MASTERARBEIT | MASTER'S THESIS

Titel | Title

The influence of oxygen on the symbiosis between environmental chlamydiae and their protist hosts

verfasst von | submitted by

Markus Arndorfer BSc

angestrebter akademischer Grad | in partial fulfilment of the requirements for the degree of

Master of Science (MSc)

Wien | Vienna, 2024

Studienkennzahl lt. Studienblatt | Degree programme code as it appears on the student record sheet:	UA 066 830
Studienrichtung lt. Studienblatt | Degree programme as it appears on the student record sheet:	Masterstudium Molecular Microbiology, Microbial Ecology and Immunobiology
Betreut von | Supervisor:	Univ.-Prof. Dr. Matthias Horn

ACKNOWLEDGEMENTS

First of all, I want to thank Prof. Matthias Horn for allowing me to do my master's thesis in his research group and for the interesting projects I was able to work on. A special thank you goes to Astrid Horn for her patient and informative supervision in the lab, in the phylogenetic and statistical analysis of all the obtained data, and for always being there to answer my questions. Additionally, I would like to thank all members of the Horn group (Matthias, Astrid, Lukas, Geli, Elisa and Flo) and Anouk Willemsen´s group for their ideas and support during group meetings and beyond. Thanks also to all the people of DOME for the nice working atmosphere. I want to thank Martin Kunert and Markus Schmid for their help with the microscopes, Stephanie Eichorst for her help with the gas chromatograph and Marc Mußmann for providing the marine sediments for my cultivation project.

A huge thank you to my family, friends and especially my twin brother Felix Arndorfer for their unconditional support and advice throughout my studies.

Table of Contents

1 INTRODUCTION

1.1 Symbiosis in protists

1.1.1 Symbiosis – an overview

Symbiosis (from the Greek sym “with” and biosis “living”) can be defined as any type of long-term interaction between two or more organisms of different species on the level of behavior, metabolism or genomes, regardless of the outcome of each partner[1–3]. Depending on the fitness effect of each partner on the other, symbiosis can be broadly divided into three types: (1) Mutualism, where both partners benefit from each other leading to a bilateral fitness increase, (2) commensalism, where the symbiont profits from the association without affecting the fitness of the host, and (3) parasitism, where one organism exploits the other to increase its fitness while harming the partner. However, many symbiotic associations are complex, poorly understood and cannot be assigned into one of these categories. Furthermore, symbiotic relationships can change over time or be highly influenced by environmental or biological factors[1,3,4]. According to the location of symbionts, it can be distinguished between ecto- and endosymbiosis: While ectosymbionts colonize the surface of their host, endosymbionts are specialized to live inside a host cell.

The dependency of the relationship can vary between symbionts: Obligate symbionts fully depend on their hosts for replication or completing their life cycle. In contrast, facultative symbionts typically also exist in a free-living stage that can survive and proliferate outside the host[1].

Symbiotic relationships are ubiquitously found on earth and have been extensively studied in multi-cellular organisms. As animals contain only a small part of the known eukaryotic diversity, findings in symbiosis research were indeed limited in their general validity[3].

More recently, the importance and distribution of symbiosis in protists, a diverse, paraphyletic group of unicellular eukaryotes, gained more attention (Figure 1): Symbiosis is found in all protist supergroups, however, in some clades like ciliates and amoebozoans such associations are documented more frequently[5–8].

The symbionts belong to different archaeal, bacterial and sometimes even other protist lineages, but members of the Chlamydiota and different phyla of Proteobacteria are more frequently found[9,10]. Potential positive or negative effects on the host have been described for some of them, however, for the majority of protist symbionts, the influence on their host remains unclear[5,11–13].

Protist endosymbionts have sometimes adapted to an intracellular lifestyle over a long evolutionary time scale and are normally characterized by genome reduction including the loss of essential metabolic pathways[14,15]. Additionally, some endosymbionts harbor specialized systems to manipulate host processes allowing the establishment of a very close and stable association. Examples are different types of secretion systems and host-targeting, eukaryotic-like effector proteins, like a Type III secretion system and a variety of effector molecules in chlamydiae[16,17]. Symbiosis in protists were mainly described as associations between two partners, however, more and more multi-partner interactions have been found in recent years[5,18–20].

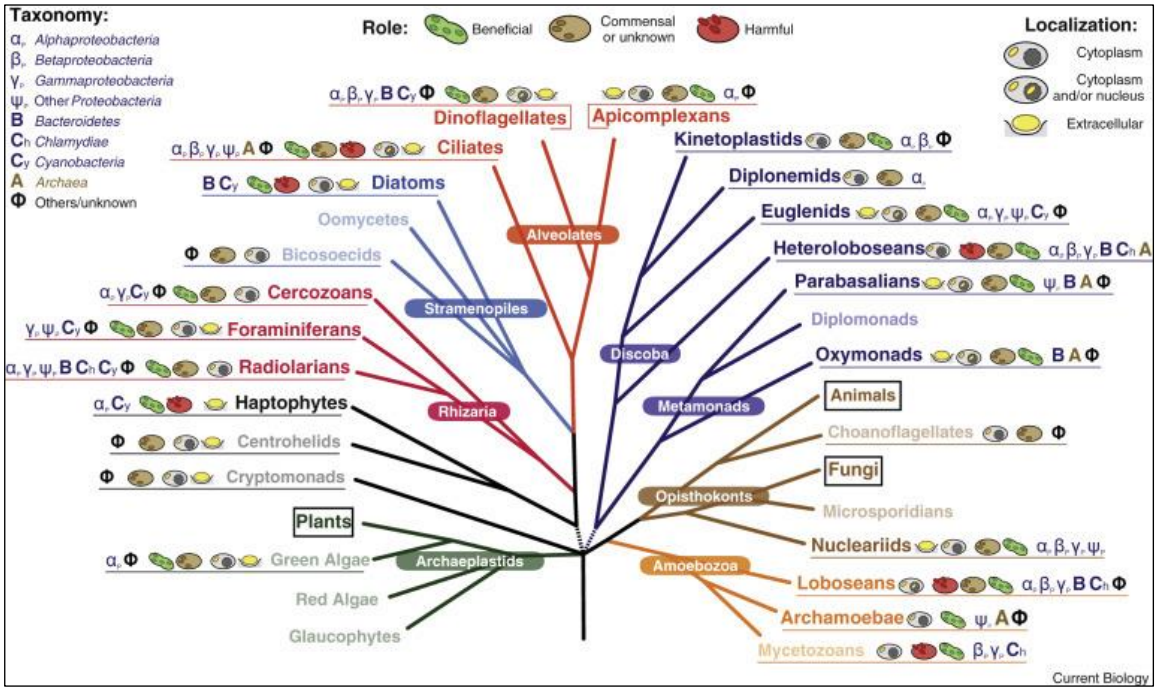

Figure 1: Phylogenetic tree of eukaryotes showing the diversity of protists and their archaeal and bacterial symbionts. Main supergroups and their lineages are depicted in different colors according to the current consensus phylogeny. For each group, symbiont taxonomy and localization as well as potential effects on the host are specified if known. The frequency of harboring symbionts in a certain lineage is indicated with faded or bold colors. Multicellular eukaryotes (not part of the protists) are shown via black squares. Figure taken from Husnik, 2021[5].

1.1.2 *Acanthamoeba* and their endosymbionts

Organisms of the genus *Acanthamoeba*, unicellular and heterotrophic eukaryotes, are members of the Amoebozoa, with a life cycle consisting of two forms. The vegetative stage, called trophozoite, is metabolically active, motile, can replicate and acts as a predator of microbes in the environment, including bacteria and yeast. Unfavored conditions like starvation or heat stress induce the transformation into cysts, which are double-walled and show a low metabolic activity allowing survival in hostile environments for years[21].

Acanthamoeba spp. can grow under oxic, microoxic as well as anoxic conditions. If oxygen is available, the energy metabolism is based mainly on oxidative phosphorylation via glycolysis/pentose phosphate pathway or fatty acid oxidation, tricarboxylic acid cycle (TCA cycle) and electron transport chain in functional mitochondria[22,23]. When facing lower oxygen concentrations or anoxia, amoebae can switch to hydrogenosome-like anaerobic ATP generation where glucose or fatty acids are fermented to H_2 and acetate via anaerobic glycolysis and the activity of the enzymes pyruvate:ferredoxin oxidoreductase, [FeFe]-hydrogenases and homologs of acetate:succinate CoA transferase and succinate thiokinase[24,25]. Cometa and colleagues have shown better growth of *Acanthamoeba* spp. under microoxic conditions than under atmospheric O_2 levels, while others found evidence for a preference towards aerobic metabolism[23,26].

Like all members of the free-living amoeba (FLA), *Acanthamoeba* spp. can colonize a broad variety of different habitats like soil, diverse fresh- and saltwater ecosystems as well as man-made environments including public water supplies, swimming pools, surgical instruments and contact lenses. *Acanthamoeba* spp. are of medical relevance as they can act as opportunistic pathogens in humans leading to diseases like granulomatous amoebic encephalitis and *Acanthamoeba* keratitis[21,27–29].

As a prevalent predator of microorganisms in the environment, *Acanthamoeba* spp. not only play a role as a regulator of microbial populations but can also serve as a host for endosymbionts that have specialized on the survival and replication inside this normally detrimental ecological niche[6,21,27,28]. Actually, up to 25% of clinical and environmental isolates of *Acanthamoeba* spp. contain associated symbionts[29].

Such obligate endosymbionts were identified as members from different taxonomic groups, including Pseudomonadota like Alpha-, Beta- and Gammaproteobacteria, Actinomycetota, Bacteroidetes, Bacillota, Chlamydiota and even Archaea[30–37]. This also includes potential pathogens of humans, that use amoeba as a "training ground" for the development of virulence traits that allow the infection of higher eukaryotes and as vehicles to colonize new environments and hosts[38].

The interactions between amoebae and their symbionts are diverse and the effects on the partners are often poorly understood[42]. In the phylum Chlamydiota, for example, symbiosis with an amoebae host can range from parasitic to neutral and sometimes even beneficial under certain environmental conditions[43]. The infection of *Acanthamoeba* with *Protochlamydia amoebophila*, on the one hand, significantly decreases the growth of the host, on the other hand, can be beneficial when the amoeba faces the amoeba parasite *Legionella pneumophila* as the endosymbionts suppress the proliferation of these pathogens. Another endosymbiont of *Acanthamoeba*, *Parachlamydia acanthamoebae*, inhibits the replication of certain giant viruses, thus protecting its host from cell lysis[44–46]. However, as this is the case for many known endosymbionts, also for the majority of chlamydiae the potential impact on their host remains unclear[47].

1.2 The phylum Chlamydiota

The bacterial phylum Chlamydiota, formerly called Chlamydiae, consists exclusively of obligate intracellular bacteria that require an eukaryotic host for their replication and survival[39]. They are related to free-living bacterial phyla including Verrucomicrobiota, Lentisphaerota, Planctomycetota and others, however, no host-independent chlamydiae have been isolated yet[40,41].

All members of the Chlamydiota share a characteristic developmental cycle (Figure 2), with two distinct morphological forms that differ in shape, localization, activity, metabolism and infectivity: Elementary bodies (EBs) are the extracellular, infective but non-replicative manifestation with a low metabolic activity that attach to a host cell which leads to their uptake via phagocytosis[42,43]. In the host cell, chlamydiae reside either in host-derived compartments called inclusions or live directly in the cytoplasm[44]. Here, EBs differentiate into reticulate bodies (RBs), the intracellular form, which uses energy from the host for their replication via binary fission, called energy parasitism[42,45].

RBs eventually convert into infective EBs, which is likely triggered by the decrease in size during cell division[46]. Last, EBs are released from the host cell by either cell lysis or inclusion extrusion and the developmental cycle can start again[9].

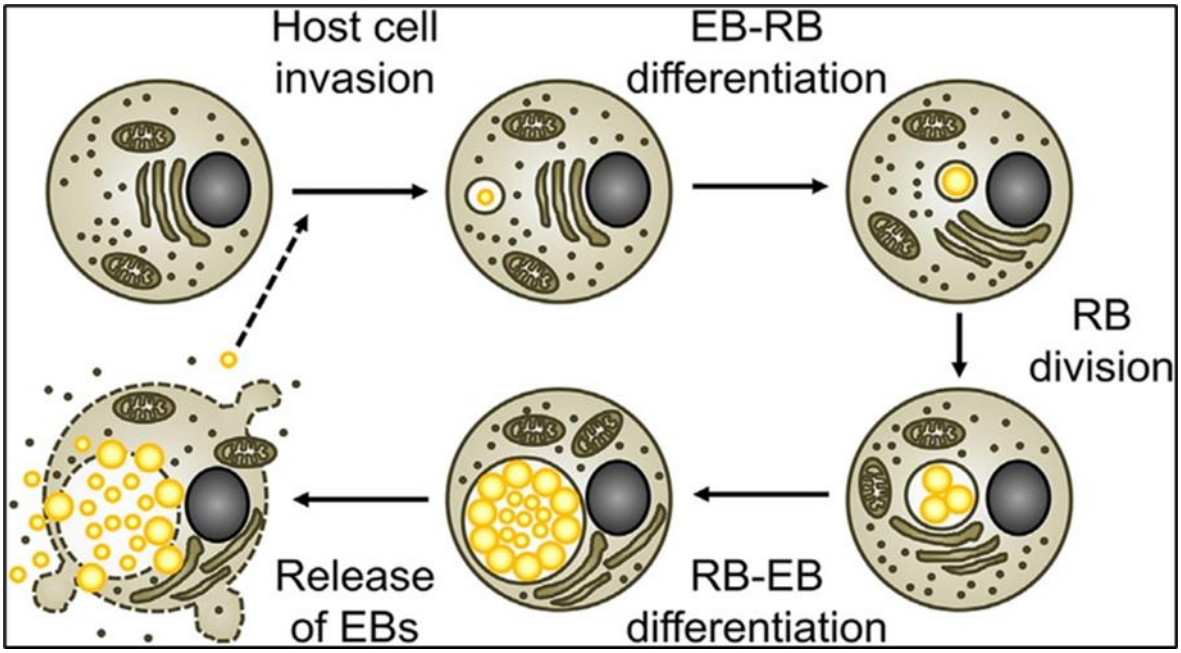

Figure 2: Biphasic developmental cycle of chlamydiae. Chlamydiae EBs infect host cells, where they differentiate into RBs, which replicate inside the host cell using energy from the host. After re-differentiation into EBs, chlamydiae are released and can invade new cells. Figure taken from Sixt, 2021[47].

Chlamydiae were originally described as a small group of animal and human pathogens with only a single family called Chlamydiaceae. This includes *Chlamydia trachomatis*, one of the most frequent causes of sexually transmitted diseases in humans that also can cause eye infections and *Chlamydophila pneumoniae*, which leads to infection in the respiratory tract in humans but can also infect other chordates[48,49].

However, in the last decades, several new families in the phylum were discovered summarized under the term Chlamydia-like organisms (CLO) or environmental chlamydiae as most of them were isolated from environmental samples but mainly to distinguish them from the family Chlamydiaceae. In contrast to this pathogenic group of Chlamydiota, CLO have a broad host range including mammals, insects, reptiles and microbial eukaryotes, so-called protists, especially the group of Amoebozoa[39,44]. Furthermore, they have - compared to members of the family Chlamydiaceae – more diverse metabolic capabilities and are less dependent on the host energy synthesis[50].

In recent years, next-generation sequencing techniques have further unveiled the extensive molecular diversity within the Chlamydiota (Figure 3). However, only a small number of chlamydiae are available as laboratory strains in host organisms while for the majority of families, not even a single representative member could be cultivated to date. Furthermore, the natural host(s) of most chlamydiae and their potential effects remain largely uncertain[41,44].

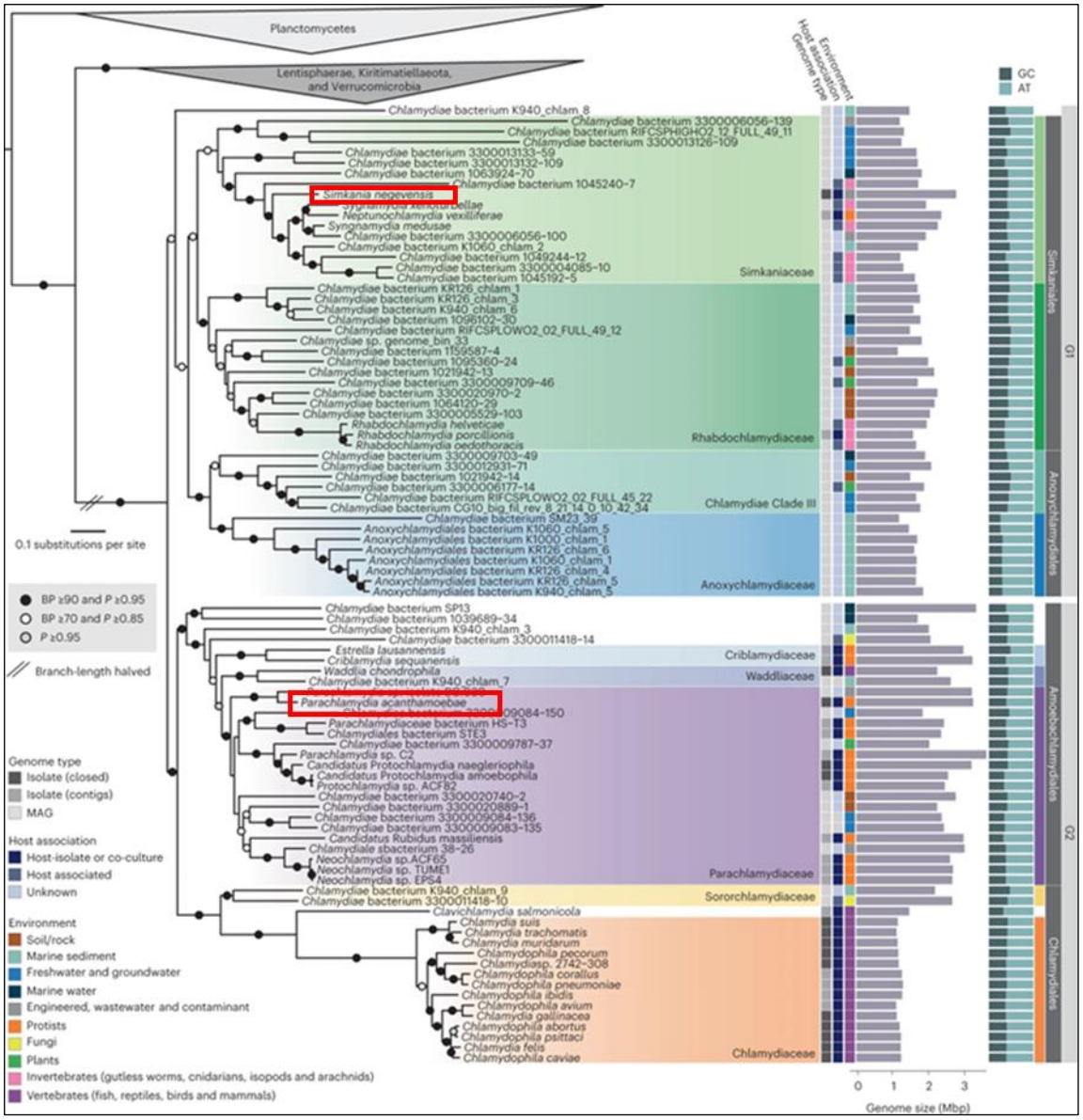

Figure 3: Phylogenetic tree of the known chlamydial diversity. The tree was calculated from 74 concatenated single-copy marker genes. The phylum Chlamydiota can be divided into groups G1 and G2 which differ in the O_2 tolerance and metabolic versatility. While the family Chlamydiaceae contains well-described species, for most chlamydial families, a low number or even no member has been cultured yet. Species marked with red boxes were used in this study. Figure adapted from Dharamshi, 2023[51].

1.2.1 *Parachlamydia acanthamoebae* UV7

Parachlamydia acanthamoebae UV7, a member of the family Parachlamydiaceae, was first isolated from activated-sludge samples of a wastewater treatment plant in Plattling, Germany via co-cultivation with symbiont-free *Acanthamoeba* sp. UWC1.

Like other members of the Parachlamydiaceae, it shares the conserved biphasic life cycle of Chlamydiota, with a rather short duration of two days from initial uptake to the release of EBs. Another commonality with almost all other Parachlamydiaceae is the replication inside host vacuoles as large, multicellular inclusions[52]. Besides amoebae, several studies indicated that UV7 can infect and replicate in human macrophages, pneumocytes, and lung fibroblasts, suggesting its potential as a new emerging human pathogen[53,54]. Like all environmental chlamydiae, *P. acanthamoebae* has an extended metabolic capability. This includes additional enzymes in sugar-metabolizing pathways, a complete TCA cycle, the potential to synthesize some amino acids on its own and a more versatile electron transport chain with additional components like the NADH dehydrogenase, accessory terminal oxidases and cytochrome c oxidases[50,55]. Beyond that, *P. acanthamoebae* encodes an acetyl-CoA synthetase, allowing the use of acetate, it potentially can grow on fatty acids and contains the more efficient F-type ATPase for energy generation[55–57].

1.2.2 *Simkania negevensis* Z

Simkania negevensis, first isolated in 1993 as a cell culture contaminant and described as a novel Chlamydia-like bacterium with unknown origin, was later assigned to the phylum Chlamydiae as the founding member of a new family called Simkaniaceae[58–60]. The natural host of *Simkania* has remained unclear until now, however, it was shown that it could replicate in various amoebae, arthropods and different mammalian cells like Vero cells, epithelial and endothelial cells and macrophages[9,58,60–64]. The developmental cycle resembles the traditional one of all chlamydiae, however, replication occurs in a single vacuole closely associated with the ER called *Simkania*-containing vacuole. In contrast to the pathogenic Chlamydiaceae, *S. negevensis* shows a prolonged life cycle of seven to twelve days and typically leaves the host without lysis[9,58,60,65,66]. Simkaniaceae share the extended metabolic features with UV7, mentioned in 1.2.1. Compared to *Parachlamydia* spp., *S. negevensis* has fewer components in its electron transport chain[58,63].

Unique genomic features of *Simkania* compared to other chlamydiae are the capability for the de-novo production of NAD from asparagine and the presence of the complete *trp*-operon, which in principle allows the synthesis of tryptophane, an important regulator of the chlamydial infection cycle[63,75,76]. Recent studies have indicated an association between *S. negevensis* and respiratory diseases in children and adolescents, including pneumonia and bronchiolitis, showing its potential as a pathogen in humans[68,77,78].

1.2.3 The family Anoxychlamydiaceae and the evolution of O_2 tolerance and metabolism in chlamydiae

Chlamydiae were originally described as aerobic to microaerobic organisms that generate energy via oxidative phosphorylation using a canonical electron transport chain. Surprisingly, a recent metagenomic study showed a relatively high abundance of chlamydiae in anoxic marine sediments leading finally to the discovery of metagenome-assembled genomes (MAGs) representing a novel obligate anaerobic chlamydial family called Anoxychlamydiaceae[41,67,68]. While several chlamydial lineages (Simkaniaceae, Parachlamydiaceae, Criblamydiaceae) have some features of a facultative anaerobic lifestyle like the acetogenic fermentation via the pyruvate dehydrogenase complex (PDC), phosphate acetyltransferase (Atp) and acetate kinase (AckA), Anoxychlamydiaceae seem to be obligate anaerobes having a variety of anaerobiosis-associated enzymes and properties: For energy conservation, they use the arginine deiminase pathway and acetogenic fermentation via the oxygen-sensitive pyruvate ferredoxin oxidoreductase (PFO). Furthermore, large parts of the TCA cycle and many components in the electron transport chain are absent. As [Fe-Fe]-hydrogenases were detected in the MAGs, fermentation was also hypothesized to be linked with H_2 production.

Until now, no cultured representative could be obtained for this family and the potential lifestyle of Anoxychlamydiaceae was described solely based on MAGs[41,68].

The discovery of several new clades in the chlamydiae and the availability of MAGs from different environmental habitats enabled a detailed phylogenetic analysis of oxygen metabolism and tolerance in the evolutionary history of Chlamydiota (Figure 3):

The last common ancestor of all chlamydiae was described as a facultatively anaerobic, motile bacterium that already lived in endosymbiosis with a eukaryotic host. The tolerance to oxygen and a more versatile metabolism evolved later via subsequent gene gain events. Based on these two features, the phylum can be divided into two major groups: The G1 group, including the families Simkaniaceae, Rhabdochlamydiaceae and the more recently described Anoxychlamydiaceae and Chlamydia Clade III (CC-III), potentially resembles more the last common chlamydial ancestor with a better adaptation to lower oxygen concentrations and a more reduced energy metabolism and respiratory chain. The G2 group in contrast is expected to be better adapted to oxygen and seems to have a more versatile metabolism and a larger variety of electron transport chain components[51]. Besides the pathogenic Chlamydiaceae, this group comprises the amoebae-infecting Parachlamydiaceae like *P. acanthamoebae*. This hypothesis about chlamydial adaptation to different oxygen regimes is at present based purely on phylogenetic and genome content analyses and has not yet been tested in laboratory experiments.

1.3 Aims of this study

This study aims to obtain more chlamydial cultures from families lacking cultivated representatives focusing on the novel, obligate anaerobic family of Anoxychlamydiaceae, which would enable follow-up experiments regarding the evolution of O_2 metabolism in Chlamydiota and provide important insights into the biology of these organisms. Here, anoxic marine sediments were used as a source as previous studies indicated a high prevalence of (anaerobic) chlamydiae in these environments[41]. Molecular techniques like PCR and droplet digital PCR (ddPCR) were applied to emphasize on the most promising sediments. Chlamydiae in these sediments and the resulting cultures were characterized by 16S rRNA gene sequencing and subsequent phylogenetic analysis. Additionally, potential host organisms were cultivated and identified via 18S rRNA gene-based phylogeny.

The second aim of this study is to test if the differences in the tolerance of oxygen exist in extant chlamydial species. Therefore two cultured representatives of each group G1 or G2 (*Simkania negevensis* and *Parachlamydia acanthamoebae* UV7), respectively, were selected to test this hypothesis experimentally.

Furthermore, the study extended the analysis of oxygen influence on the symbiosis between chlamydiae and the common laboratory and natural host, *Acanthamoeba castellanii* Neff, recently reclassified to *Acanthamoeba terricola*[69] (in the following referred to as Ac. Neff). On the host side, growth and respiration were measured under different oxygen conditions using cell counting and gas chromatography (GC) to investigate the potential effects of the associated symbionts on the host response to different O_2 levels. To study the effect of oxygen on the two chlamydial species, on the one hand, infection assays with varying O_2 levels combined with fluorescence in situ hybridization (FISH) were performed to assess the infectivity under these different conditions. On the other hand, simultaneous infections with both symbionts were carried out under low and high concentrations of oxygen to observe which organism would succeed under the given circumstances. This competition was directly quantified with a novel probe-based digital PCR (dPCR) assay over one week of incubation.

2 MATERIAL AND METHODS

2.1 Material

2.1.1 Organisms used in this study

Table 1: Organisms used in the study.

Organism	Abbreviation	Reference
Acanthamoeba terricola (ATCC30010)	Ac. Neff	Neff, 1957[70]; Corsaro *et al.*, 2024[69]
Escherichia coli TolC- (JW5503-1)	*E. coli*	Baba et al., 2006[71]
Parachlamydia acanthamoebae UV7	*P. acanthamoebae* or UV7	Collingro, Poppert *et al.*, 2005[52]
Simkania negevensis Z	*Simkania* or *S. neg*	Kahane *et al.*, 1993[58]
Acanthamoeba terricola Neff infected with *Parachlamydia acanthamoebae* UV7	Ac. Neff/UV7	
Acanthamoeba terricola Neff infected with *Simkania negevensis*	Ac. Neff/*S. neg* or Ac. Neff/*Simkania*	

2.1.2 Probes and primers

Table 2: FISH and digital PCR (dPCR) probes used in this study.

Probe name	Dye	Target	Sequence 5' – 3'	Reference
Chls-523 together with competitor probe	CY3 or CY5	Chlamydiales	CCTCCGTATTACCGCAGC	Poppert *et al.*, 2002[72]
Chlam523comp	unlabeled		CCTCCGTATTACCGCGGC	
Simneg-183	CY3 or FLUOS	*Simkania negevensis*	CAGGCTACCCCAGCTCTC	This study
UV7-763-new	CY3 (DOPE) or FLUOS	*Parachlamydia acanthamoebae* UV7	TGCTCCCCTTGCTTTCG	Collingro, Poppert *et al.*, 2005[52]
Non-EUB	CY3	Control probe complementary to EUB338	ACTCCTACGGGAGGCAGC	Wallner *et al.*, 1993[73]

SNE478_FAM	FAM	*Simkania negevensis*	{FAM}ATTGCCTAATTT GAGGGTACTTGG{BHQ-1}	This study
PAV463_HEX	HEX	*Parachlamydia acanthamoebae*	{HEX}ATTCGGCTAATTT GAGAGTACCAG{BHQ-1}	This study

Table 3: ddPCR/PCR/dPCR primers used.

Primer name	Sequence 5' – 3'	Target	Product size (nt)	Annealing T	Elongation time	Reference
515F_ mod	GTGYCAGCMG CCGCG GTAA	16S rRNA gene most bacteria	280	55°C	0:30-1:00	Walters *et al.*, 2016[86]
806R_ mod	GGACTACNVG GGTWTCTAAT					
16S1	CGGATCCTGAG AATTTGATC	16S rRNA gene Chlamy-diota	1,500	56°C	2:00	Pudjiatmoto *et al.*, 1997[87]
16S2	TGTCGACAAAG GAGGTGATCCA					
18SF	GTAGTCATATG CTTGTCTC	18S rRNA gene Amoebo-zoa	2,000	48°C	2:30	Schmitz-Esser *et al.*, 2008[88]
18SR	CGRARACCTTG TTACGAC					
18S-UniV	AACCTGGTTGA TCCTGCCAGT	18S rRNA gene Acanth-amoeba	2,000	52°C	2:30	This study
18S-UniR	GATCCTTCTGC AGGTTCACCTA C					
Chl351F_mod (either with PanR or 16S2)	GCWGCAGTCG AGRATYWTTSG C	16S rRNA gene Chlamy-diota	~1,000	58°C	2:00	unpublished
Chl40F	CRGCGTGGATG AGGCAT	16S rRNA gene	~500 (with Chl523R)	64.5°C (Chl523R)/ 56°C (16S2)	0:30-1:00 (with	Haider *et al.*, 2008[89] (only forward)

Chl523R	CCYYMC GTATTACCG CAGCT	Chlamy-diota	1500 (with 16S2)		Chl523R) 2:00 (with 16S2)	
Chl40F_mix	Forward: Equimolar mix of CAGCGTGGATG AGGCAT CGGCGTGGATG AGGCAT	16S rRNA gene Chlamy-diota	~500	64.5°C	1:00	Haider *et al.*, 2008[89] (only forward)
Chl_523R_mix (for ddPCR)	Reverse: Equimolar mix of CCCCACGTATT ACCGCAGCT CCCCCCGTATT ACCGCAGCT CCCTACGTATT ACCGCAGCT CCCTCCGTATT ACCGCAGCT CCTCACGTATT ACCGCAGCT CCTCCCGTATT ACCGCAGCT CCTTACGTATT ACCGCAGCT CCTTCCGTATT ACCGCAGCT					

Euk1385F Euk 1510R	CCCTGCCATTTGTACACAC CCTTCCGCAGGTTCACCTAC	18S rRNA gene eukaryotes	180	55°C	1:00	Amaral Zettler *et al*., 2009[90] and Lopez-Garcia *et al.*, 2003[91]
panChF2_SNE_PAV panChR2_SNE_PAV	CAACACTGGGACTGAGA AGCCGGTGCTTCTTTAC	16S rRNA gene Chlamy-diota	-	57.5°C	0:30	This study
PanF PanR	CGTGGATGAGGCATGCRAGTCG GTCATCRGCCYYACCTTVSRCRYYTCT	16S rRNA gene Chlamy-diota	1,446	65°C	2:00	Corsaro *et al.*, 2002[92]
PcF PcR	TCAGATTGAATGCTGAC TTNNGGATTTGCTTCVCC	16S rRNA gene Parachla-mydiaceae & Waddlia-ceae	1,260	60°C	2:00	Horn and Wagner, 2001[93]
SSU1 SSU2	AACCTGGTTGATCCTGCCAG GATCCTTCTGCAGGTTCACCTAT	Universal 18S rDNA	2,000	48°C	2:30	Gast *et al.*, 1994[94]
TarEuk 454F TarEuk REV3	GCTATGCGCGAGCTGC GCTATGCGCGAGCTGC	18S rRNA gene eu-karyotes	410	55°C	1:00	Stoeck *et al.*, 2010[95]

2.1.3 Chemicals and kits

Table 4: Chemicals and solutions used.

Chemical/Solution	Company
4',6'-diamidino-2-phenylindole (DAPI)	Sigma-Aldrich Handels GmbH, Vienna, Austria
6X DNA Loading Dye	Thermo Fisher Scientific Inc., Waltham, MA, USA
Biozym LE Agarose	Biozym Scientific GmbH, Hessisch Oldendorf, Germany
Calcium chloride ($CaCl_2$)	Sigma-Aldrich Handels GmbH, Vienna, Austria
Calcium chloride dihydrate ($CaCl_2$ x 2 H_2O)	Carl Roth GmbH & Co. KG, Karlsruhe, Germany
CitiFluor AF1	Citifluor Ltd., Leicester, United Kingdom
Di-Sodiumhydrogen phosphate (Na_2HPO_4)	Carl Roth GmbH & Co. KG, Karlsruhe, Germany
DNase I (lyophilized)	Zymo Research Corp., Irvine, California
EcoRI-HF restriction enzyme (#R3101S)	New England Biolabs, Ipswich, MA, USA
Ethanol absolute ≥99.8%	VWR International, Radnor, PA, USA
Ethylenediaminetetraacetic acid (EDTA)	Carl Roth GmbH + Co. KG, Karlsruhe, Germany
Formaldehyde 37% (w/w)	Carl Roth GmbH + Co. KG, Karlsruhe, Germany
Formamide deionized	Carl Roth GmbH + Co. KG, Karlsruhe, Germany
GelRed Nucleic Acid Gel Stain	VWR International, Radnor, PA, USA
GeneRuler 1kb DNA Ladder	Thermo Fisher Scientific Inc., Waltham, MA, USA
L-Glutamic Acid	Carl Roth GmbH + Co. KG, Karlsruhe, Germany
Hydrochloric acid 37% (w/w) (HCl)	Carl Roth GmbH & Co. KG, Karlsruhe, Germany
Immersol 518 F immersion oil	Carl Zeiss AG, Oberkochen, Germany
Magnesium sulfate heptahydrate ($MgSO_4$ x 7H_2O)	Sigma-Aldrich Handels GmbH, Vienna, Austria
Magnesium chloride hexahydrate ($MgCl_2$ x 6H_2O)	Carl Roth GmbH + Co. KG, Karlsruhe, Germany

Potassium chloride (KCl)	Sigma-Aldrich Handels GmbH, Vienna, Austria
Potassium dihydrogen phosphate (KH_2PO_4)	Sigma-Aldrich Handels GmbH, Vienna, Austria
Proteinase K	Takara Bio Inc., Kusatsu, Japan
QX200 ddPCR EvaGreen Supermix	Bio-Rad Laboratories, Inc., Hercules, CA, USA
Sodium chloride (NaCl)	Carl Roth GmbH + Co. KG, Karlsruhe, Germany
Sodium dodecyl sulfate (SDS)	Carl Roth GmbH + Co. KG, Karlsruhe, Germany
Sucrose	Sigma-Aldrich Handels GmbH, Vienna, Austria
Terra PCR Direct Buffer (2x, with Mg2+, dNTP)	Takara Bio Inc., Kusatsu, Japan
Terra PCR Direct Polymerase Mix (1.25 U/µl)	Takara Bio Inc., Kusatsu, Japan
Tris	Carl Roth GmbH & Co. KG, Karlsruhe, Germany
Tryptone Soy Broth	Oxoid Limited, Hampshire, UK
Yeast Extract	Oxoid Limited, Hampshire, UK

Table 5: Kits used.

Kit	Company
FastDNA Spin Kit for Soil - MP Biomedicals	Thermo Fisher Scientific Inc., Waltham, MA, USA
InnuPREP PCRpure Kit	Analytik Jena GmbH+Co. KG, Jena, Germany
QIAcuity Probe PCR Kit	QIAGEN N.V., Venlo, Netherlands
QUANTOM Total Cell Staining Kit	Logos Biosystems, Inc., Dongan-gu Anyang-si, Gyeonggi-do 14055 South Korea
Qubit 1X dsDNA High Sensitivity Assay Kit	Thermo Fisher Scientific Inc., Waltham, MA, USA
Qubit 1X RNA High Sensitivity Assay Kit	Thermo Fisher Scientific Inc., Waltham, MA, USA
Terra PCR Direct Kit	Takara Bio Inc., Kusatsu, Japan
ZymoBIOMICS DNA/RNA Miniprep Kit	Zymo Research Corp., Irvine, California

2.1.4 Disposable items

Table 6: Disposable items used.

Item	Company
BioLite Microwell Plates	Thermo Fisher Scientific Inc., Waltham, MA, USA
Corning cell strainers (50 µm)	VWR International, Radnor, PA, USA
Cover slips (12 mm)	Carl Roth GmbH & Co KG, Karlsruhe, Germany
Culture flasks (100ml) 108100 sealed with 20 mm stoppers (Butyl rubber N20)	Glasgerätebau Ochs, Bovenden / Lenglern, Germany
ddPCR 96-well Plates (semi-skirted)	Bio-Rad Laboratories, Inc., Hercules, CA, USA
ddPCR Droplet Reader Oil	Bio-Rad Laboratories, Inc., Hercules, CA, USA
DG8 Cartridges for QX200 Droplet Generator	Bio-Rad Laboratories, Inc., Hercules, CA, USA
DG8 Gaskets for Q200 Droplet Generator	Bio-Rad Laboratories, Inc., Hercules, CA, USA
Droplet Generation Oil for EvaGreen	Bio-Rad Laboratories, Inc., Hercules, CA, USA
Greiner tubes (15ml and 50ml)	Greiner Bio-One GmbH, Frickenhausen, Germany
LUNA 8-Channel Slide	Logos Biosystems, Inc., Dongan-gu Anyang-si, Gyeonggi-do 14055 South Korea
Lysing Matrix A, E tubes	MP Biomedicals, LLC, CA, USA
Manual Filter Tips (various sizes)	Biotix, San Diego, CA, USA
Microcentrifuge tubes (1.5 ml and 2ml)	Greiner Bio-One GmbH, Frickenhausen, Germany
Microscope slides, Teflon coated, 10 wells	Paul Marienfeld GmbH & Co KG, Lauda Königshofen, Germany
Minisart Syringe Filters (5 µm & 1.2 µm)	Sartorius Stedim Biotech GmbH, Göttingen, Germany
Nunclon Delta Surface cell culture flasks (various sizes)	Thermo Fisher Scientific Inc., Waltham, MA, USA
PCR 8er SoftStrips (0.2 ml)	Biozym, Hessisch Oldendorf, Germany
PCR Plate heat seal foil, piercable	Bio-Rad Laboratories, Inc., Hercules, CA, USA
Pipette tips (various sizes)	Biotix, San Diego, CA, USA
QIAcuity Nanoplate 8.5k 24/96-well, nanoplate seals and trays	QIAGEN N.V., Venlo, Netherlands
QUANTOM M50 Cell Counting Slides	Logos Biosystems, Inc., Dongan-gu Anyang-si, Gyeonggi-do 14055 South Korea
Qubit Assay Tubes	Thermo Fisher Scientific Inc., Waltham, MA, USA
Serological pipettes (various sizes)	VWR International, Radnor, PA, USA
Sterican needles (various sizes)	B. Braun Austria GmbH, Maria Enzersdorf, Austria
Syringe Omnifix 50 ml	B. Braun Austria GmbH, Maria Enzersdorf, Austria

Wide bore filter tips (200 µl)	VWR International, Radnor, PA, USA

2.1.5 Technical equipment

Table 7: Instruments used.

Instrument	Company
Anaerobic chamber (vinyl)	Accela, Prague, Czech Republik
Autoclaves: LABOKLAV 25 MV Systec VX-150 + VE-150	 SHP Steriltechnik AG, Detzel Schloß, Germany Systec GmbH, Linden, Germany
Centrifuges: Centrifuge 5804 R Centrifuge Z 366 K MiniSpin plus Rotilabo mini centrifuge	 Eppendorf AG, Hamburg Germany Hermle Labortechnik GmbH, Wehingen, Germany Eppendorf AG, Hamburg Germany Carl Roth GmbH & Co KG, Karlsruhe, Germany
ddPCR equipment : Micro TS Manual Heat Sealer QX200 Droplet Generator QX200 Droplet Reader	 Biozym Scientific GmbH, Hessisch Oldendorf, Germany Bio-Rad Laboratories, Inc., Hercules, CA, USA Bio-Rad Laboratories, Inc., Hercules, CA, USA
Dino-Lite Digital Microscopes	Dunwell Tech, Inc., Torrance, CA, USA
FastPrep-24 Classic bead beating grinder and lysis system	MP Biomedicals, LLC, CA, USA
Gas chromatograph with a pulsed discharge helium ionization detector (model TGA-6442-W-4T-PT-2He)	Valco Instruments Co. Inc., Houston, TX, USA
Gel Doc XR+ Gel Documentation System	Bio-Rad Laboratories, Inc., Hercules, CA, USA
Gel electrophoresis apparatus: Mini-Sub Cell GT Cell PowerPac Basic power supply Sub-Cell GT Cell UV-transparent gel trays + standard combs	 Bio-Rad Laboratories, Inc., Hercules, CA, USA Bio-Rad Laboratories, Inc., Hercules, CA, USA Bio-Rad Laboratories, Inc., Hercules, CA, USA Bio-Rad Laboratories, Inc., Hercules, CA, USA
Hybridization oven UE 500	Memmert GmbH & Co KG, Schwabach, Germany
Hypoxic chamber	Coy Laboratory Products, Grass Lake, MI, United States
Laminar flow hood Holten Laminair 1.8	Holten, Jouan Nordic, Allerod, Denmark

LUNA-FX7 Automated Cell Counter	Logos Biosystems, Inc., Dongan-gu Anyang-si, Gyeonggi-do 14055 South Korea
Magnetic stirrer RCT basic	IKA Werke GmbH & Co KG, Staufen, Germany
Microscopes:	
Epifluorescence microscope Axio Imager M1	Carl Zeiss AG, Oberkochen, Germany
Inverse light microscope DM IL LED	Leica Microsystems, Vienna, Austria
Thunder Epifluorescence Microscope	Leica Microsystems, Vienna, Austria
Milli-Q Integral 3 Water Purification System	Merck KGaA, Darmstadt, Germany
Multipette Stream	Eppendorf AG, Hamburg Germany
Nanodrop 1000 Spectrophotometer	Thermo Fisher Scientific Inc., Waltham, MA, USA
PCR work station	VWR International, Radnor, PA, USA
Pipetboy 2	Integra Biosciences GmbH, Biebertal, Deutschland
QIAcuity One, 2plex Device	QIAGEN N.V., Venlo, Netherlands
QUANTOM Centrifuge	Logos Biosystems, Inc., Dongan-gu Anyang-si, Gyeonggi-do 14055 South Korea
QUANTOM Tx Microbial Cell Counter	Logos Biosystems, Inc., Dongan-gu Anyang-si, Gyeonggi-do 14055 South Korea
Qubit 4 Fluorometer	Thermo Fisher Scientific Inc., Waltham, MA, USA
Research Plus Pipettes (various sizes)	Eppendorf AG, Hamburg Germany
Scales:	
OHAUS Analytical plus	OHAUS Europe GmbH, Greifensee, Switzerland
Sartorius BL6100	Sartorius AG, Göttingen, Germany
Thermocycler T100	Bio-Rad Laboratories, Inc., Hercules, CA, USA
UVP UV2 PCR Workstation	Analytik Jena GmbH+Co. KG, Jena, Germany
Vortex-Genie 2	Scientific Industries Inc., Bohemia, NY, USA
Water baths:	
Haake DC10-P5/U	Thermo Fisher Scientific Inc., Waltham, MA, USA
GFL 1004 Incubation bath	GFL Gesellschaft für Labortechnik mbH, Burgwedel, Germany
Lauda Hydro water bath	Lauda Dr. R. Wobser GmbH & Co. KG, Lauda-Königshofen, Germany

2.1.6 Software

Table 8: Software used.

Software	Company/Developer
BLASTn+2.15.0 (Basic local alignment search tool using nucleotides)	National Center for Biotechnology Information, USA
DinoCapture 2.0 version 1.5.48	Dunwell Tech, Inc., Torrance, CA, USA
Inkscape v. 1.3	Hurst, Gould, MenTaLguY, Harringto, 2003
iTol version 6.9.1	Letunic and Bork (2024)
Leica Application Suite X v. 3.0.0.15697	Carl Zeiss MicroImaging GmbH, Jena, Germany
Microsoft Office 365	Microsoft Corporation, Redmond, WA, USA
MobaXterm v. 23.2	Mobatek, Toulouse, France
QIAcuity software suite v2.5.0.1	QIAGEN N.V., Venlo, Netherlands
QX Manager 2.1.0.25	Bio-Rad Laboratories, Inc., Hercules, CA, USA
RStudio Version 2023.06.2+56	RStudio, Inc., USA
Zeiss ZEN 3.1 Version 10.0.1904	Carl Zeiss AG, Oberkochen, Germany

2.1.7 Media, buffers and solutions

10x Page Amoebic Saline (PAS):	NaCl	1.20 g
	$MgSO_4 * 7 H_2O$	0.04 g
	$CaCl_2 * 2H_2O$	0.04 g
	Na_2HPO_4	1.42 g
	KH_2PO_4	1.36 g
	ddH_2O	Ad 1L
	autoclaved	
10x Phosphate Buffered Saline (PBS):	NaCl	80.1 g
	KCl	2 g
	Na_2HPO_4	14.4 g
	KH_2PO_4	2.7 g
	ddH_2O	Ad 1L
	pH 7.3	
	autoclaved	
1x PAS:	10x PAS	100 ml
	ddH_2O	Ad 1L
	autoclaved	

1x PBS:	10x PBS	100 ml
	ddH_2O	Ad 1L
	autoclaved	
Artificial Seawater (ASW):	NaCl	26.29 g
	$MgSO_4 * 7 H_2O$	3.94 g
	$CaCl_2$	0.99 g
	$MgCl_2 * 6 H_2O$	6.09 g
	KCl	0.74 g
	ddH_2O	Ad 1L
	autoclaved	
Trypticase Soy Broth with Yeast Extract (TSY):	Tryptone Soy Broth	30 g
	Yeast extract	10 g
	ddH_2O	Ad 1L
	autoclaved	
Sucrose-Phosphate-Glutamate Buffer (SPG):	Sucrose	7.5 g
	$Na_2HPO_4 * 2 H_2O$	0.153 g
	KH_2PO_4	0.052 g
	Glutamic Acid	0.075 g
	ddH_2O	Ad 1L
	autoclaved	

10x TBE buffer:	Tris base	26.29 g
	Boric acid	3.94 g
	EDTA	0.99 g
	ddH_2O	Ad 1L
	autoclaved	
PFA [4%]:	Formalin [37%]	21.6 ml
	1x PBS	178.4 ml
NaCl [5M]:	NaCl	292.2 g
	ddH_2O	Ad 1L
Tris/HCl [1M]:	Tris	292.2 g
	ddH_2O	Ad 1L
	pH 8.0	
EDTA [0.5M]:	EDTA	186.1 g
	ddH_2O	Ad 1L
SDS [10%]:	SDS	5 g
	ddH_2O	Ad 50 ml
DAPI working solution:	DAPI stock solution	1 mg/ml
	1x MQ	1:10,000 dilution

FISH hybridization buffer (HB, 25% FA):	5M NaCl	360 µl
	1M Tris/HCl	40 µl
	Formamide (FA)	500 µl
	10 % SDS	2 µl
	ddH_2O	Ad 2 ml
FISH washing buffer (WB, for 25% FA):	5M NaCl	1.49 ml
	1M Tris/HCl	1 ml
	0.5M EDTA	0.5 ml
	ddH_20	Ad 50 ml
DNase I solution	Lyophilized DNase I	
	ZymoBIOMICS DNase/RNase-Free Water	275 µl

2.2 Methods

2.2.1 Isolation, cultivation and characterization of novel chlamydiae and their hosts from anoxic marine sediments

2.2.1.1 Sampling and sample preparation

Samples of anoxic sediments originating from 32 different locations, but pre-incubated in the laboratory, were used to cultivate potential novel chlamydiae focusing on the group of Anoxychlamydiaceae. Additional information about the samples can be found in Table 9. For the subsequent screening for the presence of chlamydiae, 0.5g of sediments were weighed into Lysing Matrix E tubes and stored at -20°C.

Table 9: Anoxic marine sediments used for chlamydiae cultivation.

Each sediment was assigned to a sample ID 1-32. The amplicon sequencing ID (JMF), sample origin, sampling date and person as well as the DNA concentrations after DNA extraction and the presence of bacterial (PCR bact) and/or chlamydial (PCR chl) DNA determined by 16S rRNA gene PCR (y=yes, n=no) are depicted in the table. HdM = Haus des Meeres Wien/Aqua Terra Zoo Vienna

Sample ID	JMF sample ID	Sample	Country	Date	Sampling person	DNA conc [ng/µl]	PCR bact	PCR chl
1		Sargasso Sea				32.2	y	n
2		BBH A	USA		Maria Mooshammer	74.1	y	n
3	JMF-2304-01-0001A/B	Elba	Italy	April 2016		12.8	y	y
4	JMF-2304-01-0002A/B	HdM Hai/ Seepferdchen 5. Stock	Austria			17.1	y	y
5		HdM Aal 3. Stock	Austria			8.4	n	n
6	JMF-2304-01-0003A/B	1770 Beach	Queensland, Australia	2018		48.4	y	y

7	JMF-2304-01-0004A/B	CBC Worm sand	Belize	April 2018		8.6	n	y
8		Egmond am See	Netherlands	24.01.2020	Marc Mussmann	7.8	y	n
9		HdM Sharktank big 2	Austria	October 2018		11.4	n	n
10		CBC	Belize	03.04.2016		11.7	y	n
11		AT Sand, HdM Atlantic tunnel	Austria			5.6	n	n
12		Janssand	Germany	28.04.2015	Marc Mussmann	10.0	y	n
13		Denmark	Denmark	14.09.2017	Anna Müller	6.3	y	n
14	JMF-2304-01-0005A/B	Kite beach	Spain	24.07.2019	Ben Yuen	13.2	y	y
15		Venice lido	Italy	2020	Marc Mussmann	6.7	y	n
16		Cassuary beach	Queensland, Australia	07.2017	Marc Mussmann	9.3	y	n
17		NB 1770 Beach	Queensland, Australia	2018	Marc Mussmann	13.9	y	n
18	JMF-2304-01-0006A/B	Castricum am See	Netherlands	24.01.2020	Marc Mussmann	7.5	y	y
19	JMF-2304-01-0007A/B	Piran Cafe	Slovenia	20.08.2020	Marc Mussmann	21.8	y	y
20	JMF-2304-01-0008A/B	Thailand	Thailand			6.0	y	y
21		China	China	2018		4.7	y	n

22	JMF-2304-01-0009A/B	Aarhus	Denmark	2020		7.1	y	y
23		Vancouver	Canada			13.9	n	n
24		Costa Rica Laska beach	Costa Rica	4.2019	Ben Yuen	42.7	n	n
25	JMF-2304-01-0010A/B	Aarhus	Denmark	20.12.2019	Kai Fiaster	4.7	y	y
26	JMF-2304-01-0011A/B	Janssand Upper flux	Germany	23.05.2017	Marc Mussmann	13.8	y	y
27	JMF-2304-01-0012A/B	Pianosa	Italy	07.2018		7.8	y	y
28	JMF-2304-01-0013A/B	Sal39 Omaha Beach	France		Marc Mussmann	28.8	y	y
29	JMF-2304-01-0014A/B	Juno Beach	France	03.2021	Marc Mussmann	18.4	y	y
30	JMF-2304-01-0015A/B	Lake Vrana	Croatia	2021	Petra Pjevac	113.2	y	y
31		Svalbard Station 52	Norway		Ken Wasmund	124.9	y	n
32	JMF-2304-01-0016A/B	Okinawa	Japan	30.06.2022	Liz Hambleton	34.5	n	y

2.1.1.2 DNA extraction, 16S rRNA gene PCR and agarose gel electrophoresis

Before cultivation, the sediments were screened for the presence of chlamydial symbionts to exclude those without any organisms of interest. Therefore, DNA was extracted from sediments 1-32 using the FastDNA Spin Kit for Soil - MP Biomedicals following the manufacturer's protocol.

Detection of chlamydiae was performed by amplifying the 16S rRNA gene via standard PCR (Tables 10 and 11) using chlamydiae-specific primers (Chl40F/Chl523R, Table 3). Additionally, a second PCR (Tables 10 and 11) using broad bacterial primers (515F/806R, Table 3) was performed as positive control on all samples. *Protochlamydia amoebophila* UWE25 DNA and MQ H_20 were used as positive and negative controls, respectively.

Table 10: Composition of reference PCR reactions. On the left: Reagents of a direct PCR assay; on the right: Reagents of a standard PCR assay. For particular PCR reactions, individual compositions are specified if performed.

Reagents (Direct PCR)	Amount per assay	Final conc.	Reagents (Standard PCR)	Amount per assay	Final conc.
Template	2 µl	-	Template	1 µl	-
2x buffer	25 µl	1x	10x buffer	2.5 µl	1x
Forward Primer (5 pmol)	3 µl	0.3 pM	Forward Primer (5 pmol)	0.5 µl	0.1 pM
Reverse Primer (5 pmol)	3 µl	0.3 pM	Reverse Primer (5 pmol)	0.5 µl	0.1 pM
Taq Polymerase	1 µl	0.025 U/µl	dNTPs (2mM each)	2.5 µl	0.2 mM
MQ H_20	16 µl	-	BSA	0.1 µl	0.08 mg/ml
-	-	-	Taq Polymerase	0.125 µl	0.025 U/µl
-	-	-	MQ H_2O	17.775 µl	-
Total volume	50 µl		Total volume	25 µl	

Table 11: Cycling conditions of a reference PCR reaction. Exact conditions may differ between individual PCR reactions and are therefore specified in Table 3 or the respective chapters of the Material and Methods section depending on the primers, template length or PCR assay used.

Step	Direct PCR		Standard PCR		
	°C	Time (min:sec)	°C	Time (min:sec)	
Initial Denaturation	98	2:00	95	3:00	
Denaturation	98	0:10 (16S)/0:30 (18S)	95	0:30	30x (16S and partial 18S)/ 35x (full-length 18S)
Annealing	Depending on the primer pair	0:15 (16S)/0:30 (18S)	Depending on the primer pair	0:30	
Elongation	68	Depending on the primer pair	72	Depending on the primer pair	
Final Elongation	68	5:00 (16S)/10:00 (18S)	72	5:00 (16S)/10:00 (18S)	
Hold	12	∞	12	∞	

The PCR products were analyzed in a 1% agarose gel along with 1kb Gene ruler as size marker and visualized with the Gel Doc system to check for the presence of chlamydial DNA in the sediments by specific bands in the gel.

2.1.1.3 Quantification of chlamydiae via droplet digital PCR (ddPCR)

For cultivation, the focus lay on sediments with a higher abundance of chlamydiae. Consequently, the cell number of chlamydiae in the chlamydiae-positive sediments (from PCR in 2.1.1.2) was determined with ddPCR (Tables 12 and 13) using the chlamydiae-specific primers Chl40F_mix and Chl523R_mix (Table 3). The extracted DNA was taken as a template and proper dilutions (1:10/1:100/1:1,000) were prepared to reach DNA concentrations between 0.1-0.5 ng/µl. As positive, negative and Non-Target (NT) controls, *Parachlamydia acanthamoebae* OEW1 DNA, MQ and NTmix/18S mock community were used.

The concentration of 16S rRNA gene copies per g sediment (cp/g) was calculated from the ddPCR results considering the amount of template in the reaction (2 µl template in 22 µl total volume), the dilution of the template and the mass of sediment used for extraction.

Table 12: Compounds of the ddPCR assay.

Reagents	Amounts per assay	Final conc.
Template	2 µl	-
2x EvaGreen Supermix	11 µl	1x
Chl40F_mix (5 µM)	0.4 µl	0.09 µM
Chl523R_mix (5 µM)	0.4 µl	0.09 µM
MQ H_20	8.2 µl	-
Total volume	22 µl	

Table 13: ddPCR cycling program.

Step	°C	Time (min:sec)		Ramp rate
Enzyme activation	95	3:00		2°/sec
Denaturation	95	0:30	40x	2°/sec
Annealing	64.5	1:00		2°/sec
Elongation	72	1:00		2°/sec
Signal stabilization	4	5:00		2°/sec
	90	5:00		2°/sec
Hold	12	∞		

2.1.1.4 16S and 18S rRNA gene amplicon sequencing

Sediments containing chlamydiae (3, 4, 6, 7, 14, 18, 19, 20, 22, 25, 26, 27, 28, 29, 30, 32) were used for chlamydiae-specific 16S rRNA gene amplicon sequencing and 18S rRNA gene amplicon sequencing targeting potential eukaryotic hosts using primer pairs Chl40F/Chl523R and 1380F/1510F, respectively (Table 3).

Sequencing was performed by the Joint Microbiome Facility (JMF)[74]. For the chlamydiae 16S amplicon sequencing results, generated ASVs were clustered on a 95% identity level using usearch and calculated into a recent 16S rRNA gene-based phylogenetic tree of the known diversity of Chlamydiota which was visualized in iTol[75,76]. For each ASV, the number of assigned reads grouped by individual sediments was depicted on the outer circle of the tree. Additionally, each sediment's taxonomic composition of chlamydiae was plotted in RStudio using phyloseq[77]. For the analysis, taxa with less than 20 reads were filtered out. Relative abundances of chlamydial families were calculated for each sediment, those results were then used to plot absolute abundances by including the ddPCR data (2.1.1.3).

The ASVs generated for the 18S rRNA gene amplicon sequencing data were used for phylogenetic and taxonomic analysis. First, general information like total read number per sample before and after filtering (all ASVs with less than ten reads were filtered out), alpha-diversity measures like Chao1 and Shannon index and eukaryotic composition in each sediment as relative abundances on supergroup and genus levels were plotted in Rstudio using phyloseq[77].

Additionally, filtered ASVs were calculated into an 18S rRNA gene-based phylogenetic tree together with the 18S rRNA gene sequences obtained from the cultures. For that, ASVs and partial 18S rRNA gene sequences from the cultures were included in the untrimmed pr2 18S rRNA database alignment from 2.1.1.6 using MAFFT and then trimmed with trimAl v1.4.rev15[78,79]. Aligned ASV and short 18S rRNA gene sequences were extracted into a new file with Python and an 18S rRNA gene-based phylogenetic tree was calculated using FastTree2 with the remaining, not-extracted aligned sequences[80]. ASV and culture 18S sequences were added to this phylogenetic tree with EPA-ng as explained in 2.1.1.6[81]. Branches in the tree were renamed using a custom Python script, and the tree was visualized in iTol[75]. For ASVs falling close to sediment culture sequences, the read number was checked to see if the cultivated organisms were high or low abundant in the sediments.

2.1.1.5 Cultivation of protists and associated chlamydiae from sediments

Twelve sediments (3, 4, 6, 7, 14, 18, 19, 20, 22, 26, 30, 32) were selected for the cultivation of protists and their associated symbionts based on the chlamydial copy number in the samples. Sediments were either directly used or filtered through a 50 µm cell strainer beforehand. Incubations were carried out either in the hypoxic tent in 24-well plates and different concentrations (1:10, 1:100, 1:1,000, 1:10,000) or anoxically in cultivation tubes.

ASW supplemented with *E. coli* food bacteria was used as a cultivation medium. After reaching a higher biomass, larger hypoxic cultures were started in 6-well plates as duplicates. Regularly, cultures were analyzed under the light microscope, the medium was exchanged and cultures were fed with fresh *E. coli*.

2.1.1.6 Taxonomic characterization of chlamydiae and their hosts in the sediment cultures via 16S/18S rRNA gene-based PCR, Sanger sequencing and phylogenetic analysis

After sufficient biomass was obtained, the cultures were screened for chlamydiae via direct PCR targeting short regions of the 16S rRNA gene followed by Sanger sequencing. For the PCR, the primer pair Chl40F/Chl523R was applied (Tables 3, 10 and 11). PCR products were separated in a 1% agarose gel along with 1kb Gene ruler as a size marker and visualized with the Gel Doc system. All PCR products with a band at the expected size in the gel were purified using the InnuPrep PCRpure Kit following the protocol of the manufacturer and were sequenced with the same primers as for the PCR reaction (in higher concentration: 10 pmol). Sanger sequencing was performed by Microsynth AG Austria and results were taxonomically assigned via NCBI Blastn.

For sediment cultures with a chlamydiae-positive Blast result, the whole 16S rRNA gene was amplified via PCR using different primer combinations (Table 3, 10 and 11) and sequenced by Microsynth AG Austria. The obtained 16S rRNA gene sequences were aligned in Geneious to produce a full-length consensus sequence if possible[82].

For phylogenetic analysis, these sequences were added to a chlamydial reference SINA alignment using MAFFT, and the alignment was trimmed using trimAl v1.4.rev15 which was the basis for the calculation of a 16S rRNA gene-based phylogenetic tree in IQ-TREE 2[78,79,83]. Afterward, the partial 16S rRNA gene sequences of sediment cultures where no full-length sequence was obtained were included in the SINA alignment and added to the phylogenetic tree using EPA-ng[81].

The phylogenetic tree was visualized in iTol, families were colored as in Dharamshi *et al.*, 2023 and branches of the potential novel chlamydiae from the sediment cultures were marked in red[51,75]. All representatives of families without a novel sediment sequence were collapsed.

Additionally, 18S rRNA gene sequences of potential hosts were obtained from the cultures via direct PCR (Table 3, 10 and 11) and Sanger sequencing (by Microsynth AG Austria) and sequences were taxonomically assigned via NCBI Blastn. Full-length 18S rRNA gene sequences were additionally calculated into an 18S rRNA-based phylogenetic tree.

Accordingly, 18S rRNA gene sequences were aligned to the pr2 18S rRNA database (v4.12.0) using MAFFT and the alignment was trimmed with trimAl v1.4.rev15[78,79]. A phylogenetic tree based on this alignment was computed in FastTree 2[80]. Afterward, partial 18S rRNA gene sequences were added to this alignment using MAFFT and added to the phylogenetic tree using EPA-ng[78,81]. Branches in the tree were renamed using a custom Python script, and the tree was visualized in iTol[75].

2.2.2 Influence of oxygen on the growth, respiration and infectivity of chlamydiae and their *Acanthamoeba* host

2.2.2.1 Comparison of growth of (un-)infected amoebae under hypoxic and oxic conditions

Unsynchronized, infected cultures of Ac. Neff/*S. neg* and Ac. Neff/UV7 as well as an uninfected Ac. Neff culture grown in culture flasks containing TSY medium were used to inoculate 12-well plates for growth comparisons under varying O_2 levels. First, the different amoebae cultures were harvested by centrifugation at 5,000 rcf for 10 min and pellets were resuspended in a small volume of TSY medium. After determining the cell concentration at the LUNA-FX7 Automated Cell Counter (Table 14), dilutions in TSY were prepared to reach an initial concentration of $5x10^4$ cells/ml per well. 2 ml of amoebae suspension diluted in TSY were seeded as triplicates for each time point of the measurement (24h, 48h, 96h and 1 week). Plates were either incubated on the bench (oxic) or in the microoxic tent (hypoxic, 1 % oxygen, N_2 as calibration gas) for the whole experiment. At each time point, samples were taken, cells were harvested by centrifugation at 5,000 rcf for 10 min, pellets were resuspended in a small volume of 1x PAS and the cell number was determined at the LUNA-FX7 Automated Cell Counter (Table 14, diluted if necessary). From the obtained cell numbers, growth curves were calculated in RStudio using ggplot2[84]. As the growth of amoebae infected with the two different symbionts was performed in separate experiments, two individual plots were generated. Additionally, significant differences (p-value < 0.05) in the growth between the different treatments were analyzed in RStudio using an ANOVA and Post-hoc Tukey test.

Table 14: Settings of the LUNA-FX7 cell counter for amoebae quantification.

Settings	Value
Min. search size	8 µm
Max. search size	30 µm
Cell detection sensitivity	5
Noise reduction	3
Dilution factor	1

2.2.2.2 Growth comparison of infected and uninfected amoebae under anoxic conditions

The growth of uninfected and UV7/*Simkania*-infected Ac. Neff was also analyzed under anoxic conditions. For the measurements, the same workflow as in 2.2.2.1 was applied (Table 14), however, plates were incubated in the anoxic tent (0 % oxygen, 2% H_2, 12% CO_2, 86% N_2) instead. Growth curves were calculated from the determined cell numbers in RStudio using ggplot2[84]. Additionally, significant differences (p-value < 0.05) in the growth between the different treatments were calculated in RStudio using an ANOVA and Post-hoc Tukey test.

2.2.2.3 Purification and quantification of EBs from supernatant of infected amoebae cultures

For further infection assays, chlamydial EBs were purified from already infected Ac. Neff/*Simkania* and Ac. Neff/UV7 cultures. To increase the yield of EBs, infected amoebae were grown in large volumes (150 ml) in TSY using Nunc TripleFlask Treated Cell Culture Flasks for at least one week and extracellular bacteria were allowed to accumulate by incubation for another week. Culture supernatant was harvested in 50 ml Falcon tubes via centrifugation at 10000 rpm (Centrifuge Z 366 K, Hermle Labortechnik GmbH, Wehingen, Germany) for 10 min and pellets were resuspended in 1x PAS. The suspension was pushed consecutively through a 5 µm and 1.2 µm filter, the filtrate was centrifuged with the same settings and the pellet was resuspended in ice-cold SPG buffer. Afterward, the resuspension was homogenized with a long 21-gauge needle. For quantification, a small volume of EB suspension was diluted 1:100 in SPG buffer and the cell number was determined with the QUANTOM Tx Microbial Cell Counter (Table 15) using the QUANTOM Total Cell Staining Kit following the protocol of the manufacturer. The remaining EB suspension was stored as 1 ml aliquots at -75°C for later infection experiments.

Table 15: Settings of the QUANTOM-Tx cell counter for EB quantification.

Settings	Value
Dilution factor	2
Min. Fluorescent object size	0.6 µm
Max. Fluorescent object size	2 µm
Size gating	0.6 ~ 2 µm
Roundness	30 %
Declustering level	7
Detection sensitivity	4
Focusing method	Autofocus
LED level	5

2.2.2.4 Respiration measurements of symbiotic and aposymbiotic Ac. Neff under oxic and hypoxic conditions using gas chromatography (GC)

Besides the growth, the respiration as released CO_2 was monitored in infected (*Simkania* and UV7) and uninfected Ac. Neff cultures under low and atmospheric O_2 levels as a measurement of host fitness.

For the experimental set-up, 100 ml sterile culture flasks (triplicates for each treatment) were filled with 20 ml TSY medium. Culture flasks were allowed to equilibrate for approximately 24 h prior to the start of the experiment at their respective atmosphere (lab bench (oxic) or in the microoxic tent (hypoxic)). The hypoxic atmosphere ([vol/vol] 1% O_2, N_2 as calibration gas) was maintained with a flexible vinyl chamber fitted with an oxygen sensor/controller. Bottles were then sealed with butyl rubber stoppers. For the infection, Ac. Neff cultures were harvested by centrifugation at 5,000 rcf for 10 min and resuspended in a small volume of TSY, also, *S. neg* and UV7 EBs were thawed in a water bath at 37°C. Amoebae cells were quantified at the LUNA-Fx7 cell counter as mentioned before (Table 14 and 2.2.2.1) and proper dilutions of Ac. Neff and the according symbionts were prepared in Falcon tubes to reach cell concentrations of $4.5x10^5$ cells/ml for the host and $9x10^6$ cells/ml for the symbionts (=multiplicity of infection (MOI) of 20, either *Simkania* or UV7) per flask.

The infection was enhanced and synchronized by centrifugation at 150 rcf for 15 min and infected or uninfected amoebae were inoculated into the culture flasks via syringes and needles.

The headspace of the respective flasks was removed by vacuum, and replaced with air at either 21% (v/v) (oxic) or 1% (v/v) (hypoxic) oxygen. All cultures were incubated at room temperature. Carbon dioxide production was monitored by gas chromatography with a pulsed discharge helium ionization detector. Two ml of headspace was sampled from each bottle every 24h (also at the beginning, time point 0) to measure the production of CO_2 via gas chromatography. After each sampling time point, the bottles were flushed and filled three times with either filtered “oxic air” or “hypoxic air” to ensure the targeted oxygen concentration. As controls, flasks with medium only and either “oxic air” or “hypoxic air” were made after the first measurement (time point 24h). Bar plots of the GC results were visualized in RStudio with ggplot2[84]. The statistical significance (ANOVA and Post-hoc Tukey test) between the different cultures was determined in RStudio.

2.2.2.5 Assessment of chlamydial infectivity under various oxygen levels

The infectivity of UV7 and *Simkania* in Ac. Neff under oxic, hypoxic and anoxic conditions was compared by counting intracellular chlamydiae after FISH.

For that, an Ac. Neff culture (in a 150 ml Nunc TripleFlask Treated Cell Culture Flask) was inoculated and grown for at least one week before the start of the experiment. Amoebae cells were harvested via centrifugation at 5,000 rcf for 10 min and cells were resuspended in TSY. Cells were quantified as described previously (Table 14 and 2.2.2.1). A proper dilution of resuspended cells was prepared in TSY. Amoebae were seeded into 24-well plates with an initial cell concentration of 2.5 x 10^4 cells/ml per well. EBs of UV7 and *Simkania* were thawed in a water bath at 37°C and diluted accordingly for the four different MOIs used (10, 30, 50, 100). Cultures were infected with 50 µl diluted EBs per well. Each infection (for the different MOI, organism and oxygen conditions) was carried out in triplicates. The infection was enhanced by centrifugation for 15 min at 150 rcf and plates were incubated at the bench (oxic), in the microoxic tent (hypoxic) or anoxic tent (anoxic). The medium was exchanged after 2h to synchronize the infection. After two days of incubation, cells were harvested and fixed for FISH analysis. For this purpose infected cells were harvested by centrifugation at 5,000 rcf for 5 min, pellets were washed in 1x PAS and fixation was performed in 4% PFA for 20 min at room temperature. Then cells were again centrifuged, washed in 1x PAS and finally resuspended in 1:1 1x PAS and 100% Ethanol.

For FISH, 10 µl of fixed cells were attached on the wells of Teflon-coated microscopy slides in the hybridization oven (FISH oven) at 46°C for 5 min. 9 µl hybridization buffer (2.1.7) and 2 µl of the specific probe (UV7-763-new-Cy3-DOPE or Simneg-183-Cy3, Table 2) were added to each well. Hybridization was performed in the FISH oven at 46°C for 2 h. Slides were washed in pre-heated washing buffer (2.1.7) at 48°C for 15 min. To remove the remaining washing buffer, slides were dipped into ice-cold ddH_2O and completely dried in the hybridization oven. Last, cells were stained with 10 µl DAPI working solution (1 µg/µl in 1x PAS) for 3 min, DAPI was removed in ice-cold 96% EtOH and samples were embedded in CitiFluor. Slides were visualized under the epifluorescence microscope and cells were counted with a counting ocular. For assessing the infectivity of the different chlamydiae under the various O_2 regimes, 50 cells were counted per well and the numbers of non- (no symbiont-associated FISH signal), low- (1-30 symbiont-associated FISH signals) and high-infected (> 30 symbiont-associated FISH signals) amoebae were determined.

2.2.2.6 Co-infection of UV7 and *Simkania* in *Acanthamoeba* under oxic and anoxic conditions

In this experiment, it should be tested which symbiont would compete better under different oxygen conditions. For this, the growth of amoebae as well as the replication of chlamydial symbionts was determined in single- (UV7 or *Simkania*) and double- (UV7 and *Simkania*) infected *A. castellanii* cultures incubated under either oxic or anoxic conditions for one week. Ac. Neff cells were harvested by centrifugation at 5,000 rcf for 10 min and resuspended in a small volume of TSY medium. The amoebae cells were quantified at the LUNA-Fx7 cell counter (2.2.2.1 and Table 14) and a proper dilution in TSY was prepared to reach 2.5 x 10^4 cells/ml and an inoculation volume of 2 ml. Diluted amoebae were inoculated in 12-well plates with four replicates per treatment. EBs of UV7 and *Simkania* were thawed in a water bath at 37°C and amoebae were infected with 50 µl of diluted EBs per well to reach a MOI of 20. The infection was enhanced by centrifugation at 150 rcf for 15 min. Plates were incubated in the 28°C climate chamber (oxic) or the anoxic tent (same temperature). After 2 h, the medium was exchanged to synchronize the infection. At six time points post infection (0h, 2h, 24h, 48h, 96h and one week), samples were taken for cell counting at the LUNA-Fx7 cell counter (2.2.2.1 and Table 14) and fixation for FISH (only for co-infected samples in two replicates). The rest of the cultures were harvested (centrifugation at 5,000 rcf for 10 min) for DNA/RNA extraction and stored at -75°C.

For fixation, cells were harvested via centrifugation at 5,000 rcf for 10 min, fixed in 4% PFA for 20 min at room temperature, washed in 1x PAS and finally resuspended in 100 µl 1:1 1x PAS and 100% EtOH.

Determined amoebae cell numbers were used to calculate growth curves as described in 2.2.2.1. Statistical significance between amoebae cell growth was tested in RStudio using an ANOVA and Post-hoc Tukey test.

FISH was performed by attaching 10 µl of PFA-fixed cells per well on FISH slides in the FISH oven for five minutes. Hybridization, washing and DAPI staining were performed as described under 2.2.2.5 with the specific probes UV7-763-new-Fluos and Simneg-183-Cy3 as well as the general Chlamydiota probe Chls-523-Cy5 (Table 2). One well per slide was hybridized as a negative control with 1 µl of Non-EUB-Cy3 probe. Cells were visualized under the Thunder epifluorescence microscope.

DNA and RNA were extracted from the harvested cells and analyzed with dPCR to quantify symbiont replication. For the extraction, DNA and RNA were co-purified using the ZymoBIOMICS DNA/RNA Miniprep Kit following the protocol of the manufacturer combined with DNase I treatment with small variations: Samples and two blank extractions were resuspended in 300 µl DNA/RNA Shield and 2 volumes of DNA/RNA Lysis buffer and cell lysis was performed without a bead beating step. All centrifugation steps were performed at 13000 rcf for 1 min unless specified in the protocol. DNase I treatment was carried out for 30 min at 37°C. DNA samples were stored at -20°C, and RNA samples at -75°C.

For quantification of chlamydiae, dPCR was performed with the extracted DNA. As pre-experiments showed a too-high probe signal for UV7 and co-infected samples to properly measure the concentration, extracted DNA was diluted 1:100 in MQ for these samples while *Simkania* DNA was used undiluted. Specific probe/primer combinations (panChF2_SNE_PAV/ panChR2_SNE_PAV primer pair and probes SNE478_FAM/ PAV463_HEX, Tables 2 and 3) labeled with two distinct fluorescent dyes (FAM/Fluorescein or HEX/Hexachlorfluorescein) were used to detect and quantify the two different chlamydiae symbionts simultaneously. For the assay, a modified protocol of the QIAcuity Probe PCR and Nanoplate Kits was carried out in 96-well, 8.5k Nanoplates (Tables 16 and 17). Blank extraction and MQ as well as *Parachlamydia acanthamoebae* OEW1 and *Simkania negevensis* Z 16S rRNA gene amplicons in two different ratios (amp 4_2 = Simkania 10^4 copies/µl : OEW1 10^2 copies/µl and amp 3_5 = Simkania 10^3 copies/µl : OEW1 10^5 copies/µl) were used as negative and positive controls, respectively.

The actual concentration of chlamydiae as cells/ml was calculated from the raw dPCR results by including reaction (12 µl) and template (2 µl) volume, dilution (1 or 100), DNA elution (100 µl) and sampling (1,890 µl) volume and the number of rRNA genes per organism (*Simkania*: 1, UV7: 3). Each sample's chlamydiae number was normalized by the measured cell number of amoebae cultures and depicted as growth curves in RStudio using ggplot2[84]. Additionally, significant differences (p-value < 0.05) in the replication of the different symbionts and oxygen concentrations were calculated in RStudio using an ANOVA and Post-hoc Tukey test.

Table 16: Components of dPCR assay

Reagents	Amounts per assay	Final conc.
Template	2 µl	-
4x Probe PCR Master Mix	3 µl	1x
10x primer/probe mix 1 (SNE_478)	1.2 µl	0.4 µM FP / 0.8 µM RP / 0.4µM probe
10x primer/probe mix 2 (UV7_483)	1.2 µl	0.4 µM FP / 0.8 µM RP / 0.4µM probe
Restriction enzyme (EcoRI)	0.5 µl	0.125 U/µl
MQ H_20	4.1 µl	-
Total volume	12 µl	

Table 17: dPCR cycling and imaging conditions

Step	Temperature	Duration (min:sec)	
Initial denaturation	95 °C	2:00	
Denaturation	95 °C	0:30	45x / 50x
Annealing	57.5 °C	0:30	
Elongation	72 °C	0:30	
Sample stabilization	40 °C	5:00	
Step	Gain	Exposure time	
Imaging	5	600 ms	

3. RESULTS

3.1 Isolation, cultivation and characterization of (anoxic) chlamydiae and their hosts from marine sediments

3.1.1 Marine sediments contain a large diversity of chlamydiae, including Anoxychlamydiaceae

For the cultivation of novel Chlamydiota, focusing on the anaerobic group of Anoxychlamydiaceae, 32 marine sediments from different locations (Table 9) were sampled and screened for the presence of chlamydiae: First, DNA was extracted from the sediments and on the one hand directly sent to 16S rRNA gene amplicon sequencing by the JMF with chlamydiae-specific primers, on the other hand, used for 16S rRNA gene-based PCR targeting chlamydiae followed by agarose gel electrophoresis. As a control, a second PCR assay was performed with general 16S rRNA gene PCR primers (see 2.1.1.2).

16S rRNA gene PCR showed the presence of chlamydial DNA in almost half of the analyzed sediments (sediments 3, 4, 6, 14, 18, 19, 20, 22, 25, 26, 27, 28, 29, 30, and 32) by a band in the agarose gel at the expected size of approximately 500 nt (data not shown). As the PCR products were not sent to sequencing, the phylogeny could not be determined via this approach, however, all sediments with a chlamydiae-positive signal were used for quantification and subsequent cultivation of the potential novel chlamydiae and their hosts.

The 16S rRNA gene amplicon sequencing generated in total 219,337 reads and 4,146 ASVs which were clustered at 95% identity and the resulting 677 ASV clusters were added to a recent 16S rRNA gene-based phylogenetic tree of the Chlamydiota group. The chlamydial families in the tree were colored as in Dharamshi *et al*[59]. Additionally, the number of reads for each ASV cluster was calculated and depicted as bars (height ~ read number) on the outer circle of the tree (Figure 4). All blue branches indicate chlamydial ASVs derived from the different marine sediments. Additionally, the chlamydial composition of each sediment sample was depicted on family-level as absolute abundance determined by normalization with a chlamydiae-specific dPCR assay (Figures 5, 6; also see 3.1.2).

In general, ASVs fell to almost all chlamydial families except for Parili-/Piscichlamydiaceae and the pathogenic Chlamydiaceae. Taking also the read number into account, well-represented groups in the sediment samples were especially Simkaniaceae, CC-III, Parasimkaniaceae and also Anoxychlamydiaceae, whereas Rhabdochlamydiaceae and Parachlamydiaceae-assigned ASVs were rarer. Moreover, in most sediments, one or maximal two ASVs dominated with other ASVs showing only low read numbers (Figure 4).

In the absolute abundance plot of chlamydial families (Figure 5), all samples showed a high number of 16S rRNA gene copies that could not be assigned to any known chlamydial family. No family was dominating in all of the sediments, however, some were found more often in specific sediments than others: Simkaniaceae in sediments 6, 19 and 32, family GCA-2709385 in sediments 3, 4, 6 and 19, Waddliaceae in sediments 6 and 19, group 2 in sediment 30 and Rhabdochlamydiaceae in sediments 4, 6 and 20.

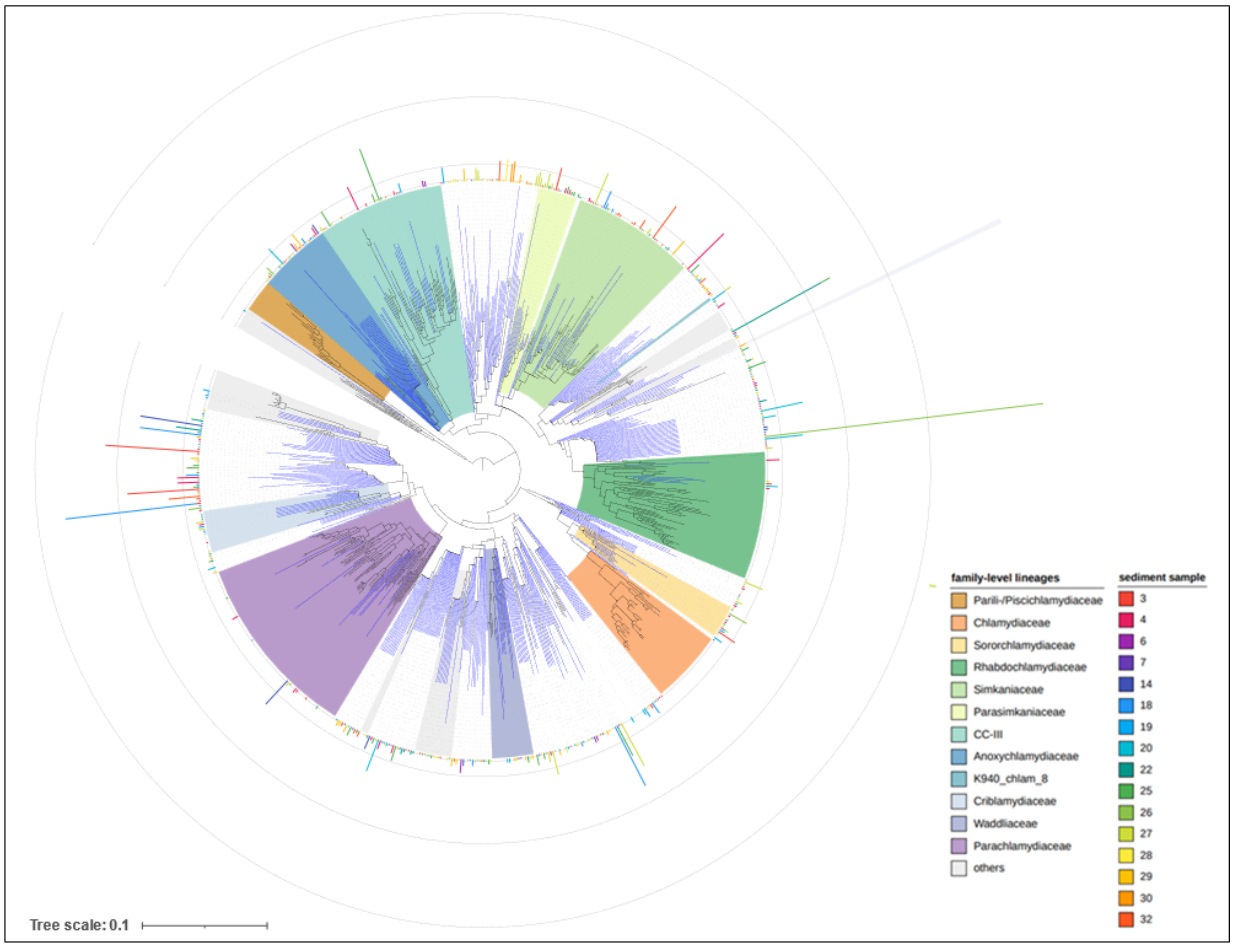

Figure 4: Chlamydiae ASV sequences from marine sediments placed in a 16S rRNA gene-based phylogenetic reference tree of Chlamydiota. Branches of sediment ASVs are depicted in blue. The different chlamydial families are colored as indicated in the legend. Bars on the outside of the tree represent the read number for each ASV, where the color shows the sediment sample ID as described in the legend. The circles surrounding the tree indicated, from the inside to the outside, 100, 1,000, 5,000 and 10,000 sequence reads, respectively.

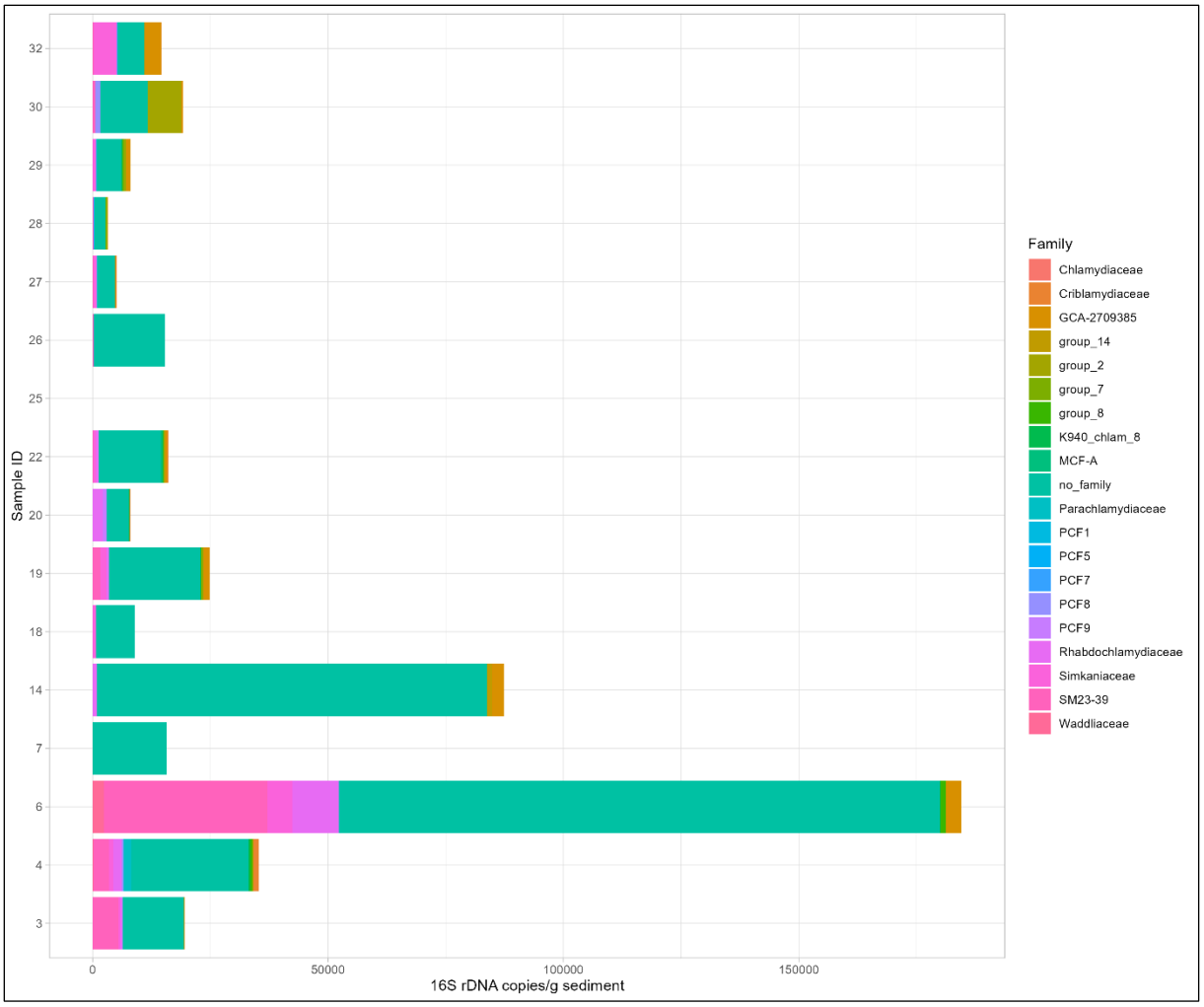

Figure 5: Absolute abundance plot of chlamydial composition in sediments. Amplicon sequencing data were first used to calculate the relative abundance of chlamydiae in the different sediment samples. By combining this with the ddPCR results, absolute abundance could be calculated and plotted as "16S rDNA copies/g sediment". The color of the bars refers to the different chlamydial families as indicated in the legend. For sediment 25, no ddPCR results were obtained allowing no presentation of absolute abundances.

3.1.2 Sediments contain a relatively high number of chlamydiae and organisms could be cultivated under hypoxic and anoxic conditions

In all sediments with a positive PCR result, chlamydiae were quantified via ddPCR and the number of 16S rRNA gene copies per g sediment was calculated (Figure 6).

In general, 16S rRNA gene copies range from 0 to almost 185,000, with the majority between 8,000 and 20,000 copies per gram sediment. The twelve sediment samples with the highest number of chlamydial 16S rRNA gene copies (sediments 3, 4, 6, 7, 14, 18, 19, 20, 22, 26, 30, and 32) were subsequently used for incubation and enrichment of protists under hypoxic and anoxic atmospheres.

All cultures could be maintained over several months intermitted by regular feeding and medium exchange and eukaryotic microorganisms could be successfully enriched (example images under 3.1.4).

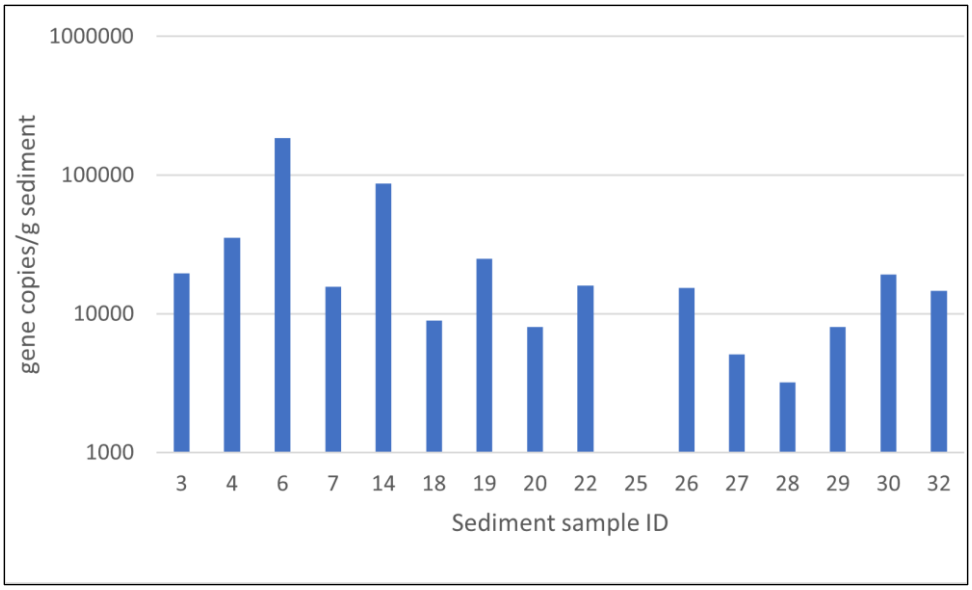

Figure 6: Chlamydial 16S rRNA gene copies in marine sediments. Chlamydial numbers derived via ddPCR are depicted as 16S rRNA gene copies per g sediment for each sediment sample.

3.1.3 Sequencing of chlamydial 16S rRNA genes of the sediment cultures reveals the successful enrichment of novel chlamydiae from a broad range of different families

The protists enriched from the sediment incubations were screened regularly for the presence of chlamydiae via direct PCR targeting a short fragment of the chlamydial 16S rRNA gene (Table 3, length approx. 500 nt) and subsequent Sanger sequencing of all PCR products with a positive result in the agarose gel (band at expected size, not shown here). In total, six different 16S rRNA gene sequences from hypoxic and anoxic cultures were obtained that were taxonomically assigned to Chlamydiota with NCBI Blastn (anoxic cultures of sediment 6, 19 and 20 as well as hypoxic cultures of sediments 4, 19 and 26). From these samples, full-length sequences of the chlamydial 16S rRNA gene were generated (Table 3) via Sanger sequencing and alignments in Geneious[82]. For the phylogenetic assignment, partial and if available, full-length 16S rRNA gene sequences were added or calculated, respectively into a 16S rRNA gene-based phylogenetic reference tree of the known diversity of Chlamydiota and visualized in iTol (Figure 7). For a better overview, subtrees were generated showing the closest related sequences to the sequences derived from the sediment samples (Figure 8).

All sequences (except for the anoxic culture of sediment 6) were affiliated with chlamydial families or groups that are less described, contain a low number of cultured representatives or are just based on 16S rRNA gene or metagenomic data. The sequence of the anoxic culture of sediment 6 was classified as a member of the Simkaniaceae, a better-described family, closely related to *Simkania negevensis*. However, no sequence was assigned to the group of Anoxychlamydiaceae.

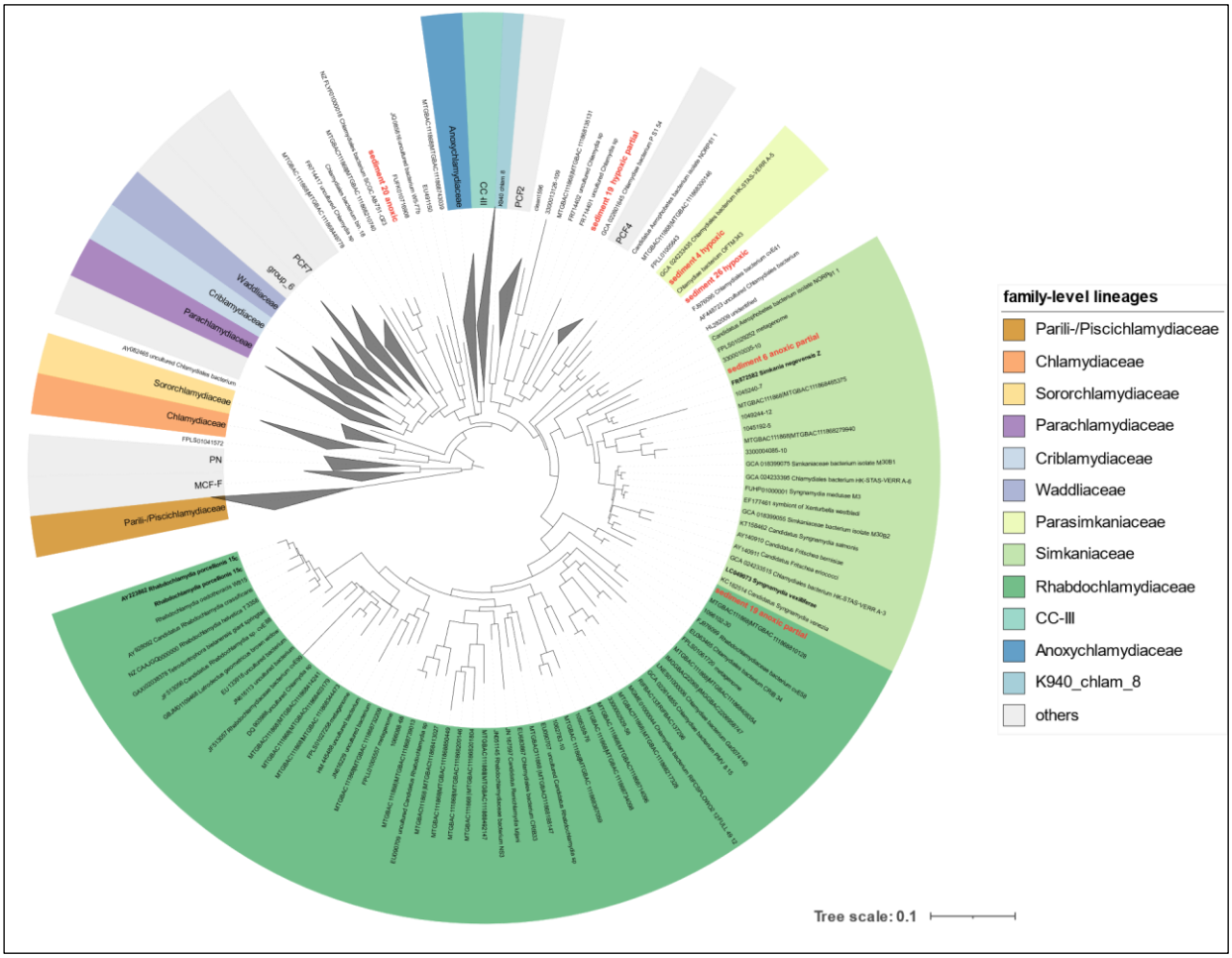

Figure 7: 16S rRNA gene-based phylogenetic tree of Chlamydiota including sequences obtained from sediment cultures. Chlamydial family-level lineages are labeled with different colors according to Dharamshi *et al.* 2023[51]. Branches of families that did not contain any novel sequences from sediment cultures (shown in red) are collapsed.

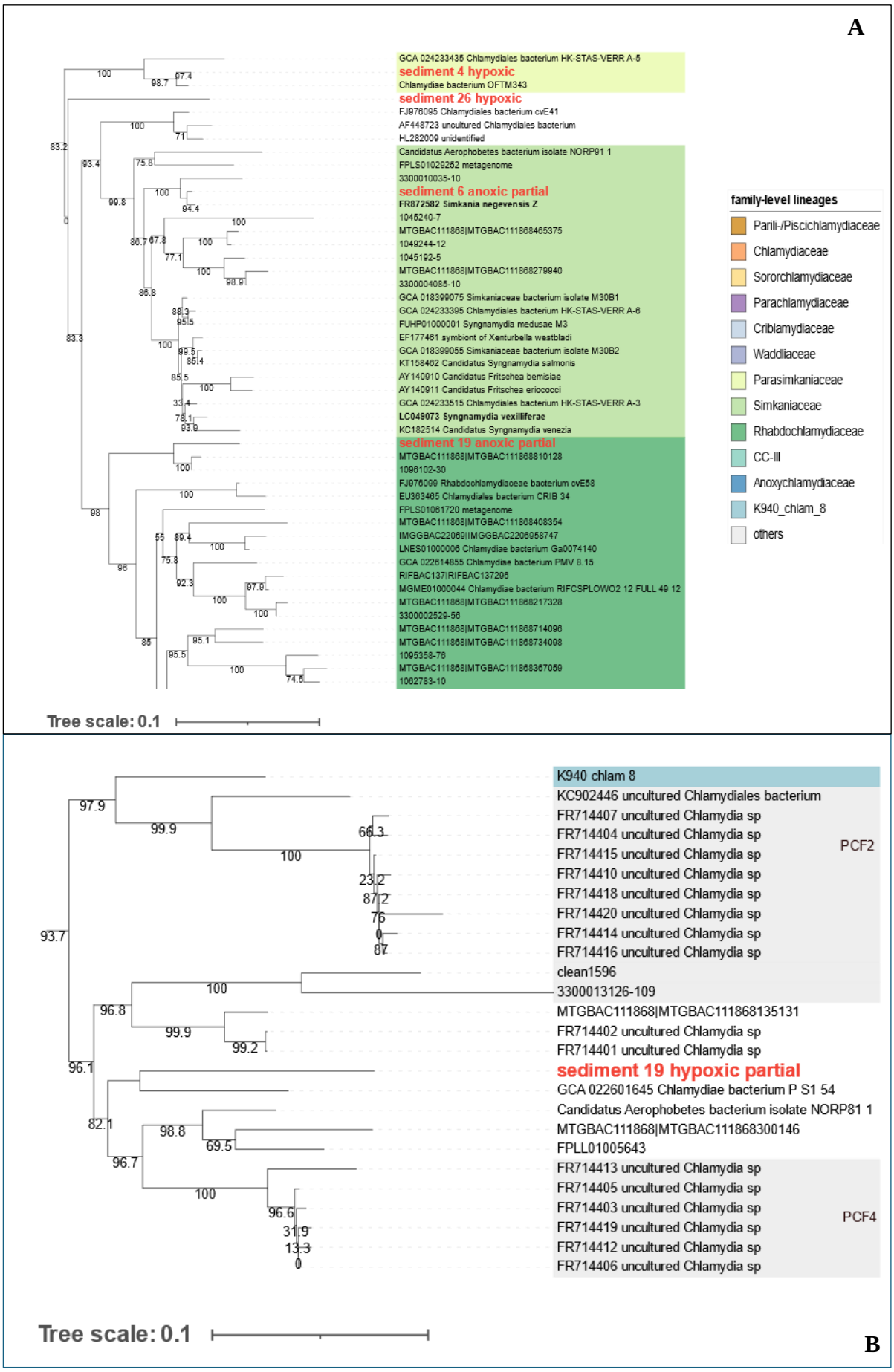
A
GCA 024233435 Chlamydiales bacterium HK-STAS-VERR A-5
sediment 4 hypoxic
Chlamydiae bacterium OFTM343
sediment 26 hypoxic
FJ976095 Chlamydiales bacterium cvE41
AF448723 uncultured Chlamydiales bacterium
HL282009 unidentified
Candidatus Aerophobetes bacterium isolate NORP91 1
FPLS01029252 metagenome
3300010035-10
sediment 6 anoxic partial
FR872582 Simkania negevensis Z
1045240-7
MTGBAC111868|MTGBAC111868465375
1049244-12
1045192-5
MTGBAC111868|MTGBAC111868279940
3300004085-10
GCA 018399075 Simkaniaceae bacterium isolate M30B1
GCA 024233395 Chlamydiales bacterium HK-STAS-VERR A-6
FUHP01000001 Syngnamydia medusae M3
EF177461 symbiont of Xenturbella westbladi
GCA 018399055 Simkaniaceae bacterium isolate M30B2
KT158462 Candidatus Syngnamydia salmonis
AY140910 Candidatus Fritschea bemisiae
AY140911 Candidatus Fritschea eriococci
GCA 024233515 Chlamydiales bacterium HK-STAS-VERR A-3
LC049073 Syngnamydia vexilliferae
KC182514 Candidatus Syngnamydia venezia
sediment 19 anoxic partial
MTGBAC111868|MTGBAC111868810128
1096102-30
FJ976099 Rhabdochlamydiaceae bacterium cvE58
EU363465 Chlamydiales bacterium CRIB 34
FPLS01061720 metagenome
MTGBAC111868|MTGBAC111868408354
IMGGBAC22069|IMGGBAC2206958747
LNES01000006 Chlamydiae bacterium Ga0074140
GCA 022614855 Chlamydiae bacterium PMV 8.15
RIFBAC137|RIFBAC137296
MGME01000044 Chlamydiae bacterium RIFCSPLOWO2 12 FULL 49 12
MTGBAC111868|MTGBAC111868217328
3300002529-56
MTGBAC111868|MTGBAC111868714096
MTGBAC111868|MTGBAC111868734098
1095358-76
MTGBAC111868|MTGBAC111868367059
1062783-10
family-level lineages
Parili-/Piscichlamydiaceae
Chlamydiaceae
Sororchlamydiaceae
Parachlamydiaceae
Criblamydiaceae
Waddliaceae
Parasimkaniaceae
Simkaniaceae
Rhabdochlamydiaceae
CC-III
Anoxychlamydiaceae
K940_chlam_8
others
Tree scale: 0.1
K940 chlam 8
KC902446 uncultured Chlamydiales bacterium
FR714407 uncultured Chlamydia sp
FR714404 uncultured Chlamydia sp
FR714415 uncultured Chlamydia sp
FR714410 uncultured Chlamydia sp
FR714418 uncultured Chlamydia sp
FR714420 uncultured Chlamydia sp
FR714414 uncultured Chlamydia sp
FR714416 uncultured Chlamydia sp
PCF2
clean1596
3300013126-109
MTGBAC111868|MTGBAC111868135131
FR714402 uncultured Chlamydia sp
FR714401 uncultured Chlamydia sp
sediment 19 hypoxic partial
GCA 022601645 Chlamydiae bacterium P S1 54
Candidatus Aerophobetes bacterium isolate NORP81 1
MTGBAC111868|MTGBAC111868300146
FPLL01005643
FR714413 uncultured Chlamydia sp
FR714405 uncultured Chlamydia sp
FR714403 uncultured Chlamydia sp
FR714419 uncultured Chlamydia sp
FR714412 uncultured Chlamydia sp
FR714406 uncultured Chlamydia sp
PCF4
Tree scale: 0.1
B

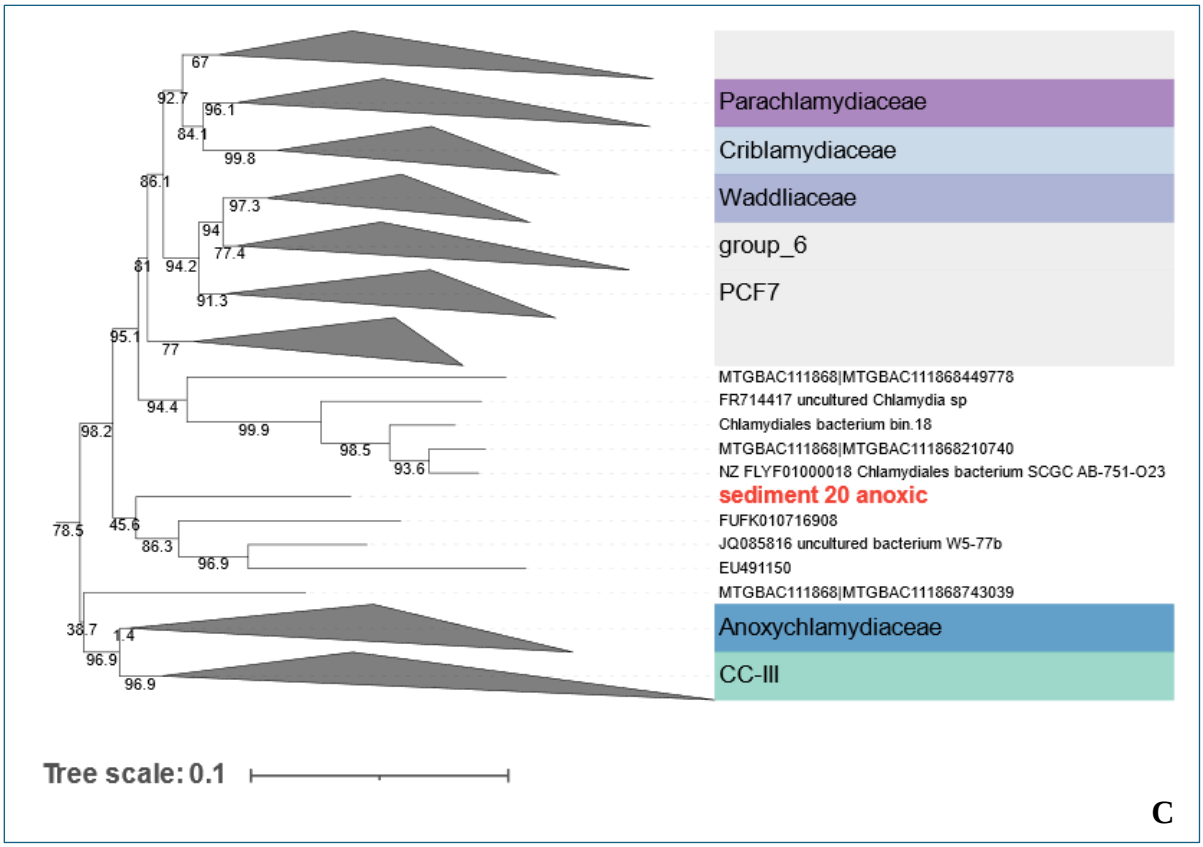

Figure 8: Subtrees of the 16S rRNA gene-based phylogenetic tree of Chlamydiota including sequences obtained from sediment cultures. Chlamydial family-level lineages are color-coded as in Fig 7. Sediment sequences are marked in red. Numbers on the branches indicate bootstrap values. **A** Subtree of the phylogenetic neighborhood of sequences from sediment 4 hypoxic, sediment 26 hypoxic, sediment 6 anoxic and sediment 19 anoxic cultures. **B** Subtree of the phylogenetic neighborhood of the sequence from sediment 19 hypoxic culture. **C** Subtree of the phylogenetic neighborhood of the sequence from sediment 20 anoxic culture.

3.1.4 Sediment cultures contain a variety of different eukaryotic organisms, including protist groups that did not harbor any known chlamydial symbionts

In addition to screening for novel chlamydiae in the cultures, potential hosts were also characterized via light microscopy and 18S rRNA gene Sanger sequencing of the cultures as well as 18S rRNA gene amplicon sequencing of the original sediment samples (Table 3).

For the 18S rRNA gene amplicon sequencing results, each sediment's read number before and after filtering (all ASVs with less than ten reads were filtered out, Figure 9) and alpha-diversity (Figure 10) were calculated and plotted. Besides that, the composition of eukaryotes in the sediments was visualized as relative abundance plots on the supergroup and genus levels (Figure 11).

In total, 171,718 reads were generated for all samples and filtering removed only 1% of the reads (Figure 9). Samples differ in the total read number, with the majority of the samples harboring more than 10,000 reads. Sediment sample 14, with roughly 200 reads, has the lowest count and can be considered an outlier (Figure 9).

When looking at different alpha-diversity measures like Shannon index or Chao1, sediment samples vary in diversity considerably. Highest diversity was found for sediment samples 32 (JMF-2304-01-0016A), 29 (JMF-2304-01-0014A) and 28 (JMF-2304-01-0013A) while samples 3 (JMF-2304-01-0001A) and 14 (JMF-2304-01-0005A) seem to be less diverse than the others (Figure 10). In the relative abundance plots of the eukaryotic composition, a high abundance of Stramenopiles could be observed in almost all sediments. A high number of ASVs in sediment 7 and 20 were assigned to Rhizaria and in the case of sediment 14 Archaeplastida. Sediment 26 contains an important proportion of Alveolata (Figure 11A). However, the majority of ASVs in all sediments could not be assigned to any known supergroup (Figure 11A) or genus (Figure 11B).

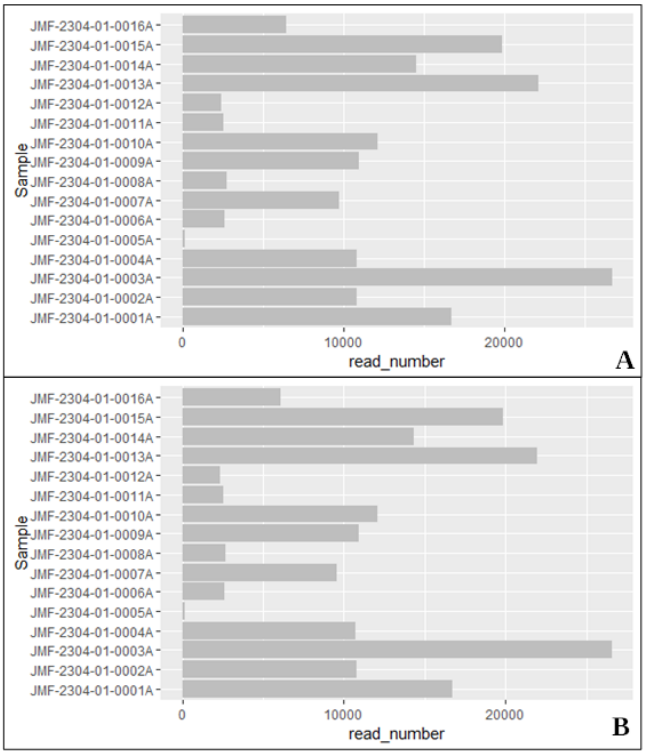

Figure 9: 18S rRNA gene amplicon sequencing read number of each sediment before (A) and after filtering (B). For filtering, all ASVs with < 10 reads were excluded. In total, from ~172,000 reads, 1,700 were filtered out.

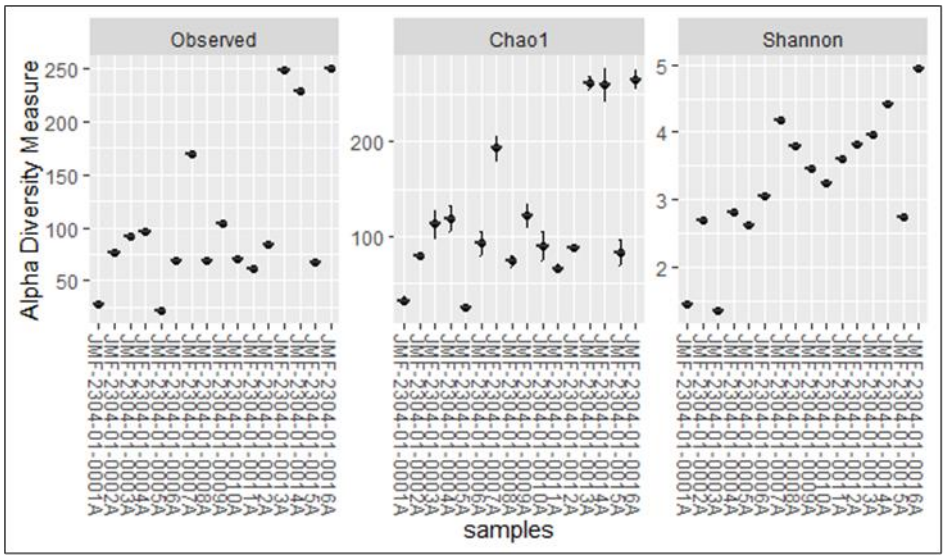

Figure 10: Alpha diversity plotted as observed diversity, Chao1 or Shannon index for each sediment sample.

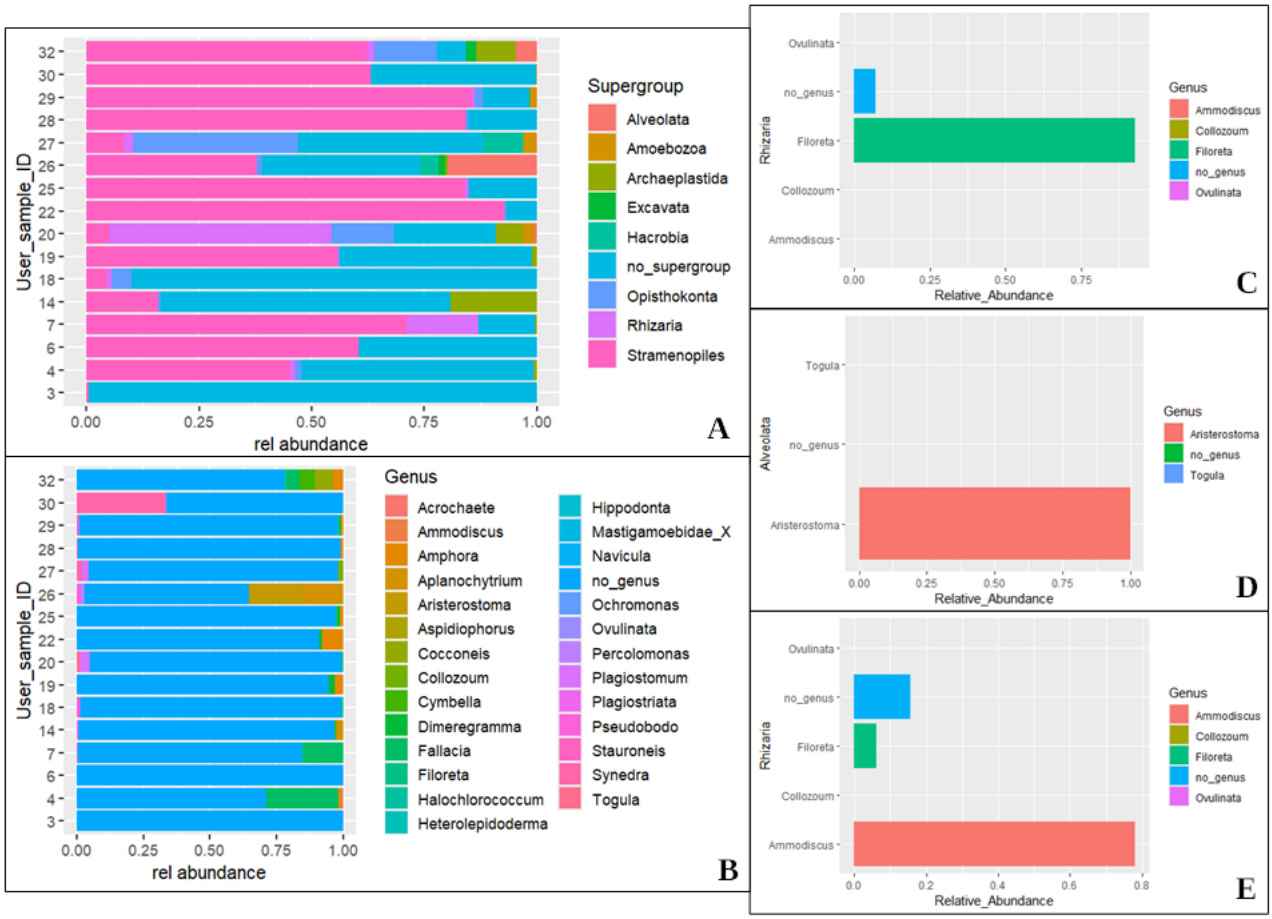

Figure 11: Relative abundance of eukaryotic 18S rRNA gene sequences in the marine sediment samples. Relative abundance sequences affiliated with eukarya on supergroup (A) or genus (B) level. Relative abundance of genera present in sediment 22 (C), 26 (D) and 19 (E) focusing on supergroups also detected in the respective cultures of each sediment.

When looking at the enrichment cultures, light microscopy confirmed the successful enrichment of eukaryotic organisms and revealed the presence of protists with different morphology, motility, color and size (Figure 12).

Additionally, 18S rRNA gene sequences could be obtained for some cultures via direct PCR followed by Sanger sequencing, indicating the successful enrichment of cultures containing single species. Results were taxonomically assigned via Blastn and calculated into an 18S rRNA gene-based phylogenetic tree for conformation of the Blast results (Figure 13). Sequences were classified into different groups (Table 18), for example, Stramenopiles (including Picophagea and diatoms), Alveolata (subgroup Ciliophora/Ciliates) and Rhizaria (subgroup Cercozoa), which are all important taxa of microbial eukaryotes where no or only a few chlamydial symbionts have been found or characterized yet. Similar results were seen in the phylogenetic analysis with the 18S rRNA-based tree. The 18S rRNA gene sequence acquired for sediment 22 anoxic culture was phylogenetically classified as *Filoreta* sp., a genus within the Rhizaria (Figure 13B). This genus was also one of the more abundant genera of Rhizaria in the amplicon sequencing of this sediment, thus, cultivation here selected for an organism that was already rather highly present in the sediment itself (Figure 11C). Similar observations were obtained for sediment 26, where the cultivated organism *Aristerostoma* sp. (Table 18, Figures 12 and 13A) was the only genus of Alveolata in the amplicon sequencing and thereby likely a quite highly abundant protist in this sediment (Figure 11D).

For other sediment cultures (like sediment 19 hypoxic culture, Figure 11E), the genus of the isolated organism (Table 18, Figures 12 and 13D) was not found in the abundance plots of the 18S amplicon data, likely because a large number of ASVs could not be assigned to a specific genus or even supergroup.

Furthermore, a combined 18S rRNA gene-based phylogenetic tree of both cultures´ and ASVs´ 18S rRNA gene sequences was calculated (not shown) and the read number of ASVs in the corresponding sediment sample falling close to culture sequences was determined to check the abundance of cultivated organisms in the sediment samples themselves. For three sediment cultures (hypoxic culture of sediment 19 and hypoxic as well as anoxic cultures of sediment 26), ASV sequences fell into the proximity of culture sequences belonging to the same sediment sample. In the case of sediment 19 hypoxic culture, one single ASV sequence (ASV_i9j_9uf) fell next to the corresponding culture sequences, showing a read number of only 1. For the anoxic and hypoxic cultures of sediment 26, in total 9 ASV sequences (ASV_igw_51l, ASV_6fv_wiu, ASV_5x8_mgp, ASV_ah5_1ys, ASV_5jq_sso, ASV_fvd_u9w,

ASV_t8x_mm5, ASV_mpx_m2m and ASV_5wp_0xs) were assigned close to the appropriate culture sequences, with read numbers between 37 and 93. To conclude, for sediment 19, a rather rare organism was cultivated, for sediment 26, a protist with a higher abundance, according to the ASV read number, was selected through cultivation.

All anoxic enrichment cultures as well as hypoxic enrichment cultures where chlamydiae were detected (4_hypoxic, 19_hypoxic and 26_hypoxic) could be maintained and are available for further characterization.

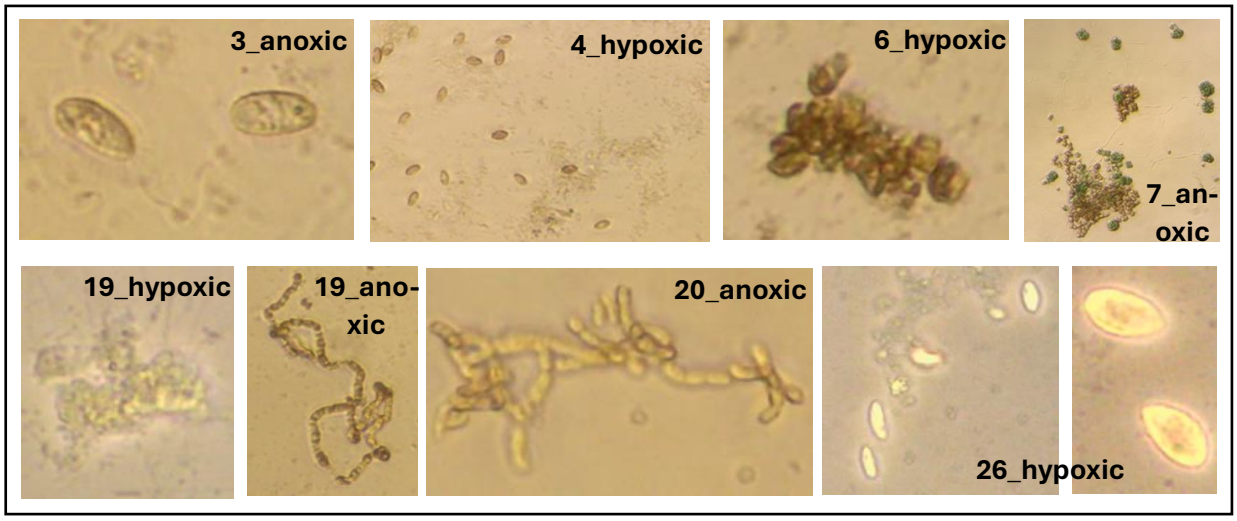

Figure 12: Light microscopy images of selected sediment cultures showing different eukaryotic organisms. For all cultures where 18S rRNA gene sequences could be obtained, the BLAST result of the closest relative is shown in Table 18.

Table 18: BLAST results of 18S rRNA gene sequences, morphological description of eukaryotes and phylogeny of chlamydial 16S rRNA gene sequences (+ sequence similarity to closest relative) in the sediment cultures.

Sediment culture ID	Morphology	BLAST result – 18S rRNA gene	Chlamydial 16S rRNA gene sequence identity
3_anoxic	Motile, large, ciliate-like organisms	*Reticulamoeba sp.* – Rhizaria/Cercozoa	-
4_hypoxic	Small, rod-shaped cells	-	Parasimkaniaceae (87.37% sequence similarity to *Simkania negevensis* Z strain)

4_anoxic	-	*Ciliophrys sp.* – Stramenopile	-
6_hypoxic	Aggregates of amorphous cells	*Picophagus flagellatus* – Stramenopiles	-
6_anoxic	-	-	Simkaniaceae (99.52% sequence similarity to *Simkania negevensis* Z strain)
7_anoxic	Green cells in aggregates, some with appendages	-	-
19_hypoxic	Amorphous cells (aggregates) with appendages	*Limnofila sp.* – Rhizaria/Cercozoa	Uncultured marine family (96% sequence similarity to Candidatus *Algichlamydia australiensis*
19_anoxic	Filamentous cells/Cells forming chains	*Nanofrustulum sp.* – Stramenopile/Diatoms	Rhabdochlamydiaceae (88.51% sequence similarity to Rhabdochlamydiaceae symbiont of *Dictyostelium giganteum* strain Digiganteum-PALH
20_anoxic	Filamentous cells/Chain-forming cells	-	Uncultured marine family (with flagellum-associated genes) (86.06% sequence similarity to *Neochlamydia* sp. Trut23-12-2015_Venoge-Embouchure)
22_anoxic	-	*Filoreta sp.* – Rhizaria/Cercozoa	-

26_hypoxic	Small and larger, motile, ciliate-like cells	*Aristerostoma sp.* – Alveolata/Ciliophora	Uncultured family (83.09% sequence similarity to *Simkania negevensis* Z strain)
26_anoxic	-	*Aristerostoma sp.* – Alveolata/Ciliophora	-
30_anoxic	-	*Halamphora sp.* – Stramenopile	-

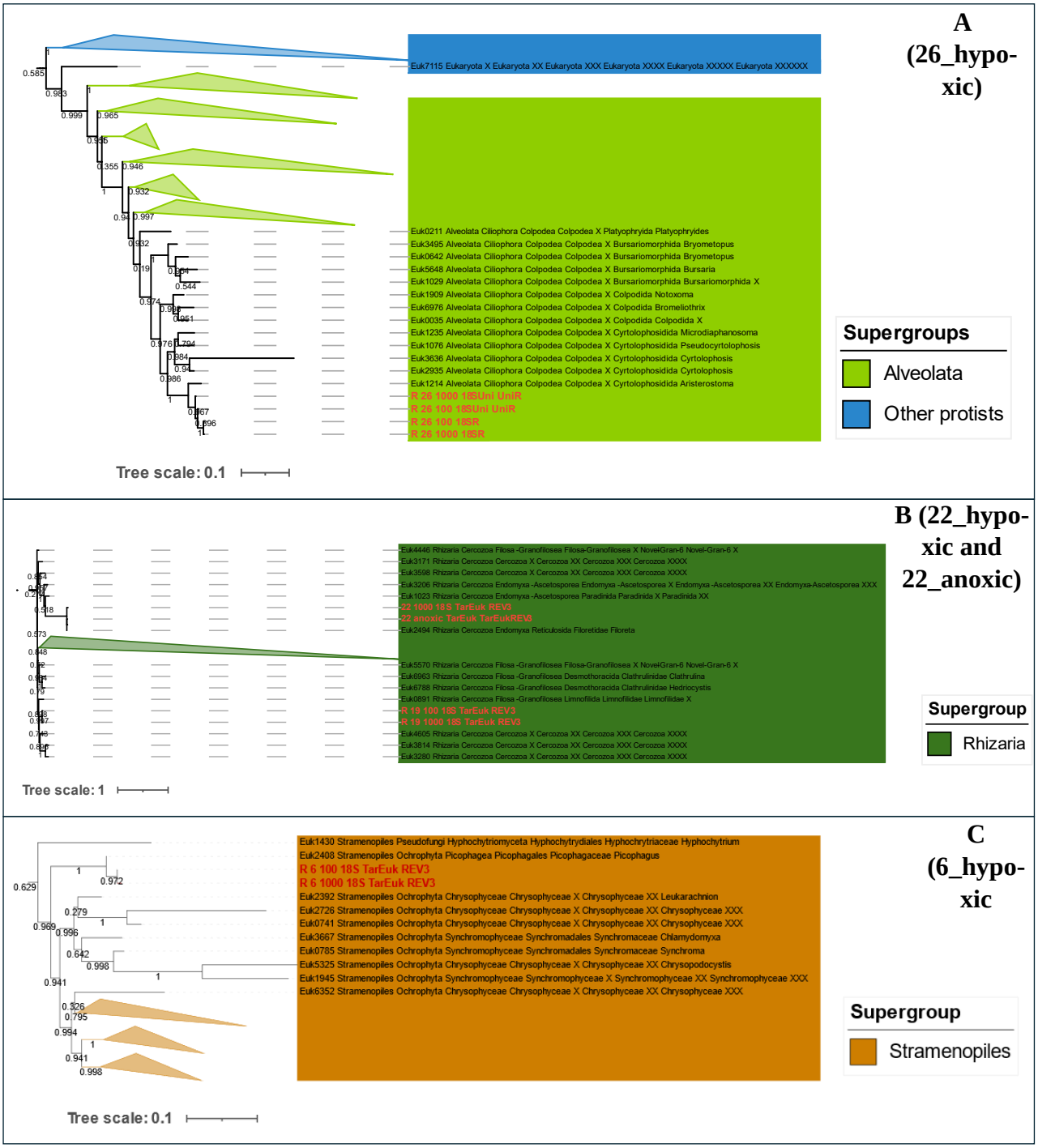
A (26_hypo-xic)
Euk7115 Eukaryota X Eukaryota XX Eukaryota XXX Eukaryota XXXX Eukaryota XXXXX Eukaryota XXXXXX
Euk0211 Alveolata Ciliophora Colpodea Colpodea X Platyophryida Platyophryides
Euk3495 Alveolata Ciliophora Colpodea Colpodea X Bursariomorphida Bryometopus
Euk0642 Alveolata Ciliophora Colpodea Colpodea X Bursariomorphida Bryometopus
Euk5648 Alveolata Ciliophora Colpodea Colpodea X Bursariomorphida Bursaria
Euk1029 Alveolata Ciliophora Colpodea Colpodea X Bursariomorphida Bursariomorphida X
Euk1909 Alveolata Ciliophora Colpodea Colpodea X Colpodida Notoxoma
Euk6976 Alveolata Ciliophora Colpodea Colpodea X Colpodida Bromeliothrix
Euk0035 Alveolata Ciliophora Colpodea Colpodea X Colpodida Colpodida X
Euk1235 Alveolata Ciliophora Colpodea Colpodea X Cyrtolophosidida Microdiaphanosoma
Euk1076 Alveolata Ciliophora Colpodea Colpodea X Cyrtolophosidida Pseudocyrtolophosis
Euk3636 Alveolata Ciliophora Colpodea Colpodea X Cyrtolophosidida Cyrtolophosis
Euk2935 Alveolata Ciliophora Colpodea Colpodea X Cyrtolophosidida Cyrtolophosis
Euk1214 Alveolata Ciliophora Colpodea Colpodea X Cyrtolophosidida Aristerostoma
R 26 1000 18SUni UniR
R 26 100 18SUni UniR
R 26 100 18SR
R 26 1000 18SR
Supergroups
Alveolata
Other protists
Tree scale: 0.1
B (22_hypo-xic and 22_anoxic)
Euk4446 Rhizaria Cercozoa Filosa -Granofilosea Filosa-Granofilosea X NoveiGran-6 Novel-Gran-6 X
Euk3171 Rhizaria Cercozoa Cercozoa X Cercozoa XX Cercozoa XXX Cercozoa XXXX
Euk3598 Rhizaria Cercozoa Cercozoa X Cercozoa XX Cercozoa XXX Cercozoa XXXX
Euk3206 Rhizaria Cercozoa Endomyxa -Ascetosporea Endomyxa -Ascetosporea X Endomyxa -Ascetosporea XX Endomyxa-Ascetosporea XXX
Euk1023 Rhizaria Cercozoa Endomyxa -Ascetosporea Paradinida Paradinida X Paradinida XX
22 1000 18S TarEuk REV3
22 anoxic TarEuk TarEukREV3
Euk2494 Rhizaria Cercozoa Endomyxa Reticulosida Filoretidae Filoreta
Euk5570 Rhizaria Cercozoa Filosa -Granofilosea Filosa-Granofilosea X NoveiGran-6 Novel-Gran-6 X
Euk6963 Rhizaria Cercozoa Filosa -Granofilosea Desmothoracida Clathrulinidae Clathrulina
Euk6788 Rhizaria Cercozoa Filosa -Granofilosea Desmothoracida Clathrulinidae Hedriocystis
Euk0891 Rhizaria Cercozoa Filosa -Granofilosea Limnofiida Limnofiilidae Limnofiilidae X
R 19 100 18S TarEuk REV3
R 19 1000 18S TarEuk REV3
Euk4605 Rhizaria Cercozoa Cercozoa X Cercozoa XX Cercozoa XXX Cercozoa XXXX
Euk3814 Rhizaria Cercozoa Cercozoa X Cercozoa XX Cercozoa XXX Cercozoa XXXX
Euk3280 Rhizaria Cercozoa Cercozoa X Cercozoa XX Cercozoa XXX Cercozoa XXXX
Supergroup
Rhizaria
Tree scale: 1
C (6_hypo-xic
Euk1430 Stramenopiles Pseudofungi Hyphochytriomyceta Hyphochytrydiales Hyphochytriaceae Hyphochytrium
Euk2408 Stramenopiles Ochrophyta Picophagea Picophagales Picophagaceae Picophagus
R 6 100 18S TarEuk REV3
R 6 1000 18S TarEuk REV3
Euk2392 Stramenopiles Ochrophyta Chrysophyceae Chrysophyceae X Chrysophyceae XX Leukarachnion
Euk2726 Stramenopiles Ochrophyta Chrysophyceae Chrysophyceae X Chrysophyceae XX Chrysophyceae XXX
Euk0741 Stramenopiles Ochrophyta Chrysophyceae Chrysophyceae X Chrysophyceae XX Chrysophyceae XXX
Euk3667 Stramenopiles Ochrophyta Synchromophyceae Synchromadales Synchromaceae Chlamydomyxa
Euk0785 Stramenopiles Ochrophyta Synchromophyceae Synchromadales Synchromaceae Synchroma
Euk5325 Stramenopiles Ochrophyta Chrysophyceae Chrysophyceae X Chrysophyceae XX Chrysopodocystis
Euk1945 Stramenopiles Ochrophyta Synchromophyceae Synchromophyceae X Synchromophyceae XX Synchromophyceae XXX
Euk6352 Stramenopiles Ochrophyta Chrysophyceae Chrysophyceae X Chrysophyceae XX Chrysophyceae XXX
Supergroup
Stramenopiles
Tree scale: 0.1

Figure 13: Selected subtrees of the 18S rRNA gene-based phylogenetic tree containing sequences of the sediment cultures. For better visualization, the closest phylogenetic taxa of each sediment sequence were pruned from the whole 18S rRNA gene-based phylogenetic tree. Triangles resemble collapsed clades, numbers on the branches represent bootstrap values. (A) Subtree containing 18S rRNA gene sequences of the sediment 26 hypoxic culture. (B) Subtree containing 18S rRNA gene sequences of the sediment 19 hypoxic culture and sediment 22 cultures. (C) Subtree containing 18S rRNA gene sequences of the sediment 6 hypoxic culture. (D) Subtree containing 18S rRNA gene sequences of the sediment 19 anoxic culture.

3.2. Influence of oxygen on the symbiosis between Ac. Neff and two different chlamydial symbionts

3.2.1 Growth of Ac. Neff differs significantly depending on host infection status and oxygen concentrations

The growth of uninfected and chlamydiae-infected (UV7 or *Simkania*) Ac. Neff was monitored over one week and compared under different oxygen regimes (oxic, hypoxic and anoxic). Starting with $5x10^4$ amoeba cells/ml in every well, amoebae were harvested and counted at the LUNA-Fx7 cell counter at each time point. The determined cell numbers were used to calculate growth curves in RStudio and visualized with ggplot2 (Figures 14, 15 and 16). Statistics (ANOVA and Post-hoc Tukey test) were performed on these data to check for significant differences in the growth of the amoebae cultures depending on O_2 level and associated symbiont. Significant p-values were plotted into the growth curves as asterisks and significance brackets (Figures 14, 15 and 16).

In general, better growth of the host was observed under high oxygen concentrations compared to hypoxic conditions (Figures 14 and 15), with significantly higher cell numbers for *Simkania*-(after four days) and uninfected hosts (after four days).

When comparing uninfected and infected hosts under oxic conditions, a significantly higher growth was observed after two days for uninfected Ac. Neff compared to UV7-infected hosts (Figure 15), which was not the case for *Simkania* (Figure 14). Under anoxic incubation, both uninfected and *S. neg*-infected hosts reached higher cell numbers compared to UV7-infected acanthamoebae, with significant differences in the growth between *Simkania*- and UV7-infected Ac.Neff (Figure 16).

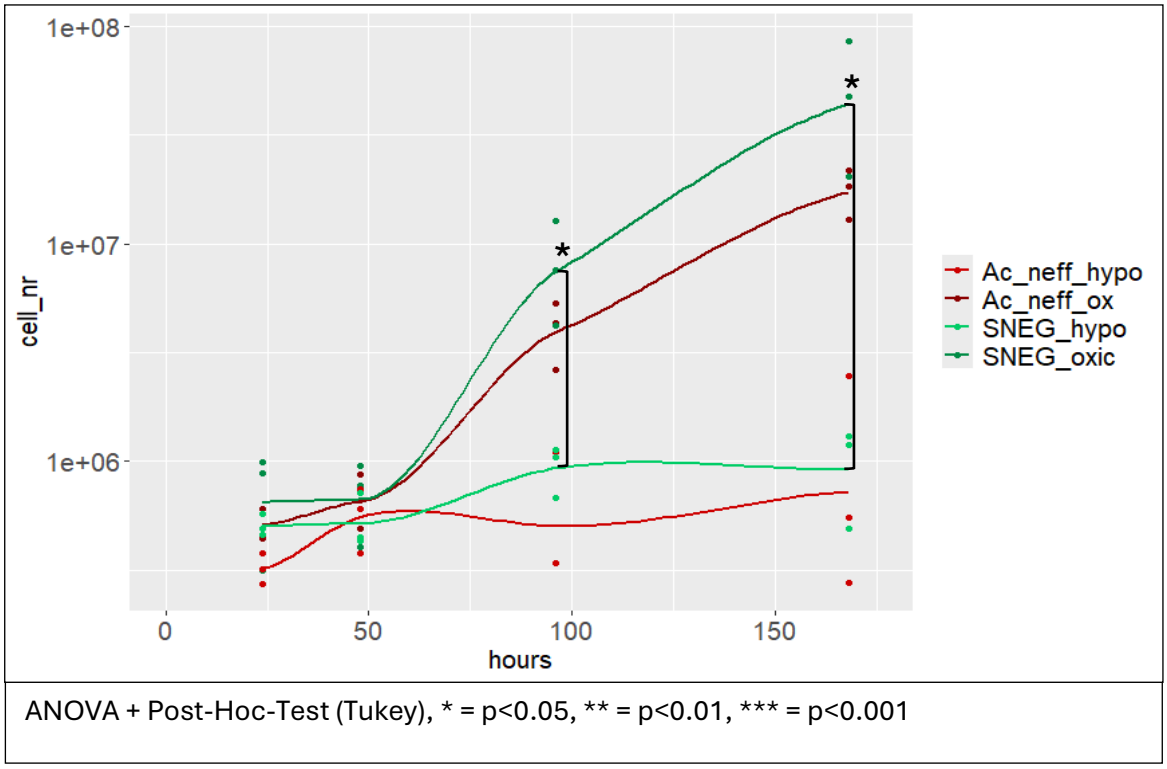

Figure 14: Oxic and hypoxic growth of *Simkania*-infected and uninfected Ac. Neff cultures. For calculating the growth curves, the mean cell numbers of the replicates were applied, while each dot represented an individual measurement in the experiment. Asterisks symbolize significant p-values (see legend) and the significance brackets the measurements where significant differences were observed.

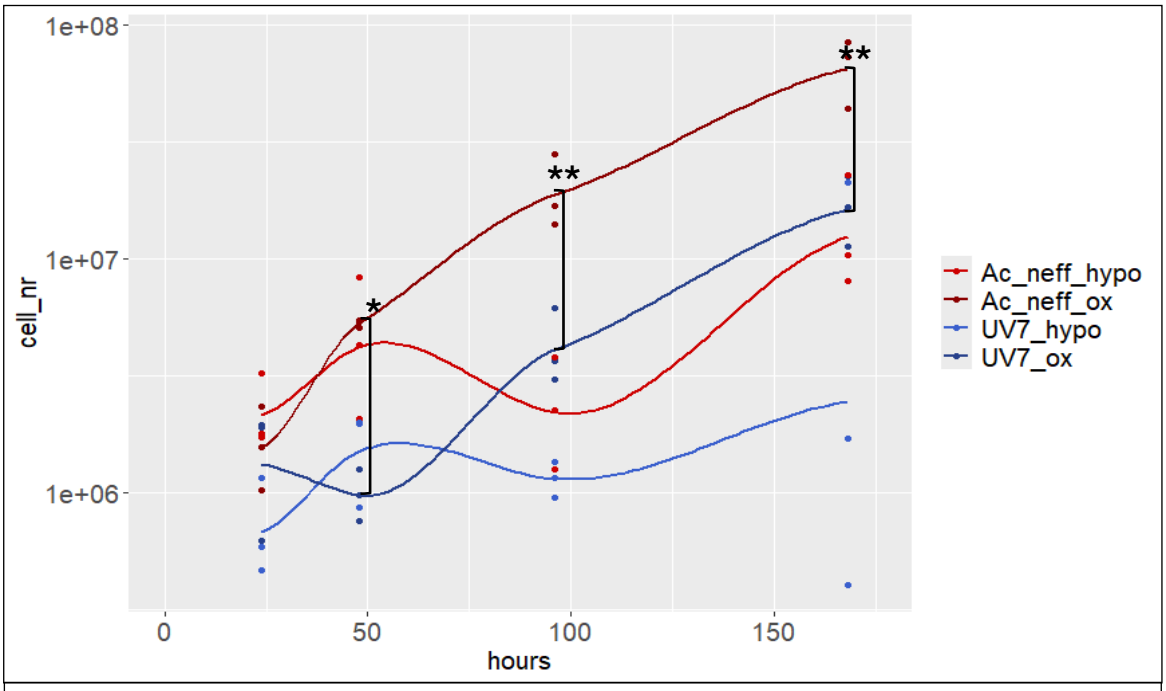

Figure 15: Oxic and hypoxic growth of UV7-infected and uninfected Ac. Neff cultures. For calculating the growth curves, the mean cell numbers of the replicates were applied, while each dot represented an individual measurement in the experiment. Asterisks symbolize significant p-values (see legend) and the significance brackets the measurements where significant differences were observed.

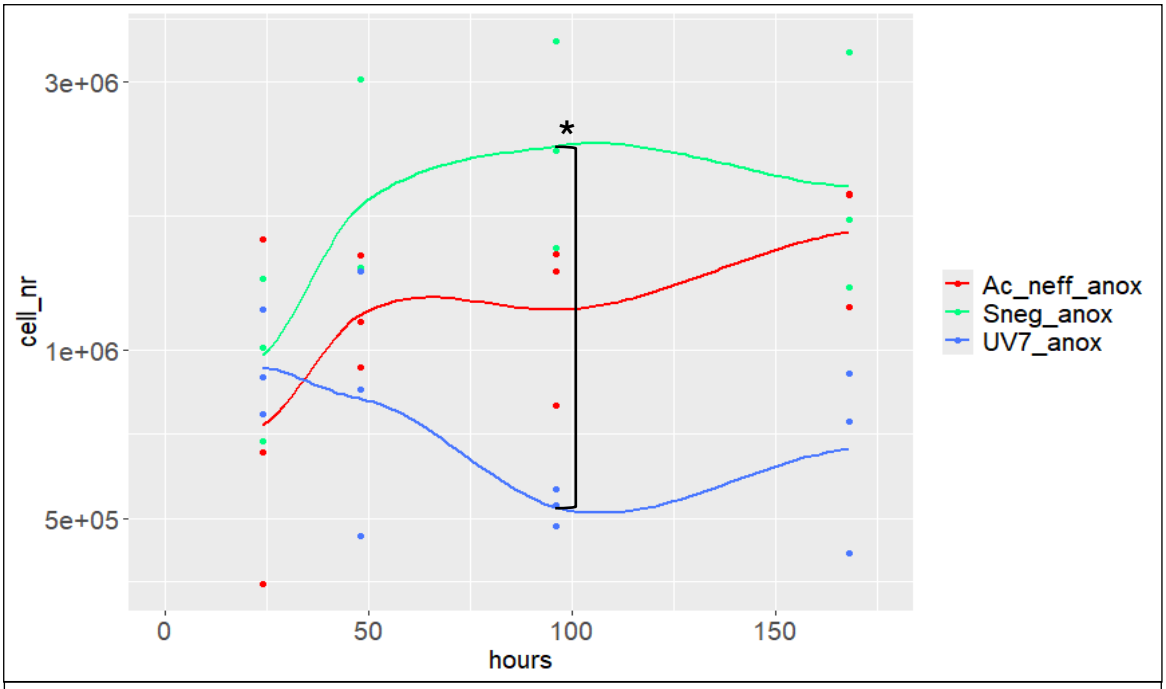

Figure 16: Anoxic growth of infected (UV7 or *Simkania*) and uninfected Ac. Neff cultures. For calculating the growth curves, the mean cell numbers of the replicates were applied, while each dot represented an individual measurement in the experiment. Asterisks symbolize significant p-values (see legend) and the significance brackets the measurements where significant differences were observed.

3.2.2 GC measurements provide first insights into respiratory activity in (un-)infected Ac. Neff cultures

The respiration in the form of produced CO_2 was measured with GC in infected (*Simkania* or UV7) and uninfected Ac. Neff cultures and compared under oxic and hypoxic incubations. For that, amoebae cultures were infected with chlamydiae (or left uninfected) in sterile culture flasks and incubated under an oxic or hypoxic atmosphere. Additionally, flasks with just TSY medium were used as controls. Every 24h, headspace was sampled and CO_2 production was assessed with gas chromatography. Results were visualized as bar charts and the statistical significance (ANOVA and Post-hoc Tukey test) was calculated and plotted as asterisks and significance brackets into the diagram (Figure 17).

Biotic gas production. All strains exhibited an increase in CO_2 after 24 hours of incubation, with CO_2 concentrations significantly higher under oxic conditions as compared to hypoxic conditions after 24 hours ($p<0.05$) (Figure 17A).

The CO_2 ranged between 2550 to 8014 ppmv under oxic conditions and 353 to 587 ppmv under hypoxic conditions after 24 hours of incubation. Similar CO_2 concentrations were observed amongst uninfected (Ac. Neff) and infected (UV7 or *Simkania*) host cultures in hypoxic atmospheres after 24 hours, yet under oxic conditions, *Simkania*-infected hosts produced significantly more CO_2 than uninfected ($p<0.001$) and UV7-infected hosts ($p<0.001$) (Figure 17A). The experiment was ended after 24 hours of incubation due to contamination of the cultures.

Abiotic gas production. Approximately 30-fold higher CO_2 concentrations were detected in the oxic atmosphere than in the hypoxic atmosphere at the start of the experiment (t=0h), suggesting an abiotic production of CO_2 from the medium. Therefore, medium controls were prepared and tested for CO_2 production after 48h and 72h of incubation. Here, a high amount of CO_2 was measured in the headspace (values between 758 and 1172 ppmv for oxic and 1238 and 1848 ppmv for hypoxic conditions after 48h of incubation), illustrating this outgassing of the medium produced abiotic CO_2 (Figure 17B).

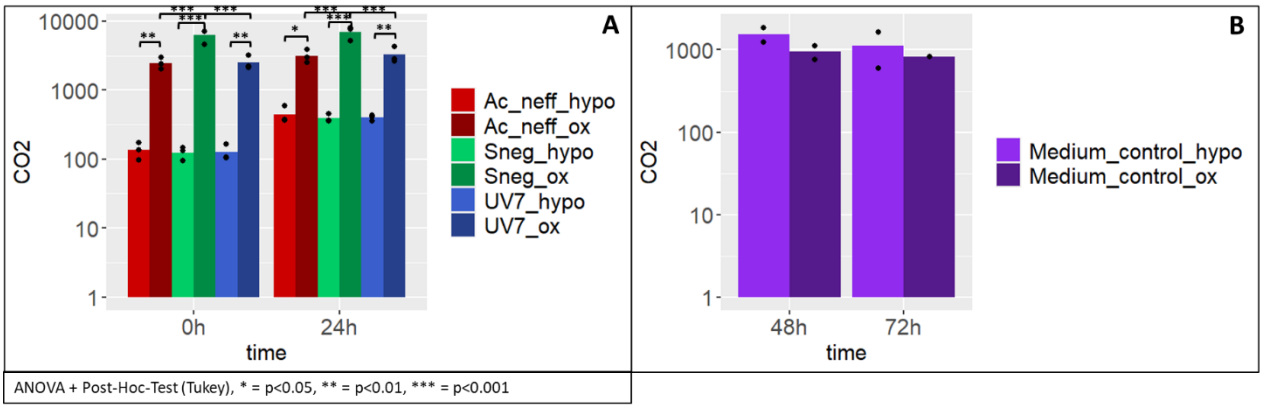

Figure 17: CO_2 concentration (in ppmv) in the headspace of amoebae cultures (A) and medium controls (B) over time. The colored bars indicate the mean value of produced CO_2 as parts per million (ppmv) while each point represents an individual measurement of the triplicates. Black asterisks symbolize significant p-values (see legend) and the significance brackets the measurements where significant differences were observed. (A) CO_2 production by infected (*Simkania* or UV7) and uninfected Ac. Neff cultures under oxic and hypoxic incubations. (B) CO_2 measurements of TSY medium controls after 48 and 72 hours.

3.2.3 Infectivity of chlamydiae differs between various oxygen conditions

The infectivity of *Simkania* and UV7 in Ac. Neff was compared under oxic, hypoxic and anoxic conditions using FISH.

For that, Ac. Neff cultures were infected as technical triplicates with either *Simkania* or UV7 in different MOIs (10, 30, 50, 100) and incubated under different O_2 regimes (oxic, hypoxic and anoxic). After two days, cells were harvested, fixed in PFA and visualized with FISH using symbiont-specific probes.

By classifying amoeba cells (n=50 per sample) under the epifluorescence microscope into non- (no symbiont-associated FISH signals), low- (< 30 symbiont-associated FISH signals) and high-infected (> 30 symbiont-associated FISH signals), the infectivity of the two symbionts under various O_2 conditions was determined (Figure 18).

For comparison, the mean value was calculated for each sample type and absolute numbers were converted into the proportions of infected cells. As expected, the proportion of infected cells correlated positively with a higher MOI, in general. While there are slight differences between the two symbionts (higher infection rate of UV7 than *Simkania* under hypoxia and the opposite for anoxic conditions) and the oxygen regimes (decreasing infectivity of UV7 under declining O_2 concentrations), the infection proportions were highly similar for all O_2 conditions and both symbionts when a MOI of 10 or 30 was used (Figure 18). As a consequence, a MOI of 20 was used in the following infection experiments.

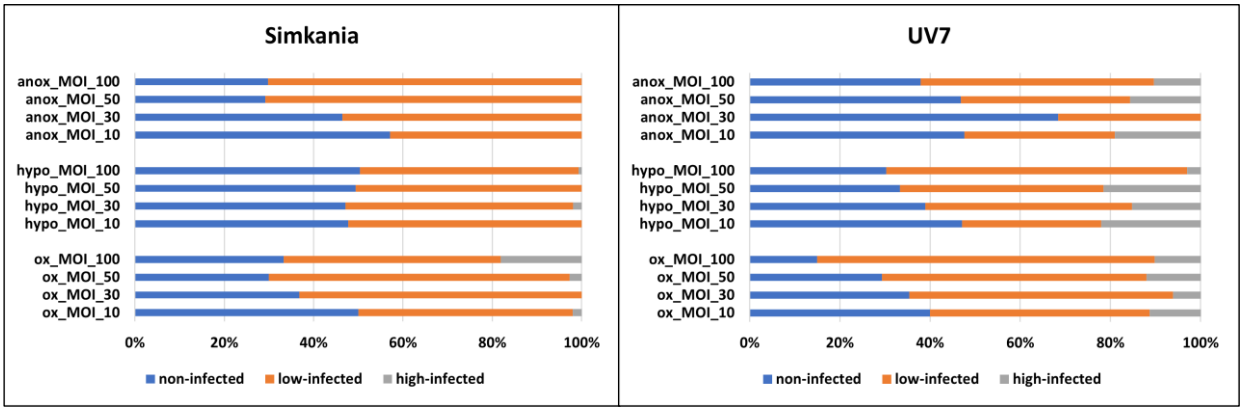

Figure 18: Proportion of infected Ac. Neff cells under different O_2 conditions. Infection with *Simkania* (left) and UV7 (right). For each sample type, mean values were calculated from triplicate assays. From top to bottom, proportions are sorted by decreasing O_2 concentration and MOI. Non-infected = 0 symbiont-related FISH signals, low-infected = 1-30 symbiont-related FISH signals and high-infected = more than 30 symbiont-related FISH signals per cell.

3.2.4 Low infection rate of *Simkania* restricted appropriate comparisons of chlamydiae replication under different oxygen regimes

The success of two chlamydial symbionts, UV7 and *Simkania*, in infecting and replicating in acanthamoebae in direct competition with each other was tested. For this purpose, single- (as control) and co-infected *Acanthamoeba* hosts were compared under oxic and anoxic conditions with dPCR and FISH with symbiont-specific probes. Additionally, host growth was assessed with the LUNA-Fx7 cell counter and calculation of growth curves in RStudio.

As already observed in growth experiments earlier (3.2.1), amoebae growth was higher under oxic than anoxic conditions, significantly after 24h and later in the incubation, however, the cell concentrations were considerably lower for all samples than in previous experiments. A significantly better growth could also be observed for oxic-grown, *Simkania*-infected hosts compared to both other oxic cultures at 96h and one week after the start of the experiment (Figure 19). This is probably due to the low infection load of *Simkania* observed in the chlamydial quantification via dPCR (Figure 20).

Looking at the success of the two different chlamydial symbionts in infecting and replicating in *Acanthamoeba* hosts, (significant) differences between UV7 and *Simkania* could be detected, with UV7 growing faster than *Simkania* under both oxic and anoxic conditions and in single- and co-infected hosts at almost every time point. Over the whole incubation time, UV7 showed a significantly higher replication under oxic than anoxic conditions, while *Simkania* tended to replicate better under anoxia, in the presence and absence of the other species. When comparing the replication of the symbionts in single- and co-infected hosts, no differences could be observed for UV7, however, *Simkania* was more replicative when UV7 was present. As large differences between *Simkania* and UV7 were already visible after 24 hours, the infection load of *Simkania* was low from the beginning and thus interpretations have to be done carefully (Figure 20). The experiment was repeated twice and the results were always the same with *Simkania* already falling behind UV7 in numbers in the co-infected host soon after the infection.

For the visualization of the symbionts in the co-infected cells, fixed cells were hybridized with the species-specific probes Sim-neg-183-Cy3 (for *Simkania*) and UV7-763-new-Fluos (for UV7) and images were taken using the Thunder microscope. For the majority of cells, FISH signals for UV7 were observed (Figure 21). *Simkania*-specific FISH signals were found rarely and if at all, only in combination with UV7-specific signals within the same amoeba cell (Figure 21A). No cell was solely infected with *Simkania*, which fits well with the results of dPCR and indicates a lower infectivity of *Simkania* EBs right from the beginning.

For representation, only three time points were depicted (Figure 21A: Anox_24h, Figure 21B: Anox_48h, Figure 21C: Anox_96h), as no real differences could be observed between the two oxygen levels or the individual time points.

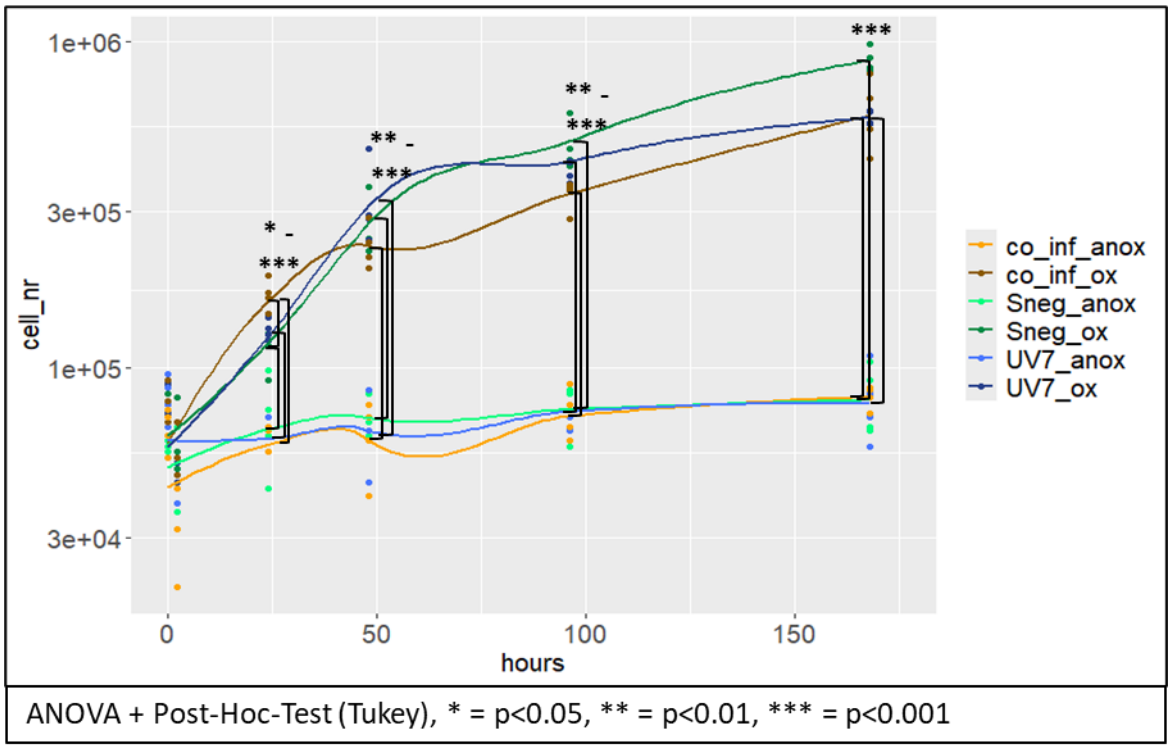

Figure 19: Growth of single- and double-infected (*Simkania* and UV7) Ac. Neff under oxic and anoxic conditions. For calculating the growth curves, the mean cell numbers of the replicates were used, while each dot represented an individual measurement in the experiment. Asterisks symbolize significant p-values (see legend) and the significance brackets the measurements where significant differences were observed.

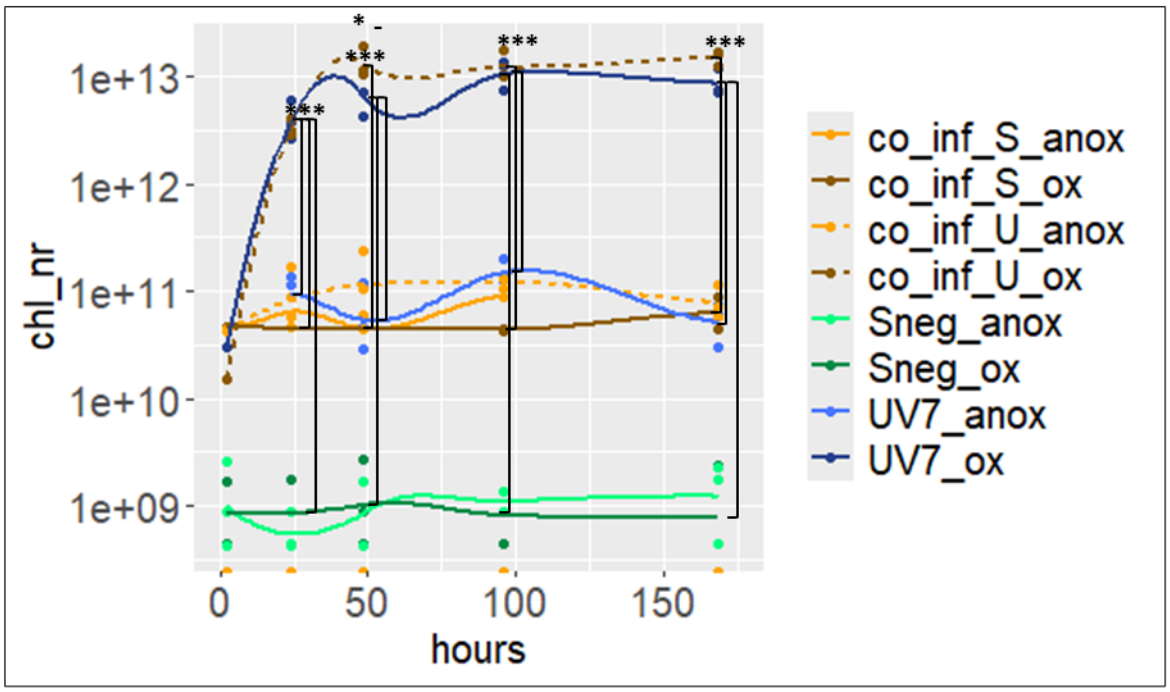

Figure 20: Replication of UV7 and *Simkania* in single- and co-infected *Acanthamoeba* hosts. Chlamydial cell numbers were normalized by the total number of amoebae hosts for each sample (Figure 19). For calculating the growth curves, the mean chlamydial cell numbers of the replicates were used, while each dot represented an individual measurement in the experiment. Asterisks symbolize significant p-values (see legend) and the significance brackets the measurements where significant differences were observed.

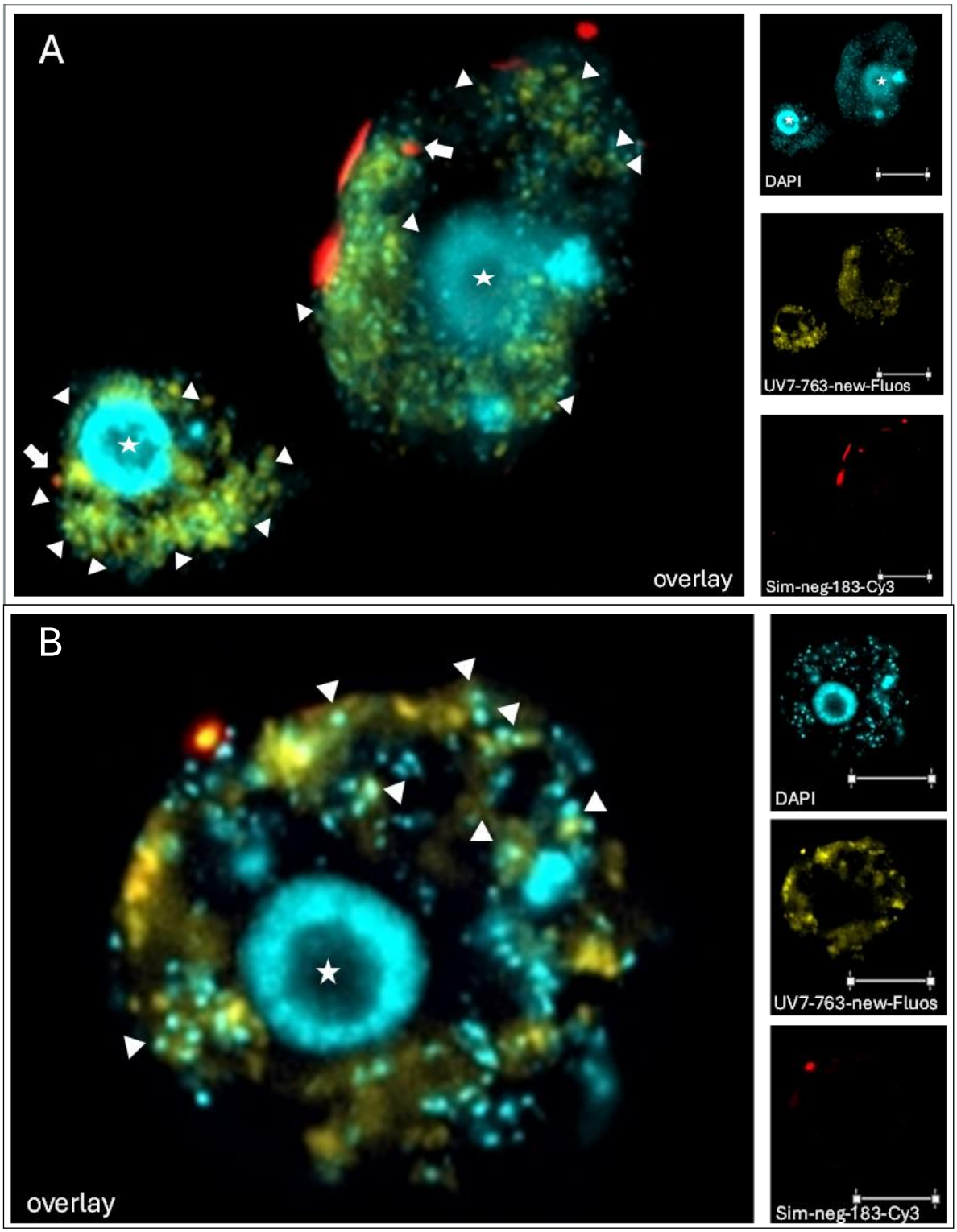
A
overlay
DAPI
UV7-763-new-Fluos
Sim-neg-183-Cy3
B
overlay
DAPI
UV7-763-new-Fluos
Sim-neg-183-Cy3

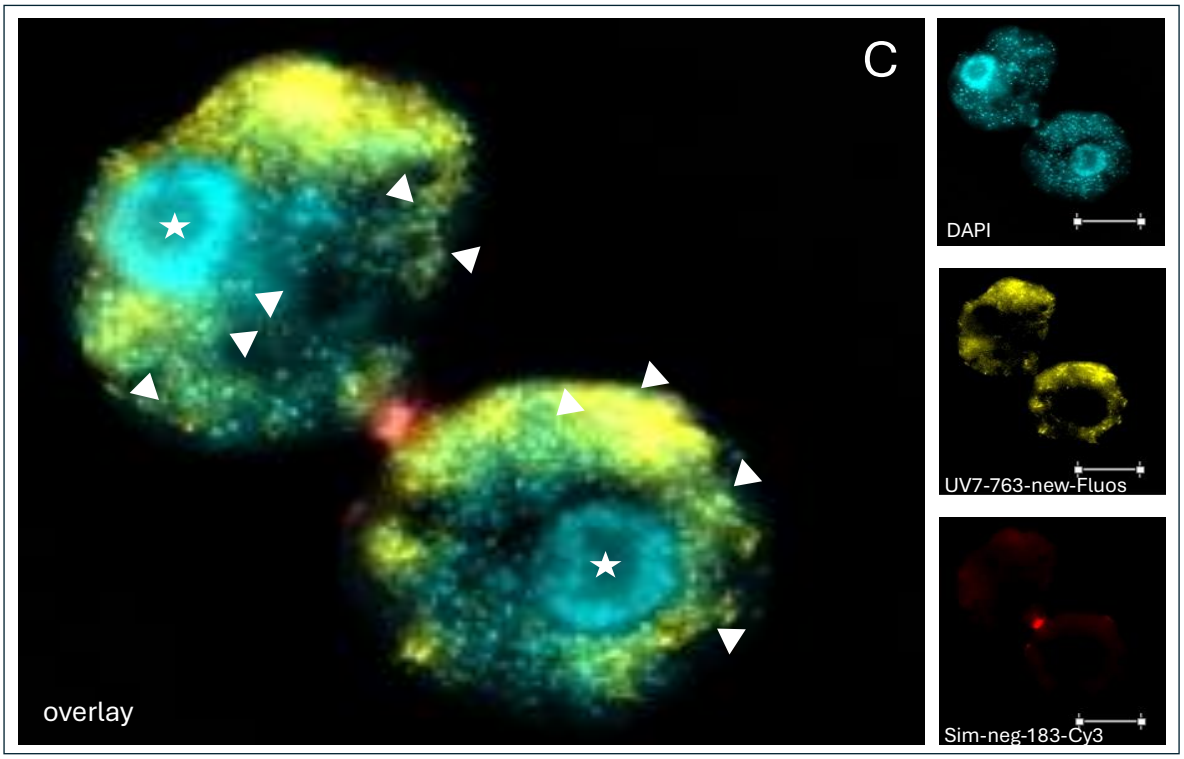

Figure 21: FISH images of co-infected amoeba cells. For hybridization, the *Simkania*-specific probe Sim-neg-183-Cy3 (in red) and UV7-specif probe UV7-763-new-Fluos (in yellow) were used. Additionally, cells were stained with DAPI (in cyan). The scale bar represents a length of 10 µm. Stars indicate the cell nucleus, triangles point toward UV7-specific FISH signals (overlay of yellow and cyan signals) and arrows toward *Simkania*-specific FISH signals (overlay of cyan and red signals). (A) FISH image of anoxic incubated, co-infected cells after 24h. (B) FISH image of an anoxic incubated, co-infected cell at timepoint 48h. (C) FISH image of anoxic incubated, co-infected cells at timepoint 96h.

4 DISCUSSION AND OUTLOOK

4.1 Marine sediments as an interesting source for cultivating novel chlamydiae

Members of the phylum Chlamydiota have been detected in various environments from soil, freshwater and marine habitats, different (in-)vertebrates and man-made systems like cooling towers and showers[44,85]. Only recently, chlamydiae were also detected in several anoxic marine sediments showing a significant abundance and high diversity. This also includes MAGs that were described as members of a novel family called Anoxychlamydiaceae, the first potentially obligate anaerobic organisms inside the Chlamydiota. Like for many other chlamydial lineages, no representative could be cultivated and thereby described more precisely[41,44,51]. This study aimed to obtain chlamydial isolates of poorly- and undescribed lineages focusing on the novel family of Anoxychlamydiaceae from 32 anoxic marine sediments from different locations worldwide.

In half of the selected sediments, chlamydiae could be detected by target-specific PCR.

Beyond, 16S rRNA gene amplicon sequencing of the original sediment samples revealed the presence of a large diversity of chlamydial families, including Simkaniaceae, Parasimkaniaceae, CC-III and most interestingly Anoxychlamydiaceae in relevant abundance, in lower abundance Rhabdochlamydiaceae and Parachlamydiaceae, demonstrating the high potential of these samples to isolate novel chlamydiae, also from lineages that lack cultivated representatives (Figure 4). The dominance of ASVs not assigned to any known chlamydial lineages suggests a remarkable and largely unexplored diversity of chlamydiae, particularly in marine sediments (Figure 5). The cultivation of these organisms would give better insights into the biology and ecology of chlamydial families that currently are based just on metagenomic data or contain only a few described species. In the case of Anoxychlamydiaceae, cultivated representatives would allow the study of their metabolism which was hypothesized to be exclusively anaerobic in recent studies[41,51]. Furthermore, it would enable a closer investigation of the evolution of oxygen tolerance and metabolism in the phylum Chlamydiota, which was in parts resolved by Dharamshi *et al.* lately[51].

To select for chlamydiae with a potential anaerobic metabolism and to focus on samples with the highest chlamydial prevalence, protist enrichment cultures were set up under hypoxic and anoxic conditions only for those twelve sediments that had the highest number of chlamydiae (Figure 6). For three hypoxic and anoxic cultures, chlamydial 16S rRNA gene sequences were obtained via PCR and Sanger sequencing, suggesting a successful enrichment of chlamydiae in the cultures simultaneously with decreased species diversity. The calculation of these sequences into a 16S rRNA gene-based phylogenetic tree of chlamydiae demonstrated the presence of mostly chlamydiae from families with none or a low number of described species, including Simkaniaceae, Rhabdochlamydiaceae, Parasimkaniaceae and unresolved lineages, however, it was not possible to isolate any members of the Anoxychlamydiaceae (Figures 7 and 8). As anoxic cultivation was carried out in culture tubes on the laboratory bench, it cannot be excluded that cultures were not fully free of oxygen. For future cultivation attempts, cultures should be incubated in anoxic atmosphere in an anaerobic tent.

The symbionts in hypoxic cultures obtained from sediment 4 and 26 were phylogenetically assigned inside/close to the Parasimkaniaceae (Figure 8A), originally described as a novel *Candidatus* family based on metagenomic data from freshwater samples and uncharacterized, sponge-associated chlamydiae and expanded by coral-associated MAGs recently. This family is closely related to Simkaniaceae, however, has on average a more compact genome and a reduced metabolic capability[68,86,87].

The sequences obtained for the anoxic cultures of sediment 6 and 19 fell into better-characterized, nevertheless poorly-studied families, Simkaniaceae and Rhabdochlamydiaceae, respectively (Figure 8A). For the organism in the anoxic culture of sediment 6, the closest branch in the tree was *Simkania negevensis*, the founding species of Simkaniaceae, originally described as a cell culture contamination[58]. In the last five years, several studies detected a high relative abundance of Simkaniaceae-assigned reads in coral-associated microbiomes and Symbiodiniaceae cultures[88–91]. A potential marine origin of *Simkania negevensis* could thereby be debated, which would be supported by the 16S rRNA gene sequences obtained from our culture of a marine sediment assigned to this species.

The rhabdochlamydial sequence of sediment 19 anoxic culture fell very basal inside this family (Figure 8A). Rhabdochlamydiaceae, proposed as one of the largest and most diverse clades inside the Chlamydiota with over 380 genus-level and 14,000 species-level lineages, contains four described species, all of the genus *Rhabdochlamydia* and all associated with arthropods like ticks, woodlice, cockroaches and spiders[92–97]. Additionally, members of this family were also frequently detected in soil and freshwater environments independent of animal hosts, suggesting that they mainly infect different hosts, most likely yet unknown protists. This was supported by the detection of novel chlamydial 16S rRNA gene sequences assigned to Rhabdochlamydiaceae in the slime mold *Dictyostelium discoideum*[98]. The host range together with a genetic set-up clearly distinct to the amoebae-infecting Parachlamydiaceae and the animal parasitic Chlamydiaceae, shows the potential of Rhabdochlamydiaceae as an interesting clade for the study of adaptation and genome evolution of Chlamydiota from protist to animal symbionts[92,98]. The organism in the culture of sediment 19, a basal, novel member of the Rhabdochlamydiaceae only moderately related to the arthropod-infecting species, could be another new protist-associated bacterium in this family with a marine, yet uncharacterized unicellular host.

The two remaining 16S rRNA gene sequences obtained, hypoxic culture of sediment 19 and anoxic culture of sediment 20, were phylogenetically classified into undescribed lineages, close to sequences derived from metagenomics/16S rRNA gene sequences or single-cell genomics without a representative species in culture (Figures 8B and 8C).

All close branches of sediment 19 hypoxic culture were either 16S rRNA gene sequences or metagenome-assembled genomes (MAGs) from marine origin, in parts associated with sponges (Figure 8B)[86,99].

In the case of sediment 20 anoxic culture, the phylogenetic closest lineages were MAGs or single-cell amplified genomes generated from marine sediments that contain at least five flagellar genes (Figure 8C). The presence of a flagellum is exceptional for Chlamydiota, as this phylum was long described as exclusively non-motile[100]. A cultivated organism harboring motility-associated genes would allow the study of the function and biology of the potential flagellum in the infection cycle of environmental chlamydiae.

To conclude, the marine sediments used for cultivation were suited to isolate novel chlamydiae with interesting features and belonging to poorly-described lineages. Even though 16S rRNA gene amplicon sequencing revealed the presence of Anoxychlamydiaceae members in the sediments (Figure 4), it was not possible to get any of them into culture. Explanations for that could be inefficient anoxic conditions as incubation was carried out on the laboratory bench and not in an anaerobic chamber or special requirements of its hosts, which were unclear as the hosts of these organisms are still unknown. Nevertheless, six (novel) chlamydiae were isolated and partly characterized, however, a visualization of them inside their hosts using FISH was not successful yet, most likely because of low available biomass and potential difficulties in permeabilizing the host cell membranes. DAPI staining, on the other hand, indicated the presence of intracellular bacteria in some host cells (data not shown), however, this could also be explained by microbial prey ingested by the host. To overcome these problems and isolate the chlamydial organisms in pure culture, a co-cultivation approach could be applied, where a different host, in most cases Acanthamoebae, as they are easy to grow in the laboratory, is offered to the culture, which is then infected by the symbionts[52]. The alternative host should show high cell growth, sufficient susceptibility to chlamydiae infection, be aposymbiotic and, for our specific purpose, grow under hypoxic and anoxic conditions. Ideally, a similar origin of host and chlamydiae (here: marine) should be considered. A disadvantage of this approach is the ignorance of the natural host, whose cultivation could also yield interesting insights.

4.2 Marine sediments harbor novel chlamydial host organisms

Besides the cultivation of chlamydiae, also their potential hosts in the sediment cultures were characterized by 18S rRNA gene-targeted Sanger sequencing. Initial screening of the sediment samples with 18S rRNA gene amplicon sequencing of DNA extracted from the sediment revealed a large variety of different eukaryotes in the sediments, including almost all important supergroups of protists (Figure 11A).

Molecular evidence suggests that protists are universal and abundant hosts of chlamydiae in various environments, however, as they are difficult to cultivate in the laboratory and extremely diverse and mostly uncharacterized, only a limited number of protist hosts are known and well-characterized, which includes mostly members of the Amoebozoa like *Acanthamoeba terricola* or *Dictyostelium discoideum*[9,39,44].

To detect and describe novel chlamydial hosts, protist enrichment cultures of the sediment samples were started, which were later on diluted to obtain pure protist cultures.

From these cultures the protist 18S rRNA gene sequences were generated via Sanger sequencing and their taxonomy was determined with phylogenetic analysis and BLAST. Protists in nine cultures (six anoxic and three hypoxic) could be characterized revealing a high diversity of eukaryotes in the different cultures, however, as sequencing results were obtained, at the same time a quite high purity of each individual culture, with only one to a few distinct species (Table 18). A similar picture was also observed by light microscopy, as the organisms show only a small number of different morphologies and cell shapes (Figure 12). Protist hosts were phylogenetically assigned to three different protist supergroups, Rhizaria, Stramenopiles and Alveolata, respectively, which all contain described (facultative) anaerobic as well as aerobic species (Figure 13 and Table 18).[101] For Rhizaria and Stramenopiles, no chlamydial-associated hosts have been isolated yet, for Alveolata, a symbiosis between a novel chlamydiae and a ciliate species was discovered recently[5,102]. In three cultures (19_hypo, 19_anox and 26_hypo), both chlamydiae and protists could be phylogenetically characterized, allowing speculations about potential symbiosis between these organisms (Figures 8 and 13, Table 18).

In the hypoxic culture of sediment 19, a Cercozoa species from the supergroup Rhizaria, quite closely related to the terrestrial or limnic genus *Limnofila*, together with an uncharacterized chlamydial species was detected (Figures 8B and 13B, Table 18). As *Limnofila* is restricted to freshwater or soil habitats, the protist in the culture likely belongs to a different, yet unknown marine genus inside the Cercozoa. Most of the organisms in this subgroup, including *Limnofila* and closely related genera, are heterotrophs that prey on bacteria and other microbes as their food source[103–105]. Although chlamydiae are able to escape host phagocytosis, it cannot be excluded that the detected chlamydiae were randomly ingested[42]. A stable symbiotic association between the two organisms has to be confirmed with FISH, which was not successful for this culture.

The anoxic culture of the same sediment selected for a relative of the diatom *Nanofrustulum*, which is part of the supergroup Stramenopiles together with a basal species of the Rhabdochlamydiaceae (Figures 8A and 19D, Table 18). No diatom host of chlamydiae was isolated before and only few protist hosts for Rhabdochlamydiaceae have been described so far[5,92,98]. Again, intracellular symbionts could not be conclusively detected via FISH with specific chlamydial probes.

Most promising were the results of the hypoxic culture of sediment 26: The protists in the culture, almost all have the same ciliate-like shape, grew in a relatively high cell density and were phylogenetically classified as relatives of *Aristerostoma*, a ciliate (Ciliophora) from the supergroup Alveolata (Figure 13A and Table 18)[106]. Additionally, chlamydial 16S rRNA gene sequences related to Parasimkaniaceae, a group without any cultured representatives, could be obtained (Figure 8A and Table 18). Notwithstanding the good growth of the ciliates, detecting chlamydiae in the culture by FISH was not possible, a potential symbiosis with the Alveolata organisms can thereby not be confirmed unequivocally.

In summary, the obtained sediment cultures in this study potentially contain novel chlamydiae from interesting clades that may live in symbiosis with members of protist supergroups that were previously not known as chlamydial hosts. FISH was not successful for any culture and therefore the final confirmation of the proposed symbioses is still missing, but protist and chlamydial organisms could be maintained for more than one year in the cultures already, ruling out the possibility of initial co-occurrence. FISH was problematic, due to low available biomass and potential difficulties to permeabilize the cell membranes of the different host organisms. Thus, a change of the growth medium that specifically selects for the protist of interest and that enables better cell growth and the use of FISH protocols adapted to the respective host could be helpful for symbiont visualization in the cultures. For the culture of sediment 26, as it contained a relative of *Aristerostoma*, cultivation in f/2 medium supplemented with a boiled wheat grain to encourage food bacteria growth or, alternatively, feeding with a few drops of *Nannochloropsis* or *Isochrysis* algae, is recommended[107,108]. A similar cultivation is in principle possible for the diatom *Nanofrustulum* relative in the anoxic culture of sediment 19, however, adjusting the light intensity could increase the growth even more[108–110]. *Limnofila sp.*, as a relative of the organisms in the hypoxic culture of sediment 19, can be cultivated in Sonneborn's Paramecium medium (ATCC Medium 802: https://www.atcc.org/~/media/91F4C9697D734A1F89DE0E2474F43743.ashx) supplemented with *Klebsiella pneumoniae* subsp. *pneumoniae* (ATCC 700831) or *Enterobacter aerogenes*

(ATCC® 13048), however, as the protists in the culture have a marine origin, the growth may not work as for the limnic relatives[103].

4.3 Chlamydial symbionts differ in their tolerance to oxygen and influence their host, *Acanthamoeba terricola*, regarding its replication and respiration

Besides the isolation of novel chlamydial symbionts with a focus on reduced oxygen conditions, a hypothesis of the evolution of oxygen tolerance and metabolism in the phylum Chlamydiota was investigated.

Two chlamydial model organisms, *Simkania negevensis* and *Parachlamydia acanthamoebae* UV7, representing members of the two proposed groups of chlamydiae regarding oxygen tolerance, group G1 and G2, respectively, were tested.

Genomic content and phylogenetic analysis suggest that G1, including *Simkania*, is better adapted to lower oxygen concentrations while G2, including UV7, prefers normoxic conditions[51]. For experimental validation, growth and respiration measurements of the host as well as infection and replication assays for the symbionts were performed, which brought some insights into the effect of oxygen on the symbiosis, however, a better adaption of *Simkania* to low and UV7 to higher O_2 concentrations was not observed.

Growth experiments of *Acanthamoeba* infected with one of the symbionts revealed significant differences in host growth under oxic, hypoxic and anoxic conditions depending on the associated chlamydial species (Figures 14, 15, 16 and 19). The most interesting observation here is the increased cell number of Ac. Neff under anoxic conditions when infected with *Simkania* compared to uninfected and UV7-infected hosts (Figure 16). Even though this refers to the amoeba, the results fit well with the hypothesis that *Simkania* is better adapted to environments with lower oxygen concentrations[51]. However, also under hypoxic and oxic conditions, host growth was improved by *Simkania* which was not observed for UV7, the effect of the symbionts seems to be thereby more species-specific and independent of the oxygen levels.

The respiration of amoebae cultures, in particular *Acanthamoeba*, was analyzed in a limited number of studies, and to the best of our knowledge, has never been investigated under different oxygen levels and for hosts with different symbionts[111–113]. Not only the growth of (apo-)symbiotic amoebae was compared under various oxygen concentrations, but also respiration as a measure of fitness was tested via gas chromatography in this study.

Although there appeared to be a great degree of outgassing due to our medium (Figure 17B – abiotic controls) and we had to contend with contamination after 24 hours, we nevertheless observed some interesting patterns in the respiration of *Acanthamoeba* sp. Higher CO_2 production was observed for all cultures under oxic conditions compared to hypoxic conditions after 24 hours, suggesting a higher respiration rate of *Acanthamoeba* sp. under elevated O_2 levels. *Simkania*-infected hosts produced significantly more CO_2 compared to UV7- and uninfected *Ac. Neff* under oxic conditions, which can be explained by the lower pathogenicity of *Simkania* compared to UV7. Results for hypoxic conditions were relatively similar for all cultures (Figure 17A).

The experimental set-up should be modified for future experiments to avoid contamination, in addition to reducing the outgassing of the medium. More specifically, more care should be taken with the incubation flasks (i.e. better sterilization of butyl rubber stoppers) and headspace sampling (i.e. sterilization of butyl rubber stoppers prior to headspace sampling). As TSY medium seems to produce copious amounts of CO_2, an alternative medium has to be considered, such as the defined axenic medium DGM-21A showing only a small amount of abiotic gas production or a 1xPAS-diluted TSY medium[114–116]. For the last option, various dilutions of TSY medium have been tested and sufficient amoebae growth is still possible in a medium with 40% TSY. Finally, CO_2 production should be normalized by cell numbers for direct comparisons across the strains.

Infection assays of *Simkania* and UV7 in *Acanthamoeba* under anoxia, hypoxia and oxic conditions revealed a similar infection efficiency of both symbionts under the various oxygen levels, however, some minor differences were observed: Slightly more hosts were infected with *Simkania* than UV7 under anoxic incubation while the opposite was detected for hypoxic and oxic conditions, however, this observation was just a trend and also varied between the replicates (Figure 18). A higher infectivity of *Simkania* under low oxygen levels and of UV7 under elevated O_2 conditions would support the hypothesis that *Simkania* as a member of the G1 group is better adapted to anoxia. In contrast, UV7 as a member of the G2 group prefers normoxic environments [41,51].

For a direct fitness comparison of *Simkania* and UV7 under oxic and anoxic conditions, acanthamoebae were co-infected with both symbionts and their replication was followed over a week. Single-infected hosts were also monitored as controls in the experiment. Fixation and FISH with *Simkania*- and UV7-specific probes were also performed to visualize the co-infected cells.

Replication assays as well as FISH indicated that the infectivity of *Simkania* EBs seems to be impaired, as no signals were obtained for the *Simkania*-specific FISH probe and the cell number of *Simkania* was far lower than UV7 in the quantification assay (Figures 20 and 21). The replication between the symbionts could thereby not be compared properly, however, a different influence of the O_2 regime was observed when looking at the chlamydial species separately, which is consistent with the proposed preference of *Simkania* to lower and UV7 to higher oxygen concentrations (Figure 20)[41,51]. A repeat of the experiment to observe any out-competition of one of the symbionts under a certain oxygen level was not successful after three times and for further attempts, the infectivity of *Simkania* has to be controlled in advance.

To conclude, none of the experiments was sufficient to confirm the hypothesis of a division of Chlamydiota into a more anaerobic G1 and a more aerobic G2 group but gave first evidence that chlamydial families differ in their tolerance and metabolism of oxygen in general[51].

The selection of the two representative organisms that were used for testing this hypothesis, was based on the availability of cultivated members from the G1 and G2 groups. Only a few isolates of the G1 group exist and thus *Simkania* was at that time the organism of choice. Since then the laboratory has acquired other G1 organisms in culture (namely members of the Parasimkaniaceae and CC-III), which might be suitable candidates to test the hypothesis in the future.

5 ABBREVIATIONS

°C	Degree Celsius
µl	microliter
µm	micrometer
µM	micromolar
anox	anoxic
ASW	Artificial Sea Water
BHQ-1	Black Hole Quencher 1
chl	Chlamydial/chlamydiae
co/co_inf	Co-infection

Co_inf_S/U	Co-infection *Simkania*/*UV7*
conc	concentration
CY3	Cyanine 3
CY5	Cyanine 5
DAPI	4’,6-diamidino-2-phenylindole
ddH_2O	Double-distilled and filtered water
ddPCR	Digital Droplet PCR
DNA	deoxyribonucleic acid
DOPE	Double Labelling of Oligonucleotide Probes
dPCR	Digital PCR
EB	elementary body
EDTA	ethylenediaminetetraacetic acid
ER	Endoplasmic reticulum
FA	Formamide
FAM	Fluorescein
FP	Forward primer
FISH	fluorescence in situ hybridization
FLUOS	fluorescein N-hydroxysuccinimidester
g	gram
GC	Gas chromatography
h	hours
HB	Hybridization buffer
HEX	Hexafluorescein
hypo	hypoxic
M	Molar
ml	milliliter

min	minutes
MOI	Multiplicity of Infection
n/nr	number
nt	nucleotide
ox	oxic
p	p-value
PAS	Page´s amoeba saline
PCR	Polymerase chain reaction
PFA	paraformaldehyde
pM	picomolar
pmol	picomol
ppm	parts per million
RB	Reticulate body
rcf	relative centrifugal force
RNA	ribonucleic acid
rpm	revolutions per minute
RP	Reverse primer
rRNA	ribosomal RNA
SDS	Sodium Dodecyl Sulfate
sec	seconds
sed	sediment
SPG	sucrose-phosphate-glutamate
T	temperature
TBE	tris-borate-EDTA buffer
TCA	trichloroacetic acid
TSY	trypticase soy broth with yeast extract

U	units
WB	Wash buffer
x	times

6 REFERENCES

1. Moya, A., Peretó, J., Gil, R. & Latorre, A. Learning how to live together: genomic insights into prokaryote–animal symbioses. *Nat. Rev. Genet.* **9**, 218–229 (2008).
2. Raina, J.-B. *et al.* Symbiosis in the microbial world: from ecology to genome evolution. *Biol. Open* **7**, bio032524 (2018).
3. Leung, T. L. F. & Poulin, R. PARASITISM, COMMENSALISM, AND MUTUALISM: EXPLORING THE MANY SHADES OF SYMBIOSES. *Vie Milieu* (2008).
4. Dimijian, G. G. Evolving together: the biology of symbiosis, part 1. *Proc. Bayl. Univ. Med. Cent.* **13**, 217–226 (2000).
5. Husnik, F. *et al.* Bacterial and archaeal symbioses with protists. *Curr. Biol.* **31**, R862–R877 (2021).
6. Horn, M. & Wagner, M. Bacterial Endosymbionts of Free-living Amoebae [1]. *J. Eukaryot. Microbiol.* **51**, 509–514 (2004).
7. Tekle, Y. I., Lyttle, J. M., Blasingame, M. G. & Wang, F. Comprehensive comparative genomics reveals over 50 phyla of free-living and pathogenic bacteria are associated with diverse members of the amoebozoa. *Sci. Rep.* **11**, 8043 (2021).
8. Görtz, H.-D. Symbiotic Associations Between Ciliates and Prokaryotes.
9. Horn, M. *Chlamydiae* as Symbionts in Eukaryotes. *Annu. Rev. Microbiol.* **62**, 113–131 (2008).

10. Boscaro, V., Husnik, F., Vannini, C. & Keeling, P. J. Symbionts of the ciliate *Euplotes* : diversity, patterns and potential as models for bacteria–eukaryote endosymbioses. *Proc. R. Soc. B Biol. Sci.* **286**, 20190693 (2019).

11. Deeg, C. M. *et al.* Chromulinavorax destructans, a pathogen of microzooplankton that provides a window into the enigmatic candidate phylum Dependentiae.

12. Farnelid, H., Tarangkoon, W., Hansen, G., Hansen, P. & Riemann, L. Putative N2-fixing heterotrophic bacteria associated with dinoflagellate–Cyanobacteria consortia in the low-nitrogen Indian Ocean. *Aquat. Microb. Ecol.* **61**, 105–117 (2010).

13. Keeling, P. J. & McCutcheon, J. P. Endosymbiosis: The feeling is not mutual. *J. Theor. Biol.* **434**, 75–79 (2017).

14. Greub, G. Environmental Metagenomic Assemblies Reveal Seven New Highly Divergent Chlamydial Lineages and Hallmarks of a Conserved Intracellular Lifestyle. *Front. Microbiol.* **9**, (2018).

15. George, E. E. Highly Reduced Genomes of Protist Endosymbionts Show Evolutionary Convergence.

16. Tseng, T.-T., Tyler, B. M. & Setubal, J. C. Protein secretion systems in bacterial-host associations, and their description in the Gene Ontology. *BMC Microbiol.* **9**, S2 (2009).

17. Cornelis, G. R. The type III secretion injectisome. (2006).

18. Lagkouvardos, I., Shen, J. & Horn, M. Improved axenization method reveals complexity of symbiotic associations between bacteria and acanthamoebae. *Environ. Microbiol. Rep.* **6**, 383–388 (2014).

19. Rossi, A. Detecting Associations Between Ciliated Protists and Prokaryotes with Culture-Independent Single-Cell Microbiomics: a Proof-of-Concept Study.

20. Dirren, S., Salcher, M. M., Blom, J. F., Schweikert, M. & Posch, T. Ménage-à-trois: The Amoeba Nuclearia sp. from Lake Zurich with its Ecto- and Endosymbiotic Bacteria. *Protist* **165**, 745–758 (2014).

21. Khan, N. A. *Acanthamoeba* : biology and increasing importance in human health. *FEMS Microbiol. Rev.* **30**, 564–595 (2006).

22. Gawryluk, R. M. R., Chisholm, K. A., Pinto, D. M. & Gray, M. W. Composition of the mitochondrial electron transport chain in Acanthamoeba castellanii: Structural and evolutionary insights. *Biochim. Biophys. Acta BBA - Bioenerg.* **1817**, 2027–2037 (2012).

23. Prescott, L. M., Hoyme, H. E., Crockett, D. & Hui, E. Carbohydrate metabolism in *Acanthamoeba castellanii* . 1. The activity of key enzymes and [^{14} C]-glucose metabolism. *Can. J. Microbiol.* **19**, 1131–1136 (1973).

24. Alves, D. D. S. M. M., Alves, L. M., Da Costa, T. L., De Castro, A. M. & Vinaud, M. C. Anaerobic Metabolism in T4 Acanthamoeba Genotype. *Curr. Microbiol.* **74**, 685–690 (2017).

25. Leger, M. M., Gawryluk, R. M. R., Gray, M. W. & Roger, A. J. Evidence for a Hydrogenosomal-Type Anaerobic ATP Generation Pathway in Acanthamoeba castellanii. *PLoS ONE* **8**, e69532 (2013).

26. Cometa, I., Schatz, S., Trzyna, W. & Rogerson, A. Tolerance of Naked Amoebae to Low Oxygen Levels with an Emphasis on the Genus Acanthamoeba.

27. Weekers, P. H. H., Bodelier, P. L. E., Wijen, J. P. H. & Vogels, G. D. Effects of Grazing by the Free-Living Soil Amoebae *Acanthamoeba castellanii, Acanthamoeba polyphaga* , and *Hartmannella vermiformis* on Various Bacteria. *Appl. Environ. Microbiol.* **59**, 2317–2319 (1993).

28. Greub, G. & Raoult, D. Microorganisms Resistant to Free-Living Amoebae. *Clin. Microbiol. Rev.* **17**, 413–433 (2004).

29. Fritsche, T. R., Gautom, R. K., Seyedirashti, S., Bergeron, D. L. & Lindquist, T. D. Occurrence of bacterial endosymbionts in Acanthamoeba spp. isolated from corneal and environmental specimens and contact lenses. *J. Clin. Microbiol.* **31**, 1122–1126 (1993).

30. Fritsche, T. R. *et al.* In Situ Detection of Novel Bacterial Endosymbionts of *Acanthamoeba* spp. Phylogenetically Related to Members of the Order *Rickettsiales*. *Appl. Environ. Microbiol.* **65**, 206–212 (1999).

31. Michel, R. & Hauröder, B. Isolation of an Acanthamoeba Strain with Intracellular Burkholderia pickettii Infection. *Zentralblatt Für Bakteriol.* **285**, 541–557 (1997).

32. Magnet, A. *et al.* Vectorial role of Acanthamoeba in Legionella propagation in water for human use. *Sci. Total Environ.* **505**, 889–895 (2015).

33. Yu, H. S. *et al.* Natural occurrence of Mycobacterium as an endosymbiont of Acanthamoeba isolated from a contact lens storage case. *Korean J. Parasitol.* **45**, 11 (2007).

34. Horn, M. *et al.* Members of the *Cytophaga–Flavobacterium–Bacteroides* phylum as intracellular bacteria of acanthamoebae: proposal of ' *Candidatus* Amoebophilus asiaticus'. *Environ. Microbiol.* **3**, 440–449 (2001).

35. Hajialilo, E. *et al.* Molecular characterization of bacterial, viral and fungal endosymbionts of Acanthamoeba isolates in keratitis patients of Iran. *Exp. Parasitol.* **200**, 48–54 (2019).

36. Fritsche, T. R. *et al.* Phylogenetic Diversity among Geographically Dispersed *Chlamydiales* Endosymbionts Recovered from Clinical and Environmental Isolates of *Acanthamoeba* spp. *Appl. Environ. Microbiol.* **66**, 2613–2619 (2000).

37. Hoffmann, R., Michel, R., Müller, K. D. & Schmid, E. N. Archaebacteria like endocytobiotic organisms isolated from Acanthamoeba sp (gr II). *Endocytobiosis Cell Res.* **12**, 185–188 (1998).

38. Molmeret, M., Horn, M., Wagner, M., Santic, M. & Abu Kwaik, Y. Amoebae as Training Grounds for Intracellular Bacterial Pathogens. *Appl. Environ. Microbiol.* **71**, 20–28 (2005).

39. Taylor-Brown, A., Vaughan, L., Greub, G., Timms, P. & Polkinghorne, A. Twenty years of research into Chlamydia-like organisms: a revolution in our understanding of the biology and pathogenicity of members of the phylum Chlamydiae. *Pathog. Dis.* **73**, 1–15 (2015).

40. Wagner, M. & Horn, M. The Planctomycetes, Verrucomicrobia, Chlamydiae and sister phyla comprise a superphylum with biotechnological and medical relevance. *Curr. Opin. Biotechnol.* **17**, 241–249 (2006).

41. Dharamshi, J. E. *et al.* Marine Sediments Illuminate Chlamydiae Diversity and Evolution. *Curr. Biol.* **30**, 1032-1048.e7 (2020).

42. AbdelRahman, Y. M. & Belland, R. J. The chlamydial developmental cycle: Figure 1. *FEMS Microbiol. Rev.* **29**, 949–959 (2005).

43. König, L. *et al.* Biphasic Metabolism and Host Interaction of a Chlamydial Symbiont. *mSystems* **2**, e00202-16 (2017).

44. Collingro, A., Köstlbacher, S. & Horn, M. Chlamydiae in the Environment. *Trends Microbiol.* **28**, 877–888 (2020).

45. Trentmann, O., Horn, M., Van Scheltinga, A. C. T., Neuhaus, H. E. & Haferkamp, I. Enlightening Energy Parasitism by Analysis of an ATP/ADP Transporter from Chlamydiae. *PLoS Biol.* **5**, e231 (2007).

46. Lee, J. K. *et al.* Replication-dependent size reduction precedes differentiation in Chlamydia trachomatis. *Nat. Commun.* **9**, 45 (2018).

47. Sixt, B. S. Host cell death during infection with *Chlamydia* : a double-edged sword. *FEMS Microbiol. Rev.* **45**, fuaa043 (2021).

48. Bébéar, C. & De Barbeyrac, B. Genital Chlamydia trachomatis infections. *Clin. Microbiol. Infect.* **15**, 4–10 (2009).

49. Taylor, H. R., Burton, M. J., Haddad, D., West, S. & Wright, H. Trachoma. *The Lancet* **384**, 2142–2152 (2014).

50. Omsland, A., Sixt, B. S., Horn, M. & Hackstadt, T. Chlamydial metabolism revisited: interspecies metabolic variability and developmental stage-specific physiologic activities. *FEMS Microbiol. Rev.* **38**, 779–801 (2014).

51. Dharamshi, J. E. *et al.* Gene gain facilitated endosymbiotic evolution of Chlamydiae. *Nat. Microbiol.* **8**, 40–54 (2023).

52. Collingro, A. *et al.* Recovery of an environmental chlamydia strain from activated sludge by co-cultivation with Acanthamoeba sp. *Microbiology* **151**, 301–309 (2005).

53. Casson, N., Medico, N., Bille, J. & Greub, G. Parachlamydia acanthamoebae enters and multiplies within pneumocytes and lung fibroblasts. *Microbes Infect.* **8**, 1294–1300 (2006).

54. Greub, G., Mege, J.-L. & Raoult, D. *Parachlamydia acanthamoeba* Enters and Multiplies within Human Macrophages and Induces Their Apoptosis. *Infect. Immun.* **71**, 5979–5985 (2003).

55. Collingro, A. *et al.* Unity in Variety--The Pan-Genome of the Chlamydiae. *Mol. Biol. Evol.* **28**, 3253–3270 (2011).

56. Kumari, S., Tishel, R., Eisenbach, M. & Wolfe, A. J. Cloning, characterization, and functional expression of acs, the gene which encodes acetyl coenzyme A synthetase in Escherichia coli. *J. Bacteriol.* **177**, 2878–2886 (1995).

57. Perzov, N., Padler-Karavani, V., Nelson, H. & Nelson, N. Features of V-ATPases that distinguish them from F-ATPases. *FEBS Lett.* **504**, 223–228 (2001).

58. Kahane, S., Gonen, R., Sayada, C., Elion, J. & Friedman, M. G. Description and partial characterization of a new chlamydia-like microorganism. *FEMS Microbiol. Lett.* **109**, 329–333 (1993).

59. Everett, K. D. E. & Andersen, A. A. The Ribosomal Intergenic Spacer and Domain I of the 23S rRNA Gene Are Phylogenetic Markers for Chlamydia spp. *Int. J. Syst. Bacteriol.* **47**, 461–473 (1997).

60. Vouga, M., Baud, D. & Greub, G. *Simkania negevensis* , an insight into the biology and clinical importance of a novel member of the *Chlamydiales* order. *Crit. Rev. Microbiol.* **43**, 62–80 (2017).

61. Kahane, S., Dvoskin, B., Mathias, M. & Friedman, M. G. Infection of *Acanthamoeba polyphaga* with *Simkania negevensis* and *S. negevensis* Survival within Amoebal Cysts. *Appl. Environ. Microbiol.* **67**, 4789–4795 (2001).

62. Croxatto, A. *et al.* Presence of Chlamydiales DNA in ticks and fleas suggests that ticks are carriers of Chlamydiae. *Ticks Tick-Borne Dis.* **5**, 359–365 (2014).

63. Kahane, S., Fruchter, D., Dvoskin, B. & Friedman, M. G. Versatility of Simkania negevensis infection in vitro and induction of host cell inflammatory cytokine response. *J. Infect.* **55**, e13–e21 (2007).

64. Kahane, S., Dvoskin, B. & Friedman, M. G. The role of monocyte/macrophages as vehicles of dissemination of *Simkania negevensis* : an *in vitro* simulation model. *FEMS Immunol. Med. Microbiol.* **52**, 219–227 (2008).

65. Mehlitz, A. *et al.* The chlamydial organism *S imkania negevensis* forms ER vacuole contact sites and inhibits ER-stress: *Simkania* vacuole formation and ER-stress inhibition. *Cell. Microbiol.* **16**, 1224–1243 (2014).

66. Pilhofer, M. *et al.* Architecture and host interface of environmental chlamydiae revealed by electron cryotomography. *Environ. Microbiol.* **16**, 417–429 (2014).

67. Stairs, C. W. *et al.* Chlamydial contribution to anaerobic metabolism during eukaryotic evolution. *Sci. Adv.* **6**, eabb7258 (2020).

68. Köstlbacher, S. *et al.* Pangenomics reveals alternative environmental lifestyles among chlamydiae. *Nat. Commun.* **12**, 4021 (2021).

69. Corsaro, D., Mrva, M., Colson, P. & Walochnik, J. Validation and redescription of Acanthamoeba terricola Pussard, 1964 (Amoebozoa: Acanthamoebidae). *Eur. J. Protistol.* **94**, 126091 (2024).

70. Neff, R. J. Purification, Axenic Cultivation, and Description of a Soil Amoeba, Acanthamoeba sp. *J. Protozool.* **4**, 176–182 (1957).

71. Baba, T. *et al.* Construction of *Escherichia coli* K-12 in-frame, single-gene knockout mutants: the Keio collection. *Mol. Syst. Biol.* **2**, 2006.0008 (2006).

72. Poppert, S., Essig, A., Marre, R., Wagner, M. & Horn, M. Detection and Differentiation of Chlamydiae by Fluorescence In Situ Hybridization. *Appl. Environ. Microbiol.* **68**, 4081–4089 (2002).

73. Wallner, G., Amann, R. & Beisker, W. Optimizing fluorescent in situ hybridization with rRNA-targeted oligonucleotide probes for flow cytometric identification of microorganisms. *Cytometry* **14**, 136–143 (1993).

74. Pjevac, P. *et al.* An Economical and Flexible Dual Barcoding, Two-Step PCR Approach for Highly Multiplexed Amplicon Sequencing. *Front. Microbiol.* **12**, 669776 (2021).

75. Letunic, I. & Bork, P. Interactive Tree of Life (iTOL) v6: recent updates to the phylogenetic tree display and annotation tool. *Nucleic Acids Res.* gkae268 (2024) doi:10.1093/nar/gkae268.

76. Edgar, R. C. Search and clustering orders of magnitude faster than BLAST. *Bioinformatics* **26**, 2460–2461 (2010).

77. McMurdie, P. J. & Holmes, S. phyloseq: An R Package for Reproducible Interactive Analysis and Graphics of Microbiome Census Data. *PLoS ONE* **8**, e61217 (2013).

78. Katoh, K. MAFFT: a novel method for rapid multiple sequence alignment based on fast Fourier transform. *Nucleic Acids Res.* **30**, 3059–3066 (2002).

79. Capella-Gutiérrez, S., Silla-Martínez, J. M. & Gabaldón, T. trimAl: a tool for automated alignment trimming in large-scale phylogenetic analyses. *Bioinformatics* **25**, 1972–1973 (2009).

80. Price, M. N., Dehal, P. S. & Arkin, A. P. FastTree 2 – Approximately Maximum-Likelihood Trees for Large Alignments. *PLoS ONE* **5**, e9490 (2010).

81. Barbera, P. *et al.* Data from: EPA-ng: massively parallel evolutionary placement of genetic sequences. 16601287 bytes [object Object] https://doi.org/10.5061/DRYAD.KB505NC (2018).

82. Kearse, M. *et al.* Geneious Basic: An integrated and extendable desktop software platform for the organization and analysis of sequence data. *Bioinformatics* **28**, 1647–1649 (2012).

83. Minh, B. Q. *et al.* IQ-TREE 2: New Models and Efficient Methods for Phylogenetic Inference in the Genomic Era. *Mol. Biol. Evol.* **37**, 1530–1534 (2020).

84. Wickham, H. *Ggplot2*. (Springer International Publishing, Cham, 2016). doi:10.1007/978-3-319-24277-4.

85. Lienard, J. *et al.* Prevalence and diversity of Chlamydiales and other amoeba-resisting bacteria in domestic drinking water systems. *New Microbes New Infect.* **15**, 107–116 (2017).

86. Dharamshi, J. E. *et al.* Genomic diversity and biosynthetic capabilities of sponge-associated chlamydiae. *ISME J.* **16**, 2725–2740 (2022).

87. Maire, J., Collingro, A., Horn, M. & Van Oppen, M. J. H. Chlamydiae in corals: shared functional potential despite broad taxonomic diversity. *ISME Commun.* **4**, ycae054 (2024).

88. Wada, N. *et al.* High-resolution spatial and genomic characterization of coral-associated microbial aggregates in the coral *Stylophora pistillata*. *Sci. Adv.* **8**, eabo2431 (2022).

89. Chan, W. Y., Peplow, L. M., Menéndez, P., Hoffmann, A. A. & Van Oppen, M. J. H. The roles of age, parentage and environment on bacterial and algal endosymbiont communities in *Acropora* corals. *Mol. Ecol.* **28**, 3830–3843 (2019).

90. Maire, J. *et al.* Colocalization and potential interactions of *Endozoicomonas* and chlamydiae in microbial aggregates of the coral *Pocillopora acuta*. *Sci. Adv.* **9**, eadg0773 (2023).

91. Buerger, P., Vanstone, R. T., Maire, J. & Van Oppen, M. J. H. Long-Term Heat Selection of the Coral Endosymbiont Cladocopium C1acro (Symbiodiniaceae) Stabilizes Associated Bacterial Communities. *Int. J. Mol. Sci.* **23**, 4913 (2022).

92. Halter, T. *et al.* Ecology and evolution of chlamydial symbionts of arthropods. *ISME Commun.* **2**, 45 (2022).

93. Lagkouvardos, I. *et al.* IMNGS: A comprehensive open resource of processed 16S rRNA microbial profiles for ecology and diversity studies. *Sci. Rep.* **6**, 33721 (2016).

94. Pillonel, T. *et al.* Sequencing the Obligate Intracellular Rhabdochlamydia helvetica within Its Tick Host Ixodes ricinus to Investigate Their Symbiotic Relationship. *Genome Biol. Evol.* **11**, 1334–1344 (2019).

95. Kostanjšek, R., Štrus, J., Drobne, D. & Avguštin, G. 'Candidatus Rhabdochlamydia porcellionis', an intracellular bacterium from the hepatopancreas of the terrestrial isopod Porcellio scaber (Crustacea: Isopoda). *Int. J. Syst. Evol. Microbiol.* **54**, 543–549 (2004).

96. Corsaro, D. *et al.* 'Candidatus Rhabdochlamydia crassificans', an intracellular bacterial pathogen of the cockroach Blatta orientalis (Insecta: Blattodea). *Syst. Appl. Microbiol.* **30**, 221–228 (2007).

97. Vanthournout, B. & Hendrickx, F. Endosymbiont Dominated Bacterial Communities in a Dwarf Spider. *PLOS ONE* **10**, e0117297 (2015).

98. Haselkorn, T. S. *et al.* Novel Chlamydiae and *Amoebophilus* endosymbionts are prevalent in wild isolates of the model social amoeba *Dictyostelium discoideum*. *Environ. Microbiol. Rep.* **13**, 708–719 (2021).

99. Pizzetti, I., Fazi, S., Fuchs, B. M. & Amann, R. High abundance of novel environmental chlamydiae in a Tyrrhenian coastal lake (Lago di Paola, Italy). *Environ. Microbiol. Rep.* **4**, 446–452 (2012).

100. Collingro, A. *et al.* Unexpected genomic features in widespread intracellular bacteria: evidence for motility of marine chlamydiae. *ISME J.* **11**, 2334–2344 (2017).

101. Gawryluk, R. M. R. & Stairs, C. W. Diversity of electron transport chains in anaerobic protists. *Biochim. Biophys. Acta BBA - Bioenerg.* **1862**, 148334 (2021).

102. Wang, R. *et al.* " *Candidatus* Euplotechlamydia quinta," a novel chlamydia-like bacterium hosted by the ciliate *Euplotes octocarinatus* (Ciliophora, Spirotrichea). *J. Eukaryot. Microbiol.* **70**, e12945 (2023).

103. Bass, D. *et al.* Phylogeny of Novel Naked Filose and Reticulose Cercozoa: Granofilosea cl. n. and Proteomyxidea Revised. *Protist* **160**, 75–109 (2009).

104. Dumack, K., Fiore-Donno, A. M., Bass, D. & Bonkowski, M. Making sense of environmental sequencing data: Ecologically important functional traits of the protistan groups Cercozoa and Endomyxa (Rhizaria). *Mol. Ecol. Resour.* **20**, 398–403 (2020).

105. Dumack, K. *et al.* Contrasting protist communities (Cercozoa: Rhizaria) in pristine and earthworm-invaded North American deciduous forests. *Biol. Invasions* **24**, 1345–1357 (2022).

106. Foissner, W., Stoeck, T., Agatha, S. & Dunthorn, M. Intraclass Evolution and Classification of the Colpodea (Ciliophora): CLASS COLPODEA. *J. Eukaryot. Microbiol.* **58**, 397–415 (2011).

107. Gachon, C. M. M. *et al.* The Culture Collection of Algae and Protozoa (CCAP): A biological resource for protistan genomics. *Gene* **406**, 51–57 (2007).

108. Guillard, R. R. L. & Ryther, J. H. STUDIES OF MARINE PLANKTONIC DIATOMS: I. CYCLOTELLA NANA HUSTEDT, AND DETONULA CONFERVACEA (CLEVE) GRAN. *Can. J. Microbiol.* **8**, 229–239 (1962).

109. Morales, E. A., Novais, M. H., García, M. L., Maidana, N. I. & Morais, M. M. Two new species of Nanofrustulum (Bacillariophyta) from temporary rivers in the Alentejo region, southern Portugal. *Nova Hedwig.* **117**, 71–92 (2023).

110. Erdoğan, A. *et al.* Manipulation in Culture Conditions of Nanofrustulum shiloi for Enhanced Fucoxanthin Production and Isolation by Preparative Chromatography. *Molecules* **28**, 1988 (2023).

111. Lloyd, D., Edwards, S. W. & Fry, J. C. Temperature-compensated oscillations in respiration and cellular protein content in synchronous cultures of Acanthamoeba castellanii. *Proc. Natl. Acad. Sci.* **79**, 3785–3788 (1982).

112. Martín-Pérez, T., Criado-Fornelio, A., Ávila-Blanco, M. & Pérez-Serrano, J. Development and optimization of new culture media for Acanthamoeba spp. (Protozoa: Amoebozoa). *Eur. J. Protistol.* **64**, 91–102 (2018).

113. Crawford, D., Rogerson, A. & Laybourn-Parry, J. Respiration of the marine amoeba Trichosphaerium sieboldi determined by 14C labelling and Cartesian diver methods. *Mar. Ecol. Prog. Ser.* **112**, 135–142 (1994).

114. Schuster, F. L. Cultivation of Pathogenic and Opportunistic Free-Living Amebas. *Clin. Microbiol. Rev.* **15**, 342–354 (2002).

115. Byers, T. J., Akins, R. A., Maynard, B. J., Lefken, R. A. & Martin, S. M. Rapid Growth of Acanthamoeba In Defined Media; Induction of Encystment By Glucose-Acetate Starvation. *J. Protozool.* **27**, 216–219 (1980).

116. Sixt, B. S. *et al.* Metabolic Features of Protochlamydia amoebophila Elementary Bodies – A Link between Activity and Infectivity in Chlamydiae. *PLoS Pathog.* **9**, e1003553 (2013).

„Ich habe mich bemüht, sämtliche Inhaber*innen der Bildrechte ausfindig zu machen und ihre Zustimmung zur Verwendung der Bilder in dieser Arbeit eingeholt. Sollte dennoch eine Urheberrechtsverletzung bekannt werden, ersuche ich um Meldung bei mir.“

"I have made every effort to identify all copyright holders and obtain their consent for using the images in this work. If a copyright infringement is discovered, I kindly request that it be reported to me."

7 ABSTRACT

The phylum Chlamydiota contains obligate intracellular bacteria dependent on eukaryotic hosts for replication and key metabolite acquisition. Initially described as a small group of human pathogens with a characteristic developmental cycle, chlamydiae have since been found in different environments, infecting various hosts, especially unicellular protists. Recently, chlamydial sequences from marine anoxic sediments were classified as a novel family called Anoxychlamydiaceae, the first obligate anaerobic chlamydial lineage. Furthermore, phylogenetic reconstruction of oxygen tolerance and metabolism in the phylum revealed two contrasting groups, G1 and G2, that differ in their preferred oxygen level and versatility of their energy metabolism.

As no cultivated Anoxychlamydiaceae members are available and their host organisms are unknown, this study aimed to isolate novel chlamydiae adapted to low oxygen concentration, focusing on Anoxychlamydiaceae, and their hosts from marine sediments and characterize them taxonomically. Additionally, differences in chlamydial G1 and G2 group oxygen tolerance were experimentally tested by growth, infection and respiratory assays, using two chlamydial laboratory strains, *Simkania negevensis* and *Parachlamydia acanthamoebae*.

Novel chlamydiae were successfully cultivated within protist enrichment cultures obtained from marine sediments, albeit no Anoxychlamydiaceae were retrieved. Potential hosts were assigned to protist supergroups, including Rhizaria and Stramenopiles, which so far have not been described as chlamydial hosts.

The oxygen tolerance hypothesis could not be proven successfully with the tested organisms. However, *Acanthamoeba*'s differential growth and respiration rates under varying oxygen levels during chlamydial infection provided first evidence for different oxygen adaptations within chlamydiae. These results will allow future studies further exploring this hypothesis.

8 ZUSAMMENFASSUNG

Das Phylum Chlamydiota umfasst obligat intrazelluläre Bakterien, die für Replikation und den Erwerb bestimmter Metabolite auf eukaryotische Wirte angewiesen sind. Ursprünglich als eine kleine Gruppe menschlicher Krankheitserregern mit einem charakteristischen Entwicklungszyklus beschrieben, wurden Chlamydien inzwischen in vielen verschiedenen Habitaten nachgewiesen, in denen sie unterschiedliche Wirten infizieren, insbesondere einzellige Protisten. Unlängst wurden Chlamydiensequenzen aus anoxischen marinen Sedimenten in eine neuartige Familie namens Anoxychlamydiaceae eingeordnet, die als erste obligat anaerobe Gruppe innerhalb der Chlamydiota gilt. In diesem Zusammenhang wurde auch die Evolution von Sauerstofftoleranz und -stoffwechsel innerhalb des Phylums rekonstruiert, wobei zwei Gruppen, G1 und G2, identifiziert wurden, die sich in ihrem bevorzugten Sauerstoffgehalt und der Vielseitigkeit ihres Energiestoffwechsels unterscheiden.

Da bisher keine Vertreter der Anoxychlamydiaceae in Kultur vorliegen und ihre Wirtsorganismen unbekannt sind, war das Ziel dieser Studie, neuartige Chlamydien, insbesondere Anoxychlamydiaceae, mitsamt ihrer Wirtsorganismen aus marinen Sedimenten zu kultivieren und taxonomisch zu charakterisieren. Zusätzlich wurden Unterschiede in der Sauerstofftoleranz der chlamydialen G1- und G2-Gruppen mit zwei repräsentativen Chlamydienarten, *Simkania negevensis* und *Parachlamydia acanthamoebae*, experimentell durch Wachstums-, Infektions- und Respirationsanalysen untersucht.

Es gelang, neuartige Chlamydien aus marinen Sedimenten zu kultivieren, darunter aber keine Anoxychlamydiaceae. Potenzielle Wirtsorganismen wurden verschiedenen Protistensupergruppen zugeordnet, einschließlich Rhizaria und Stramenopilen, die bisher nicht als Chlamydienwirtszellen beschrieben wurden.

Die Hypothese zur Sauerstofftoleranz konnte mit den ausgewählten Chlamydienarten nicht eindeutig bestätigt werden. Dennoch lieferten unterschiedliche Wachstums- und Respirationsraten der Amöbenwirtszellen während einer Chlamydieninfektion unter verschiedenen Sauerstoffbedingungen erste Hinweise auf unterschiedliche Sauerstoffanpassung innerhalb der Chlamydiota. Ergebnisse dieser Studie bilden eine Grundlage für zukünftige Forschungen, die diese Hypothese näher untersuchen.

9 SUPPLEMENTS

Script for phylogenetic tree calculation of 16S rRNA gene amplicon sequencing data

1. Cluster ASV sequences

-) Determine ASV occurrences (in Excel)

-) Generate a text file with fasta header name and name to replace it (name name size=x)

-) Exchange name with awk and manipulation by hand afterward:

```
awk 'FNR==NR { a[">"$1]=$2; next } $1 in a { sub(/>/,">"a[$1]"|",$1)}1'
DADA2_ASVs_size.txt DADA2_ASVs_short.fna > DADA2_ASVs_short_size.fna
```

```
module load usearch usearch -sortbylength DADA2_ASVs_short_size.fna -fastaout
DADA2_ASVs_short_size_sorted.fna usearch -cluster_smallmem
DADA2_ASVs_short_size_sorted.fna -centroids DADA2_ASVs_OTUs95.fasta -id 0.95 -
query_cov 0.9 -sizein -sizeout -sortedby length -uc DADA2_ASVs_OTUs95.uc
```

-> only clusters with reads >19 were used for tree! n=677

2. Add sequences to tree

-) Add sequences from sediment sequencing

-) Align with mafft to existing full length 16S alignment:

```
mafft --addfragments cluster95_all.fna --keeplength --6merpair --thread 1
Chlamydiae_GEM_CHls_Silva138_16S_drep99_aligned_trim_forClavi3.fasta >
Chlamydiae_GEM_CHls_Silva138_16S_drep99_aligned_trim_forClavi3_with_cluster95_all.a
ln
```

-) Add sequences to tree:

```
module load epa-ng epa-ng -s
Chlamydiae_GEM_CHls_Silva138_16S_drep99_aligned_trim_forClavi3.fasta -t
Clavi7_GEM_trimal.treefile -q cluster95_all_aln2_Chlamydiae_GEM.aln -m SYM+I+R10
```

-) Make file readable:

```
module load pplacer guppy tog epa_result.jplace
```

-) Rename tree (script to rename tips in a phylo tree using tab delim name file: 16Snames_2_tax.txt):

```
python rename_nodes.py 16Snames_2_tax.txt epa_result.tog.tre
```

```
import sys import re
```

-) Infile of names:

```
names_in = open(sys.argv[1], 'r')
```

```
names_hash = {}
```

```
for line in names_in: line = line.rstrip('\n') old,new = line.split('\t')
names_hash[old] = new
```

```
names_in.close()
```

-) Inpfile of tree:

```
tree_file_path = sys.argv[2] tree_in = open(tree_file_path, 'r')
```

-) Tree output file that has new names:

```
tree_out = open(tree_file_path+"_rn.nwk", 'w')
```

```
for line in tree_in: for key in names_hash: if key in line: line = re.sub(key,
names_hash[key], line)
```

```
print line tree_out.write(line) print("new tree saved to: " +
tree_file_path+"_rn.nwk") tree_out.close()
```

-) Put file in iTOL

Supplement 1: Work-flow and commands for phylogenetic tree calculation of 16S rRNA gene amplicon sequencing data

Script for absolute abundance plot of chlamydiae in the sediments

1. Import all necessary files

```
setwd("//share.univie.ac.at/DOME/staff/arndorfer/Markus Arndorfer/JMF-2304-01/JMF-2304-01__all__rRNA_SSU_040_523_Chlamydia__JMFR_MSHS_KMHHM")
```

```
OTU <- read.table("DADA2_counts_as_matrix.tsv", header=TRUE, row.names=1, check.names=F)
OTU <- as.matrix(OTU, rownames = 1)
```

```
TAX <- read.table("DADA2_ASVs.rRNA_SSU.custom_reference.DADA2_classified.tsv", sep = "\t", header = T, row.names=1, na.strings=c("","NA"))
TAX$Family <- TAX$Family %>% replace_na("no_family")
TAX$Genus <- TAX$Genus %>% replace_na("no_genus")
TAX <- as.matrix(TAX)
```

```
Sample <- read.table("metadata_Chl.txt", sep="\t", header=TRUE, row.names=1)
```

2. Generate phyloseq object

```
PS_all <- phyloseq(otu_table(OTU, taxa_are_rows=T), tax_table(TAX), sample_data(Sample))
PS_all
```

3. Filter out samples with no abundance

```
PS <- prune_samples(sample_sums(PS)>0, PS)
```

4. Include only taxa with more than 20 reads (on average) in at least 5% of samples

```
filter <- phyloseq::genefilter_sample(PS, filterfun_sample(function(x) x >= 20))
```

5. Calculate relative abundance plots

```
PS2_taxtree_ra = PS2 %>% tax_glom(taxrank = "Family") %>% transform_sample_counts(function(x) {x/sum(x)}) %>% psmelt() %>% arrange(Family)
```

```
P_ra <- ggplot(PS2_taxtree_ra, aes(x = Sample, y = Abundance, fill = Family)) +
geom_bar(stat = "identity") +
theme(axis.text.x = element_text(angle = 45, hjust =1)) +
theme_light() +
coord_flip() +
xlab("") +
ylab("rel abundance")

ggsave("chl_rel_ab.png", width = 10, height = 15)
```

6. Plot absolute abundance with ddPCR data

```
PS2_taxtree_ab <- PS2_taxtree_ra %>% mutate(absnr = Abundance * cp_per_g_sediment)

P_absnr <- ggplot(PS2_taxtree_ab, aes(x = fct_reorder(User_sample_ID,
as.numeric(as.character(User_sample_ID))), y = absnr, fill = Family)) +
geom_bar(stat = "identity") +
theme(axis.text.x = element_text(angle = 45, hjust =1)) +
theme_light() +
theme(axis.text.y = element_text()) +
xlab("Sample ID") +
ylab("16S rDNA copies/g sediment") +
coord_flip()

ggsave("Chl_absnr_final_high.png", width =12, height =10)
```

Supplement 2: Work-flow and Rstudio commands for absolute abundance plot of chlamydiae in the sediments

Script for 18S rRNA gene amplicon sequencing data analysis

1. Load required packages

```
library(tinytex)
library(phyloseq)
library(plyr)
library(ggplot2)
library(gridExtra)
library(vegan)
library(magrittr)
library(tidyr)
library(RColorBrewer)
library (forcats)
```

2. Import all necessary files

```
setwd("//share.univie.ac.at/DOME/staff/arndorfer/Markus Arndorfer/JMF-2304-01/JMF-2304-01__all__rRNA_SSU_Euk_D__JMFR_MSHS_KMHHM")

OTU_18S <- read.table("DADA2_counts_as_matrix.tsv", header=TRUE, row.names=1, check.names=F)
OTU_18S <- as.matrix(OTU_18S, rownames = 1)

TAX_18S <- read.table("DADA2_ASVs.rRNA_SSU.PR2_reference.DADA2_classified.tsv", header = TRUE, row.names=1, sep= "\t" , na.strings=c("","NA"))

TAX_18S$Class <- TAX_18S$Class %>% replace_na("no_class")
TAX_18S$Division <- TAX_18S$Division %>% replace_na("no_division")
TAX_18S$Supergroup <- TAX_18S$Supergroup %>% replace_na("no_supergroup")
TAX_18S$Order <- TAX_18S$Order %>% replace_na("no_order")
TAX_18S$Family <- TAX_18S$Family %>% replace_na("no_family")
TAX_18S$Genus <- TAX_18S$Genus %>% replace_na("no_genus")
TAX_18S$Species <- TAX_18S$Species %>% replace_na("no_species")

TAX_18S <- as.matrix(TAX_18S)

Sample_18S <- read.table("metadata_18S_mod.csv", sep=",", header=TRUE, row.names=1)
```

3. Generate phyloseq object

```
PS_all <- phyloseq(otu_table(OTU_18S, taxa_are_rows=TRUE), tax_table(TAX_18S),
sample_data(Sample_18S))
PS_all
```

4. Check read number and ASV number

```
reads_samples_all <- data.frame(sample_sums(PS_all))
total_read_sums_all <- sum(reads_samples_all)
reads_ASV_all <- data.frame(taxa_sums(PS_all))
```

5. Rename reads_samples_all column to read_number and add Sample ID column

```
names(reads_samples_all)[1] <- "read_number"
reads_samples_all <- cbind(Sample = rownames(reads_samples_all),
reads_samples_all)
rownames(reads_samples_all) <- NULL
reads_samples_all$Sample_ID <-
factor(c(3,4,6,7,14,18,19,20,22,25,26,27,28,29,30,32))
```

6. Get basic overview over composition

```
plot_bar(PS_all, fill="Supergroup")
plot_bar(PS_all)

ggplot(data=reads_samples_all, aes(x=Sample_ID, y=read_number)) +
geom_bar(stat="identity", fill="grey") +
coord_flip()
```

7. Plot alpha diversity

```
plot_richness(PS_all, measures=c("Observed","Chao1","Shannon")) + geom_boxplot()
```

8. Plot a rarefaction curve

-) force matrix and transform in long format for vegan:

```
mat_18S <- as(t(otu_table(PS_all)), "matrix") rarecurve(mat_18S, step = 50, col = "blue", label = FALSE)
```

9. Include only taxa with more than 10 reads (on average) in at least 5% of samples

```
filter_PS <- phyloseq::genefilter_sample(PS_all, filterfun_sample(function(x) x >= 10)) #10), A = 0.05*nsamples(PS1))
PS_f <- prune_taxa(filter_PS, PS_all)
PS_f
```

-) Check read number and ASV number after filtering:

```
reads_samples_PS_f <- data.frame(sample_sums(PS_f)) #read sums per sample
total_read_sumsPS_f <- sum(reads_samples_PS_f)
reads_ASV_PS_f <- data.frame(taxa_sums(PS_f))
```

10. Rename reads_samples_PS_f, add Sample ID column and plot read number

```
names(reads_samples_PS_f)[1] <- "read_number"
reads_samples_PS_f <- cbind(Sample = rownames(reads_samples_PS_f), reads_samples_PS_f)
rownames(reads_samples_PS_f) <- NULL

reads_samples_PS_f$Sample_ID <- factor(c(3,4,6,7,14,18,19,20,22,25,26,27,28,29,30,32))

ggplot(data=reads_samples_PS_f, aes(x=Sample_ID, y=read_number)) + geom_bar(stat="identity", fill="grey") + coord_flip()
```

11. Extract ASV from otu table

```
ASV <- otu_table(PS_f)
write.csv (ASV,"ASV.csv")
```

12. Get basic overview over composition after filtering

```
Abund = plot_bar(PS_f, fill = "Supergroup")
Abund + geom_bar(aes(color = Supergroup, fill = Supergroup), stat="identity")
```

```
ggsave("Abund_supergroups_euk.png")
```

13. Transform to relative abundance and generate basic relative abundance plots

-) Relative abundance of supergroups:

```
PS_f_ra = PS_f %>% tax_glom(taxrank = "Supergroup") %>%
transform_sample_counts(function(x) {x/sum(x)}) %>% psmelt() %>%
arrange(Supergroup)
PS_f_ra$User_sample_ID <- as.character(PS_f_ra$User_sample_ID)
PS_f_ra$User_sample_ID <- fct_reorder(PS_f_ra$User_sample_ID,PS_f_ra$Sample)
ggplot(PS_f_ra, aes(x = User_sample_ID, y = Abundance, fill = Supergroup)) +
geom_bar(stat = "identity") +
coord_flip() +
ylab("rel abundance")
```

-) Relative abundance of genera:

```
PS_f_ra2 = PS_f %>% tax_glom(taxrank = "Genus") %>%
transform_sample_counts(function(x) {x/sum(x)}) %>% psmelt() %>% arrange(Genus)
PS_f_ra2$User_sample_ID <- as.character(PS_f_ra2$User_sample_ID)
PS_f_ra2$User_sample_ID <- fct_reorder(PS_f_ra2$User_sample_ID,PS_f_ra2$Sample)
ggplot(PS_f_ra2, aes(x = User_sample_ID, y = Abundance, fill = Genus)) +
geom_bar(stat = "identity") +
theme(legend.key.size = unit(0.5, "cm")) +
coord_flip() +
ylab("rel abundance")
```

13. Focus on specific supergroups and plot rel. abundance of their genera

-) Replace "Stramenopiles" with the supergroup of interest:

```
target_supergroup6 <- "Stramenopiles"
```

-) Specify the sample of interest:

```
target_sample6 <- "JMF-2304-01-0003A"
```

-) Extract the taxonomic table from the phyloseq object:

```
tax_table6 <- tax_table(PS_f)
```

-) Identify the rows in the taxonomic table that match the target supergroup:

```
supergroup_rows6 <- which(tax_table6[, "Supergroup"] == target_supergroup6)
```

-) Extract the genera corresponding to these rows:

```
genera6 <- unique(tax_table6[supergroup_rows6, "Genus"])
```

-) Print the genera:

```
print(genera6)
```

-) Filter the phyloseq object to keep only the taxa from the target supergroup:

```
PS_f_supergroup6 <- subset_taxa(PS_f, Supergroup == target_supergroup6)
```

-) Aggregate the data at the genus level:

```
PS_f_genus6 <- tax_glom(PS_f_supergroup6, taxrank = "Genus")
```

-) Extract the OTU table and subset it to the target sample:

```
abundance_matrix6 <- otu_table(PS_f_genus6)
target_sample_abundance6 <- abundance_matrix6[, target_sample6]
```

-) Calculate the relative abundance for the target sample:

```
relative_abundance6 <- target_sample_abundance6 / sum(target_sample_abundance6)
```

-) Convert relative abundance to a data frame for easier handling:

```
relative_abundance_df6 <- data.frame( Genus = as(tax_table(PS_f_genus6)[,
"Genus"], "character"), RelativeAbundance = as.numeric(relative_abundance6) )
```

-) Print the relative abundance data frame for the target sample:

```
print(relative_abundance_df6)
```

-) Plot the relative abundance using ggplot2:

```
ggplot(relative_abundance_df6, aes(x = Genus, y = RelativeAbundance, fill =
Genus)) +
geom_bar(stat = "identity") +
coord_flip() +
xlab("Stramenopiles") +
ylab("Relative_Abundance")
```

Supplement 3: Work-flow and Rstudio commands for analysis of the 18S rRNA gene amplicon sequencing data

Script for the calculation of the chlamydial 16S rRNA gene-based phylogenetic tree with full-length and short 16S rRNA gene sequences from sediment cultures

-) Reference tree: IQ tree Chl_Nov2022 from Nov 2022 including IMG metagenome 16S seqs and all novel chlamydial sequences

-) Reference alignment: SILVA alignment

1. Add full (>1200 nt) 16S rRNA gene sequences from sediment cultures to reference alignment with mafft

```
module load mafft
mafft --add 16S_full_length_sediment_cultures.fna Chl_Nov2022_SilvaAli.fasta > Chl_Nov2022_SilvaAli_with_full_16S_sediment.fasta
```

2. Trim sequences with trimal 1.4.1 on Lisc server

```
module load trimal
trimal -in Chl_Nov2022_SilvaAli_with_full_16S_sediment.fasta -out Chl_Nov2022_SilvaAli_with_full_16S_sediment_trimal.fasta -gappyout
```

3. Calculate tree with IQ-TREE v 2.2.5

```
iqtree2 -nt 8 -B 1000 -alrt 1000 -m SYM+R10 -s Chl_Nov2022_SilvaAli_with_full_16S_sediment_trimal.fasta -pre Chl_reference_tree_with_full_16S_seq_sediment
```

4. Add short 16S rRNA gene sequences from sediment cultures to the alignment generated above

```
module load mafft
mafft --addfragments [shortseqs.fasta] --6merpair --keeplength --thread -1 Chl_Nov2022_SilvaAli_with_full_16S_sediment_trimal.fasta > [out.aln]
```

5. Extract fasta headers to extract short aligned fasta seqs from whole alignment to be able to add them to tree

-) Extract fasta headers:

```
grep '^>' [shortseqs.fasta] | grep -o '^\S*' | sed 's/>//' > [header.txt]
```

-) Extract aligned short seqs from out.aln file:

```
python3 extract_fasta.py [out.aln] [header.txt] > [shortseqs_toChl16S.aln]
```

extract_fasta.py script:

```
from Bio import SeqIO
import sys
wanted = [line.strip() for line in open(sys.argv[2])]
seqiter = SeqIO.parse(open(sys.argv[1]), 'fasta')
SeqIO.write((seq for seq in seqiter if seq.id in wanted), sys.stdout, "fasta")
```

6. Add aligned sequences to reference tree with full-length 16S rRNA gene sequences with epa-ng

```
module load conda
```

```
conda activate epa-ng
epa-ng -s Chl_Nov2022_SilvaAli_with_full_16S_sediment_trimal.fasta -t
Chl_reference_tree_with_full_16S_seq_sediment -q [shortseqs_toChl16S.aln] -m
SYM+I+R10
```

7. Extract a readable tree with pplacer

```
module load pplacer
guppy tog epa_result.jplace
```

8. Replace names of Chl16S sequences in tog.tre

```
python rename_nodes.py [reftree_names_families.txt] [tree file]
```

rename_nodes.py script:

```
import sys
import re
```

#Infile of names

```
names_in = open(sys.argv[1], 'r')
```

```
names_hash = {}

for line in names_in: line = line.rstrip('\n') old,new = line.split('\t')
names_hash[old] = new

names_in.close()

#Inpfile of tree
tree_file_path = sys.argv[2]
tree_in = open(tree_file_path, 'r')

#tree output file that has new names
tree_out = open(tree_file_path+"_rn.nwk", 'w')

for line in tree_in: for key in names_hash: if key in line: line = re.sub(key,
names_hash[key], line)

#print line
tree_out.write(line)
print ("new tree saved to: " + tree_file_path+"_rn.nwk")
tree_out.close()
```

Supplement 4: Work-flow and commands for calculating the phylogenetic tree of chlamydiae 16S rRNA gene sequences from the sediment cultures

Script for the calculation of 18S rRNA gene-based phylogenetic tree of the sediment cultures 18S rRNA gene sequences

-) 18S tree with full and partial 18S Sanger sequences

-) Used database: pr2 18S rRNA database v4.12.0

-) With sequences longer 1200 nt, clustered at 95% sequence id with usearch, without Fungi & Metazoa sequences

-) Aligned to SINA 18S alignment

1. Full-length 18S sequences aligned with mafft to SINA alignment

```
mafft --add sediment18S.fasta --auto pr2_centroids95_noFungiMetazoa_sinaaln.aln > sediment18S_aln2_pr2_centroids95_noFungiMetazoa_2.aln
```

-) Check alignment in SeaView

2. Trim alignment with trimal v1.4.rev15

```
trimal -in sediment18S_aln2_pr2_centroids95_noFungiMetazoa_2.aln -out sediment18S_aln2_pr2_centroids95_noFungiMetazoa_2_trimal.fasta -gappyout
```

3. Run fasttree on slurm with fasttree.sh

fasttree.sh script:

```
#!/bin/bash
#
#SBATCH --job-name=FastTree
#SBATCH --cpus-per-task=1
#SBATCH --mem=20000
#SBATCH --mail-type=ALL
#SBATCH --output=log/FastTree-%j.out
#SBATCH --error=log/FastTree-%j.err

#start tree
#sbatch FastTree.sh sediment18S_aln2_pr2_centroids95_noFungiMetazoa_2_trimal.fasta
```

```
QUERYFILE=$1

module load conda
conda activate fasttree-2.1.11

# the FastTree-command
FastTree -nt -gtr $QUERYFILE > $QUERYIFLE_fasttree.nwk

echo done
```

4. Replace names in file with cluster centroid sequence name

```
python rename_nodes.py [numbers2header.txt] [tree file]
```

Commands of rename_nodes.py script in Supplement 4

5. Add short 18S rRNA gene sequences to ref tree

Same commands as used in Supplement 4

Supplement 5: Workflow and commands for the calculation of 18S rRNA gene-based phylogenetic tree of the sediment cultures 18S rRNA gene sequences

Script for the calculation of 18S rRNA gene-based phylogenetic tree of the sediment cultures 18S rRNA gene and ASV sequences

-) used pr2 18S rRNA database v4.12.0

1. 18S sequences aligned with mafft to SINA alignment

```
module load mafft
mafft --add 18S_short_ASV_sequences.txt --auto
sediment18S_aln2_pr2_centroids95_noFungiMetazoa_2.aln >
ASV_sediment18S_aln2_pr2_centroids95_noFungiMetazoa_2.aln
```

-) check alignment in SeaView

2. Trim alignment with trimal v1.4.rev15

```
module load trimal
trimal -in ASV_sediment18S_aln2_pr2_centroids95_noFungiMetazoa_2.aln -out
ASV_sediment18S_aln2_pr2_centroids95_noFungiMetazoa_2_trimal.fasta -gappyout
```

3. Extract ASV and short sequences into new file

```
grep '^>' 18S_short_ASV_sequences.txt | grep -o '^\S*' | sed 's/>//' >
header_ASV_short18S.txt
```

```
module load python3
python3 extract_fasta.py
ASV_sediment18S_aln2_pr2_centroids95_noFungiMetazoa_2_trimal.fasta
header_ASV_short18S.txt > ASV_trimmed.aln
```

Commands of extract_fasta.py file in Supplement 4

4. Extract all other sequences into seperate file

```
grep '^>' sediment18S_aln2_pr2_centroids95_noFungiMetazoa_2.aln | grep -o '^\S*' |
sed 's/>//' > header_rest.txt
```

```
python3 extract_fasta.py
ASV_sediment18S_aln2_pr2_centroids95_noFungiMetazoa_2_trimal.fasta header_rest.txt
> 18S_and_reference_trimmed.aln
```

Commands of extract_fasta.py file in Supplement 4

5. Run fasttree of aligned reference and full-length 18S rRNA gene sequences on slurm with fasttree.sh

-) Used file: 18S_and_reference_trimmed.aln

Same commands as used in Supplement 5

6. Add ASV trimmed aligned sequences to reference tree with epa-ng

```
module load conda
conda activate epa-ng
epa-ng -s 18S_and_reference_trimmed.aln -t 18S_reference_trimmed_tree.nwk -q
ASV_trimmed.aln -m SYM+I+R10
```

7. Extract a readable tree with pplacer

Same commands used as in Supplement 4

8.Replace names in file with cluster centroid sequence name

```
python3 rename_nodes.py numbers2header.txt 18S_seq_ASV_trimmed.tog.tre
```

Commands of rename_nodes.py script in Supplement 4

Supplement 6: Workflow and commands for the calculation of 18S rRNA gene-based phylogenetic tree of the sediment cultures 18S rRNA gene and ASV sequences

Script for growth curve calculation for the different amoebae cultures and symbiont replication as well as their statistical analysis

1. Load required RStudio packages

```
library(ggplot2)
```

```
library(reshape2)
```

```
library(tidyr)
```

2. Import growth data from textfiles

```
data1 <- read.table("Growth_experiment_SNEG_oxic_hypoxic_2024.txt", sep="\t", header=TRUE)
```
#OR

```
data1 <- read.table("Growth_experiment_Ac_neff_symbionts_anox_2024.txt", sep="\t", header=TRUE)
```
#OR

```
data1 <- read.table("Growth_experiment_UV7_oxic_hypoxic_2024.txt", sep="\t", header=TRUE)
```
#OR

```
data1 <- read.table("Growth_Ac_neff_Sim_UV7_coinfection.txt", sep="\t", header=TRUE)
```
#OR

```
data1 <- read.table("Competition_chlamydiae_cell_conc_normalized.txt", sep="\t", header=TRUE)
```

3. Transform table from wide format to long format

```
data1_melted <- gather(data1, hours, cell_nr, X24h:X168h)
```
#OR

```
data1_melted <- gather(data1, hours, cell_nr, X0h:X168h)
```
#OR

```
data1_melted <- gather(data1, hours, chl_nr, X2h:X168h)
```

4. Check if cell numbers are really numbers

```
is.numeric(data1_melted$cell_nr)
```
#OR

```
is.numeric(data1_melted$chl_nr)
```

5. Sort timepoints correctly

```
timepoints <- c("X24h","X48h","X96h","X168h")
```
#OR

```
timepoints <- c("X0h","X2h","X24h","X48h","X96h","X168h")
```
#OR

```
timepoints <- c("X2h","X24h","X48h","X96h","X168h")
```

6. Change order of timepoints in dataframe

```
data1_melted$hours <- factor(data1_melted$hours, levels = timepoints)
```

7. Change level names of factor time

```
levels(data1_melted$hours) <-c("24","48","96","168")
```
#OR

```
levels(data1_melted$hours) <-c("0","2","24","48","96","168")
```
#OR

```
levels(data1_melted$hours) <-c("2","24","48","96","168")
```

8. Change hours from factor to numeric

```
data1_melted$hours <- as.numeric(as.character(data1_melted$hours))
```

9. Plot growth data with ggplot

```
ggplot(data1_melted, aes(x = hours, y = cell_nr, color = strain2, group = strain2)) +
scale_color_manual(values=c("red3","red4","springgreen3","springgreen4")) +
geom_point() +
theme(legend.title=element_blank()) +
geom_smooth(se=F, method = "loess") +
scale_y_log10() +
xlim(0,175) +
theme(legend.text=element_text(size=15)) +
theme(axis.text.x = element_text(size = 15)) +
theme(axis.text.y = element_text(size = 15)) +
theme(axis.title=element_text(size=15))
```

#OR

```
ggplot(data1_melted, aes(x = hours, y = cell_nr, color = strain2, group = strain2)) +
scale_color_manual(values=c("red1","springgreen1","royalblue1")) +
geom_point() +
theme(legend.title=element_blank()) +
geom_smooth(se=F, method = "loess") +
scale_y_log10() +
xlim(0,175) +
theme(legend.text=element_text(size=15)) +
theme(axis.text.x = element_text(size = 15)) +
theme(axis.text.y = element_text(size = 15)) +
theme(axis.title=element_text(size=15))
```

#OR

```
ggplot(data1_melted, aes(x = hours, y = cell_nr, color = strain2, group = strain2)) +
scale_color_manual(values=c("red3","red4","royalblue3","royalblue4")) +
geom_point() +
theme(legend.title=element_blank()) +
geom_smooth(se=F, method = "loess") +
scale_y_log10() +
xlim(0,175) +
theme(legend.text=element_text(size=15)) +
theme(axis.text.x = element_text(size = 15)) +
theme(axis.text.y = element_text(size = 15)) +
theme(axis.title=element_text(size=15))
```

#OR

```
ggplot(data1_melted, aes(x = hours, y = cell_nr, color = strain2, group = strain2)) +
scale_color_manual(values=c("orange1","orange4","springgreen1","springgreen4","royalblue1","royalblue4")) +
geom_point() +
theme(legend.title=element_blank()) +
geom_smooth(se=F, method = "loess") +
scale_y_log10() +
xlim(0,175) +
theme(legend.text=element_text(size=15)) +
theme(axis.text.x = element_text(size = 15)) +
```

```
theme(axis.text.y = element_text(size = 15)) +
theme(axis.title=element_text(size=15))
```

#OR

```
ggplot(data1_melted, aes(x = hours, y = chl_nr, group = strain2, color = strain2,
linetype = strain3)) +
scale_color_manual(values=c("orange1","orange4","orange1","orange4","springgreen1"
,"springgreen4","royalblue1","royalblue4")) +
geom_point() +
theme(legend.title=element_blank()) +
geom_smooth(aes(color = strain2, linetype = strain3), se=F, method = "loess") +
scale_y_log10() +
xlim(0,175) +
guides( color = guide_legend(override.aes = list(linetype = c("solid",
"solid","dashed","dashed", "solid","solid","solid", "solid"))), linetype = "none")
+
theme(legend.text=element_text(size=15)) +
theme(axis.text.x = element_text(size = 15)) +
theme(axis.text.y = element_text(size = 15)) +
theme(axis.title=element_text(size=15))

ggsave ("name")
```

10. Statisical analysis for significance

-) ANOVA:

```
summary(aov(data1$cell_nr_Xh ~ data1$Species))
```
#OR

```
summary(aov(data$chl_nr_Xh ~ data$Species))
```

-) Tukey Post-hoc test:

```
TukeyHSD(aov(data1$cell_nr_Xh ~ data1$Species))
```
#OR

```
TukeyHSD(aov(data$chl_nr_Xh ~ data$Species))
```

Supplement 7: RStudio code for growth curve calculation for the different amoebae cultures and symbiont replication as well as their statistical analysis (2.2.2.1, 2.2.2.2 and 2.2.2.6)

Script for visualization of the GC results and their statistical analysis

1. Load required Rstudio packages

```
library(ggplot2)
library(reshape2)
library(tidyr)
```

2. Import GC data from textfiles

```
data1 <- read.table("GC_CO2_ppm.txt", sep="\t", header=TRUE)
data2 <- read.table("GC_CO2_mean_ppm.txt" , sep="\t", header=TRUE)
data3 <- read.table("GC_medium_control_ppm.txt" , sep="\t", header=TRUE)
data4 <- read.table("GC_medium_control_mean_ppm.txt" , sep="\t", header=TRUE)
```

3. Transform table from wide format to long format

```
data1_melted <- gather(data1, time, CO2, X0h:X24h)
data2_melted <- gather(data2, time, CO2, X0h:X24h)
data3_melted <- gather(data3, time, CO2, X48h:X72h)
data4_melted <- gather(data4, time, CO2, X48h:X72h)
```

4. Check if CO2 values are really numbers

```
is.numeric(dataX_melted$CO2)
```

5. Sort timepoints correctly

```
timepoints <- c("X0h","X24h")
timepoints_2 <- c("X48h","X72h")
```

6. Change order of timepoints in dataframe

```
data1_melted$time <- factor(data1_melted$time, levels = timepoints)
data2_melted$time <- factor(data2_melted$time, levels = timepoints)
data3_melted$time <- factor(data3_melted$time, levels = timepoints_2)
data4_melted$time <- factor(data4_melted$time, levels = timepoints_2)
```

8. Remove X before hours

```
levels(data1_melted$time) <-c("0h","24h")
levels(data2_melted$time) <-c("0h","24h")
levels(data3_melted$time) <- c("48h", "72h")
levels(data4_melted$time) <- c("48h", "72h")
```

9. Plot GC data with ggplot

```
ggplot() +
geom_col(data=data2_melted, aes(x = time, y = CO2, fill = strain2, group = strain2), position = "dodge") +
geom_point(data = data1, aes(x=time, y = CO2, group = strain2), position = position_dodge(width = 0.9)) +
scale_fill_manual(values=c("red3","red4", "springgreen3", "springgreen4", "royalblue3","royalblue4")) +
theme(legend.title=element_blank()) +
theme(legend.text=element_text(size=15)) +
theme(axis.text.x = element_text(size = 15)) +
theme(axis.text.y = element_text(size = 15)) +
theme(axis.title=element_text(size=15)) +
scale_y_log10()
```

```
ggplot() +
geom_col(data=data4_melted, aes(x = time, y = CO2, fill = strain2, group = strain2), position = "dodge") +
geom_point(data = data3_melted, aes(x=time, y = CO2, group = strain2), position = position_dodge(width = 0.9)) +
scale_fill_manual(values=c("purple2","purple4")) +
theme(legend.title=element_blank()) +
theme(legend.text=element_text(size=15)) +
theme(axis.text.x = element_text(size = 15)) +
theme(axis.text.y = element_text(size = 15)) +
theme(axis.title=element_text(size=15)) +
scale_y_log10()
```

10. Statisical analysis for significance

-) ANOVA:

```
summary(aov(dataX$CO2_Xh ~ dataX$Species))
```

-) Tukey Post-hoc test:

```
TukeyHSD(aov(dataX$CO2_Xh ~ dataX$Species))
```

Supplement 8: Workflow and RStudio code for visualization of the GC results and their statistical analysis (2.2.2.4)

Supplement 9: Overview of ANOVA test result regarding cell growth and respiration. Significant p-values are marked with an asterisk.

Experiment	Time after incubation	df	Sum Sq	Mean Sq	F value	p-value
Simkania (2.2.2.1)	24h	3	2.462e+11	8.206e+10	2.242	0.161
	48h	3	6.143e+10	2.048e+10	0.468	0.713
	96h	3	1.121e+14	3.737e+13	7.227	0.0115*
	168h	3	5.064e+15	1.688e+15	6.143	0.018*
UV7 (2.2.2.1)	24h	3	3.503e+12	1.168e+12	2.506	0.133
	48h	3	4.438e+13	1.479e+13	5.464	0.0244*
	96h	3	6.688e+14	2.229e+14	14.99	0.0012*
	168h	3	6.834e+15	2.278e+15	13.37	0.00175*
Anoxia (2.2.2.2)	24h	2	3.045e+10	1.522e+10	0.085	0.92
	48h	2	1.725e+12	8.625e+11	2.209	0.191
	96h	2	5.638e+12	2.819e+12	7.154	0.0258
	168h	2	3.179e+12	1.590e+12	3.301	0.108
GC (2.2.2.4)	0h	5	86915240	17383048	40.5	4.17e-07*
	24h	5	102469408	20493882	33.69	1.16e-06*
Competition experiment (2.2.2.6)	2h	5	3.596e+12	5.138e+11	1.419	0.265
	24h	5	3.193e+15	4.562e+14	19.32	1.09e-06*
	48h	5	9.921e+15	1.417e+15	22.78	3.44e-07*
	96h	5	4.768e+15	6.811e+14	29.35	5.59e-08*
	168h	5	2.391e+15	3.416e+14	23.54	2.72e-07*

Supplement 10: List of p-values of the pairwise post-hoc Tukey test regarding cell growth under oxic vs. hypoxic conditions (2.2.2.1). The significant p-values are marked with an asterisk.

	96h			
	Sneg_ox	Sneg_hypo	Ac_neff_ox	Ac_neff_hypo
Sneg_ox	---	0.0189389*	0.1986140	---
Sneg_hypo	0.0189389*	---	---	0.9972756
Ac_neff_ox	0.1986140	---	---	0.3072180
Ac_neff_hypo	---	0.9972756	0.3072180	---
	168h			
	Sneg_ox	Sneg_hypo	Ac_neff_ox	Ac_neff_hypo
Sneg_ox	---	0.0242833*	0.1363226	---
Sneg_hypo	0.0242833*	---	---	0.9999998
Ac_neff_ox	0.1363226	---	---	0.6301922
Ac_neff_hypo	---	0.9999998	0.6301922	---
	48h			
	UV7_ox	UV7_hypo	Ac_neff_ox	Ac_neff_hypo
UV7_ox	---	0.9655225	0.0489926*	---
UV7_hypo	0.9655225	---	---	0.1429672
Ac_neff_ox	0.0489926*	---	---	0.9898782
Ac_neff_hypo	---	0.1429672	0.9898782	---
	96h			
	UV7_ox	UV7_hypo	Ac_neff_ox	Ac_neff_hypo
UV7_ox	---	0.7591908	0.0052970*	---
UV7_hypo	0.7591908	---	---	0.9761281
Ac_neff_ox	0.0052970*	---	---	0.0026299*

Ac_neff_hypo	---	0.9761281	0.0026299*	---
	168h			
	UV7_ox	UV7_hypo	Ac_neff_ox	Ac_neff_hypo
UV7_ox	---	0.8263038	0.0063830*	---
UV7_hypo	0.8263038	---	---	0.9402291
Ac_neff_ox	0.0063830*	---	---	0.0044430*
Ac_neff_hypo	---	0.9402291	0.0044430*	---

Supplement 11: List of p-values of the pairwise post-hoc Tukey test regarding cell growth under anoxic conditions (2.2.2.2). The significant p-values are marked with an asterisk.

	96h		
	Ac_neff_anox	Sneg_anox	UV7_anox
Ac_neff_anox	---	0.1186102	0.4199458
Sneg_anox	0.1186102	---	0.0225697*
UV7_anox	0.4199458	0.0225697*	---

Supplement 12: List of p-values of the pairwise post-hoc Tukey test regarding respiration (2.2.2.4). The significant p-values are marked with an asterisk.

	0h					
	Ac_neff_ox	Ac_neff_hypo	Sneg_ox	Sneg_hypo	UV7_ox	UV7_hypo
Ac_neff_ox	---	0.0092593*	0.0001506*	---	0.9999952	---
Ac_neff_hypo	0.0092593*	---	---	1.0000000	---	1.0000000
Sneg_ox	0.0001506*	---	---	0.0000010*	0.0001779*	---
Sneg_hypo	---	1.0000000	0.0000010*	---	---	1.0000000
UV7_ox	0.9999952	---	0.0001779*	---	---	0.0073160*
UV7_hypo	---	1.0000000	---	1.0000000	0.0073160*	---

	24h					
	Ac_neff_ox	Ac_neff_hypo	Sneg_ox	Sneg_hypo	UV7_ox	UV7_hypo
Ac_neff_ox	---	0.0111637*	0.0006613*	---	0.9999729	---
Ac_neff_hypo	0.0111637*	---	---	0.9999994	---	0.9999997
Sneg_ox	0.0006613*	---	---	0.0000029*	0.0008565*	---
Sneg_hypo	---	0.9999994	0.0000029*	---	---	1.0000000
UV7_ox	0.9999729	---	0.0008565*	---	---	0.0074764*
UV7_hypo	---	0.9999997	---	1.0000000	0.0074764*	---

Supplements 13: Number and proportion (%) of non-infected (NI), low-infected (LI) and high-infected (HI) amoebae cells

	NI	LI	HI	%NI	%LI	%HI
Sneg_ox_MOI10_1	26	24	0	52.00%	48.00%	0.00%
Sneg_ox_MOI10_2	25	23	2	50.00%	46.00%	4.00%
Sneg_ox_MOI10_3	24	25	1	48.00%	50.00%	2.00%
Sneg_ox_MOI30_1	16	20	0	44.44%	55.56%	0.00%
Sneg_ox_MOI30_2	19	31	0	38.00%	62.00%	0.00%
Sneg_ox_MOI30_3	15	35	0	30.00%	70.00%	0.00%
Sneg_ox_MOI50_1	17	33	0	34.00%	66.00%	0.00%
Sneg_ox_MOI50_2	16	32	2	32.00%	64.00%	4.00%
Sneg_ox_MOI50_3	12	36	2	24.00%	72.00%	4.00%
Sneg_ox_MOI100_1	11	26	1	28.95%	68.42%	2.63%
Sneg_ox_MOI100_2	15	12	23	30.00%	24.00%	46.00%
Sneg_ox_MOI100_3	20	29	1	40.00%	58.00%	2.00%
UV7_ox_MOI10_1	15	28	7	30.00%	56.00%	14.00%
UV7_ox_MOI10_2	27	18	5	54.00%	36.00%	10.00%
UV7_ox_MOI10_3	18	27	5	36.00%	54.00%	10.00%
UV7_ox_MOI30_1	7	9	0	43.75%	56.25%	0.00%
UV7_ox_MOI30_2	12	20	3	34.29%	57.14%	8.57%
UV7_ox_MOI30_3	10	19	2	32.26%	61.29%	6.45%
UV7_ox_MOI50_1	20	23	7	40.00%	46.00%	14.00%
UV7_ox_MOI50_2	9	36	5	18.00%	72.00%	10.00%
UV7_ox_MOI50_3	15	29	6	30.00%	58.00%	12.00%

UV7_ox_MOI100_1	12	34	4	24.00%	68.00%	8.00%
UV7_ox_MOI100_2	6	32	5	13.95%	74.42%	11.63%
UV7_ox_MOI100_3	1	29	4	2.94%	85.29%	11.76%
Sneg_hypo_MOI10_1	13	8	0	61.90%	38.10%	0.00%
Sneg_hypo_MOI10_2	16	17	0	48.48%	51.52%	0.00%
Sneg_hypo_MOI10_3	3	10	0	23.08%	76.92%	0.00%
Sneg_hypo_MOI30_1	9	10	1	45.00%	50.00%	5.00%
Sneg_hypo_MOI30_2	1	4	0	20.00%	80.00%	0.00%
Sneg_hypo_MOI30_3	15	13	0	53.57%	46.43%	0.00%
Sneg_hypo_MOI50_1	11	15	0	42.31%	57.69%	0.00%
Sneg_hypo_MOI50_2	26	24	0	52.00%	48.00%	0.00%
Sneg_hypo_MOI50_3	5	4	0	55.56%	44.44%	0.00%
Sneg_hypo_MOI100_1	25	25	0	50.00%	50.00%	0.00%
Sneg_hypo_MOI100_2	20	18	1	51.28%	46.15%	2.56%
Sneg_hypo_MOI100_3	25	25	0	50.00%	50.00%	0.00%
UV7_hypo_MOI10_1	14	10	7	45.16%	32.26%	22.58%
UV7_hypo_MOI10_2	13	9	6	46.43%	32.14%	21.43%
UV7_hypo_MOI10_3	5	2	2	55.56%	22.22%	22.22%
UV7_hypo_MOI30_1	2	2	0	50.00%	50.00%	0.00%
UV7_hypo_MOI30_2	9	13	1	39.13%	56.52%	4.35%
UV7_hypo_MOI30_3	12	12	8	37.50%	37.50%	25.00%
UV7_hypo_MOI50_1	5	15	3	21.74%	65.22%	13.04%
UV7_hypo_MOI50_2	10	7	7	41.67%	29.17%	29.17%
UV7_hypo_MOI50_3	2	1	1	50.00%	25.00%	25.00%
UV7_hypo_MOI100_1	0	2	0	0.00%	100.00%	0.00%
UV7_hypo_MOI100_2	5	9	0	35.71%	64.29%	0.00%
UV7_hypo_MOI100_3	5	11	1	29.41%	64.71%	5.88%
Sneg_anox_MOI10_1	7	5	0	58.33%	41.67%	0.00%
Sneg_anox_MOI10_2	1	1	0	50.00%	50.00%	0.00%
Sneg_anox_MOI10_3	0	0	0	0.00%	0.00%	0.00%
Sneg_anox_MOI30_1	0	2	0	0.00%	100.00%	0.00%
Sneg_anox_MOI30_2	8	8	0	50.00%	50.00%	0.00%
Sneg_anox_MOI30_3	5	5	0	50.00%	50.00%	0.00%
Sneg_anox_MOI50_1	2	6	0	25.00%	75.00%	0.00%
Sneg_anox_MOI50_2	1	9	0	10.00%	90.00%	0.00%
Sneg_anox_MOI50_3	4	2	0	66.67%	33.33%	0.00%

Sneg_anox_MOI100_1	8	20	0	28.57%	71.43%	0.00%
Sneg_anox_MOI100_2	3	10	0	23.08%	76.92%	0.00%
Sneg_anox_MOI100_3	3	3	0	50.00%	50.00%	0.00%
UV7_anox_MOI10_1	0	0	0	0.00%	0.00%	0.00%
UV7_anox_MOI10_2	10	7	4	47.62%	33.33%	19.05%
UV7_anox_MOI10_3	0	0	0	0.00%	0.00%	0.00%
UV7_anox_MOI30_1	2	0	0	100.00%	0.00%	0.00%
UV7_anox_MOI30_2	2	1	0	66.67%	33.33%	0.00%
UV7_anox_MOI30_3	22	11	0	66.67%	33.33%	0.00%
UV7_anox_MOI50_1	4	2	4	40.00%	20.00%	40.00%
UV7_anox_MOI50_2	5	5	0	50.00%	50.00%	0.00%
UV7_anox_MOI50_3	6	5	1	50.00%	41.67%	8.33%
UV7_anox_MOI100_1	9	9	2	45.00%	45.00%	10.00%
UV7_anox_MOI100_2	1	4	1	16.67%	66.67%	16.67%
UV7_anox_MOI100_3	1	2	0	33.33%	66.67%	0.00%

Supplement 14: List of p-values of the pairwise post-hoc Tukey test regarding cell growth in the competition experiment (2.2.2.6). The significant p-values are marked with an asterisk.

	0h					
	co_inf_ox	co_inf_anox	Sneg_ox	Sneg_anox	UV7_ox	UV7_anox
co_inf_ox	---	0.5035792	0.9797739	---	0.9986691	---
co_inf_anox	0.5035792	---	---	0.8150109	---	0.2120004
Sneg_ox	0.9797739	---	---	0.2396168	0.9995368	---
Sneg_anox	---	0.8150109	0.2396168	---	---	0.0203518*
UV7_ox	0.9986691	---	0.9995368	---	---	0.9124460
UV7_anox	---	0.2120004	---	0.0203518*	0.9124460	---
	24h					
	co_inf_ox	co_inf_anox	Sneg_ox	Sneg_anox	UV7_ox	UV7_anox
co_inf_ox	---	0.0000018*	0.0327039*	---	0.0750526	---
co_inf_anox	0.0000018*	---	---	0.9933635	---	0.9999947

Sneg_ox	0.0327039*	---	---	0.0039682*	0.9980178	---
Sneg_anox	---	0.9933635	0.0039682*	---	---	0.9980615
UV7_ox	0.0750526	---	0.9980178	---	---	0.0006757*
UV7_anox	---	0.9999947	---	0.9980615	0.0006757*	---
	48h					
	co_inf_ox	co_inf_anox	Sneg_ox	Sneg_anox	UV7_ox	UV7_anox
co_inf_ox	---	0.0011431*	0.8197368	---	0.2011585	---
co_inf_anox	0.0011431*	---	---	0.9998186	---	0.9999958
Sneg_ox	0.8197368	---	---	0.0001553*	0.8332203	---
Sneg_anox	---	0.9998186	0.0001553*	---	---	0.9999920
UV7_ox	0.2011585	---	0.8332203	---	---	0.0000117*
UV7_anox	---	0.9999958	---	0.9999920	0.0000117*	---
	96h					
	co_inf_ox	co_inf_anox	Sneg_ox	Sneg_anox	UV7_ox	UV7_anox
co_inf_ox	---	0.0000004*	0.0014137*	---	0.2706747	---
co_inf_anox	0.0000004*	---	---	0.9999996	---	0.9999999
Sneg_ox	0.0014137*	---	---	<0.0000001*	0.1347729	---
Sneg_anox	---	0.9999996	<0.0000001*	---	---	1.0000000
UV7_ox	0.2706747	---	0.1347729	---	---	<0.0000001*
UV7_anox	---	0.9999999	---	1.0000000	<0.0000001*	---
	168h					
	co_inf_ox	co_inf_anox	Sneg_ox	Sneg_anox	UV7_ox	UV7_anox
co_inf_ox	---	0.0000001*	0.0006275*	---	0.9970604	---
co_inf_anox	0.0000001*	---	---	1.0000000	---	1.0000000
Sneg_ox	0.0006275*	---	---	<0.0000001*	0.0002443*	---
Sneg_anox	---	1.0000000	<0.0000001*	---	---	1.0000000

UV7_ox	0.9970604	---	0.0002443*	---	---	0.0000001*
UV7_anox	---	1.0000000	---	1.0000000	0.0000001*	---

Supplement 15: List of p-values of the pairwise post-hoc Tukey test regarding chlamydiae replication in the competition experiment (2.2.2.6). The significant p-values are marked with an asterisk.

	24h							
	Sneg_ox	Sneg_anox	UV7_ox	UV7_anox	co_inf_S_ox	co_inf_U_ox	co_inf_S_anox	Co_inf_U_anox
Sneg_ox	---	1.0000000	0.0000080*	---	1.0000000	---	---	---
Sneg_anox	1.0000000	---	---	0.9998938	---	---	0.9999994	---
UV7_ox	0.0000080*	---	---	0.0000149*	---	0.0554383	---	---
UV7_anox	---	0.9998938	0.0000149*	---	---	---	---	1.0000000
co_inf_S_ox	1.0000000	---	---	---	---	0.0032738*	0.9999994	---
co_inf_U_ox	---	---	0.0554383	---	0.0032738*	---	---	0.0071960*
co_inf_S_anox	---	0.9999994	---	---	0.9999994	---	---	0.9999981
co_inf_U_anox	---	---	---	1.0000000	---	0.0071960*	0.9999981	---
	48h							
	Sneg_ox	Sneg_anox	UV7_ox	UV7_anox	co_inf_S_ox	co_inf_U_ox	co_inf_S_anox	Co_inf_U_anox
Sneg_ox	---	1.0000000	0.0201823*	---	1.0000000	---	---	---

Sneg_anox	1.0000000	---	---	0.9999993	---	---	1.0000000	---
UV7_ox	0.0201823*	---	---	0.0290632*	---	0.0010219*	---	---
UV7_anox	---	0.9999993	0.0290632*	---	---	---	---	0.9999992
co_inf_S_ox	1.0000000	---	---	---	---	0.0000015*	1.0000000	---
co_inf_U_ox	---	---	0.0010219*	---	0.0000015*	---	---	0.0000025*
co_inf_S_anox	---	1.0000000	---	---	1.0000000	---	---	0.9999873
co_inf_U_anox	---	---	---	0.9999992	---	0.0000025*	0.9999873	---
	96h							
	Sneg_ox	Sneg_anox	UV7_ox	UV7_anox	co_inf_S_ox	co_inf_U_ox	co_inf_S_anox	Co_inf_U_anox
Sneg_ox	---	1.0000000	0.0000581*	---	1.0000000	---	---	---
Sneg_anox	1.0000000	---	---	0.9995598	---	---	1.0000000	---
UV7_ox	0.0000581*	---	---	0.0001370*	---	0.2612498	---	---
UV7_anox	---	0.9995598	0.0001370*	---	---	---	---	1.0000000
co_inf_S_ox	1.0000000	---	---	---	---	0.0000012*	1.0000000	---
co_inf_U_ox	---	---	0.2612498	---	0.0000012*	---	---	0.0000023*
co_inf_S_anox	---	1.0000000	---	---	1.0000000	---	---	0.9999278

co_inf_U_anox	---	---	---	1.000000	---	0.000002	0.9999278	---
	168h							
	Sneg_ox	Sneg_anox	UV7_ox	UV7_anox	co_inf_S_ox	co_inf_U_ox	co_inf_S_anox	Co_inf_U_anox
Sneg_ox	---	1.0000000	0.002884*	---	1.000000	---	---	---
Sneg_anox	1.000000	---	---	0.999996	---	---	1.0000000	---
UV7_ox	0.002884*	---	---	0.004781*	---	0.010157*	---	---
UV7_anox	---	0.9999946	0.004781*	---	---	---	---	1.0000000
co_inf_S_ox	1.000000	---	---	---	---	0.000002*	1.0000000	---
co_inf_U_ox	---	---	0.010157*	---	0.000002*	---	---	0.0000031*
co_inf_S_anox	---	1.0000000	---	---	1.000000	---	---	0.9999697
co_inf_U_anox	---	---	---	1.000000	---	0.000003*	0.9999697	---